

THE EFFECT OF NITROGEN DEPRIVATION ON STABLE ISOTOPE ^{15}N
FRACTIONATION AND PREFERENCE OF AMMONIUM, NITRATE, AND UREA
BY MARINE DINOFLAGELLATES AND A RAPHIIDOPHYTE

by

Kugako Sugimoto

B. S., University of Hawaii at Manoa, 1994

A THESIS SUBMITTED IN PARTIAL FULFILMENT OF THE REQUIREMENTS
FOR THE DEGREE OF MASTER OF SCIENCE
in
THE FACULTY OF GRADUATE STUDIES
(Department of Earth and Ocean Sciences)

We accept this thesis as conforming to the required standard

THE UNIVERSITY OF BRITISH COLUMBIA

OCTOBER 1998

© Kugako Sugimoto, 1998

In presenting this thesis in partial fulfilment of the requirements for an advanced degree at the University of British Columbia, I agree that the Library shall make it freely available for reference and study. I further agree that permission for extensive copying of this thesis for scholarly purposes may be granted by the head of my department or by his or her representatives. It is understood that copying or publication of this thesis for financial gain shall not be allowed without my written permission.

Department of Earth and Ocean Sciences

The University of British Columbia
Vancouver, Canada

Date December 1, 1998

ABSTRACT

Nitrogen (N) preference and the uptake response of N-replete and N-starved dinoflagellate *Amphidinium carterae* and *Prorocentrum micans*, and the chloromonad (Raphidophyte) *Heterosigma carterae* grown on NH_4^+ , NO_3^- , and urea were determined by N disappearance rates and uptake rates. N-replete cells preferentially took up NH_4^+ in the presence of three N forms. Urea was the second preference. NO_3^- was taken up last. N-replete *Heterosigma carterae* exhibited a strong preference for NH_4^+ uptake and its ratio of uptake preference of the three N sources relative to urea was 10 (NH_4^+):0.1 (NO_3^-):1 (urea). These ratios suggest a strong influence of NH_4^+ on NO_3^- uptake. However, the concentration of NO_3^- decreased rapidly when only NO_3^- and urea were present in a medium. This order of preference remained the same after N deprivation. However, N-deplete *P. micans* and *A. carterae* decreased their preference for NO_3^- relative to both NH_4^+ and urea from 1.9 (NH_4^+):0.6 (NO_3^-):1 (urea) to 1.5:0.5:1 and from 6.9 (NH_4^+):-0.2 (NO_3^-):1 (urea) to 7.5:-1.1:1 respectively. On the other hand, N-deprived *H. carterae* increased its preference for NO_3^- relative to both NH_4^+ and urea from 10 (NH_4^+):0.1 (NO_3^-):1 (urea) to 7.5:0.2:1. The N uptake preference depended on the interactions of each N source.

N-starved *H. carterae* in a batch culture grown on NH_4^+ showed an immediate NH_4^+ uptake after the re-addition of NH_4^+ and ceased uptake for a short period and started to take up NH_4^+ again. This NH_4^+ uptake pattern existed, but was not evident in *H. carterae* grown on three N sources.

Diel patterns of nitrate (NO_3^-) uptake under a light:dark (14L:10D) cycle were investigated in a batch culture of *H. carterae* which is known as a diel vertical migrator. The concentration of NO_3^- in the culture decreased mostly during light periods, and hardly decreased or even increased (i.e. efflux) during dark periods. NO_3^- -starved *H. carterae* showed NO_3^- uptake during the dark period. NO_3^- -starved cells grown under a light:dark cycle exhibited a longer period of no uptake after the re-addition of NO_3^- than when grown under continuous light.

The impact of N deprivation on N isotope fractionation by marine phytoplankton grown on NH_4^+ , NO_3^- , and urea, or only NO_3^- was examined by using the predicted model of $\delta^{15}\text{N}$ of particulate nitrogen (PN). The mechanism of isotope fractionation (ϵ) for *P. micans*, *A. carterae*, and *H. carterae* changed rapidly with N availability. The best fit $\epsilon(\text{NH}_4^+)$ value for N-deprived *A. carterae* and *H. carterae* decreased from 20 and 24‰ to 4 and < 4‰ respectively following the re-supply of the three N sources while the $\epsilon(\text{NH}_4^+)$ for *P. micans* increased from 12‰ to 20‰. $\epsilon(\text{NO}_3^-)$ for *H. carterae* grown on NO_3^- also increased, probably due to the increased, efflux of dissolved organic N (DON) during the N deprivation.

LIST OF CONTENT

Abstract.....	ii
List of Tables	vii
List of Figures.....	viii
Acknowledgments	xvi
Introduction	
Overview.....	1
Ammonium (NH_4^+).....	2
Nitrate (NO_3^-).....	2
Urea ($\text{CO}(\text{NH}_2)_2$).....	2
Physiology.....	3
Uptake.....	3
Assimilation.....	5
Kinetic parameters.....	7
Starvation and rapid uptake.....	7
Ecology.....	8
Interactions	
1) NH_4^+ and NO_3^-	8
2) Effect of starvation on interaction between NH_4^+ and NO_3^-	9
3) Effect of light limitation on the interaction between NH_4^+ and NO_3^-	10
4) Interactions between NH_4^+ and urea.....	10
5) Interactions between NO_3^- and urea.....	11
6) Field study.....	12
Isotopic fractionation.....	13
Isotope expression.....	13
Isotope fractionations.....	14
Nitrogen isotope fractionation by phytoplankton.....	15
N utilization by dinoflagellates and flagellates.....	17
The species studied.....	18
1) <i>Amphidinium carterae</i>	18
2) <i>Heterosigma carterae</i>	19
3) <i>Prorocentrum micans</i>	20
Objectives	22
Materials and Methods	23
Culture methods.....	23
Biomass, particulate N and nutrient analysis.....	26
Rate measurements.....	26
Uptake rate.....	27
Nitrogen isotope analysis.....	27
Calculations of the fractionation factor.....	28
Multiple N source uptake model.....	29

Part I	
Results.....	30
<i>Prorocentrum micans</i> grown on and re-supplied with NH_4^+ , NO_3^- , and urea (Experiment 1).....	30
<i>Amphidinium carterae</i> grown on and re-supplied with NH_4^+ , NO_3^- , and urea (Experiment 2).....	37
<i>Heterosigma carterae</i> grown on and re-supplied with NH_4^+ , NO_3^- , and urea (Experiment 3).....	46
<i>Heterosigma carterae</i> grown on and re-supplied with NO_3^- (Experiment 4).....	54
<i>Heterosigma carterae</i> grown on and re-supplied with NO_3^- under L:D cycle lights (Experiment 5).....	58
<i>Heterosigma carterae</i> grown on and re-supplied with NH_4^+ under continuous light (Experiment 6).....	63
Discussion.....	74
N Preference change	
1) period I.....	74
2) period II.....	77
Cellular physiological state	
1) Surge uptake.....	79
2) Ammonium uptake in N-deplete phase.....	80
3) Nitrate uptake in N-deplete phase.....	82
4) Urea uptake in N-deplete phase.....	83
N interaction.....	84
Increased concentration and efflux of N.....	88
Ecology.....	89
Growth rate.....	91
Light:Dark cycle	
1) Cell division and fluorescence number.....	93
2) Uptake diel periodicity.....	94
3) <i>Heterosigma carterae</i> and dark NO_3^- uptake.....	96
Conclusions	98
Future studies	100
Part II Isotope fractionation	
Results	
1) <i>Prorocentrum micans</i> grown on NH_4^+ , NO_3^- , and urea.....	101
2) <i>Amphidinium carterae</i> grown on NH_4^+ , NO_3^- , and urea.....	105
3) <i>Heterosigma carterae</i> grown on NH_4^+ , NO_3^- , and urea.....	109
4) <i>Heterosigma carterae</i> grown on NO_3^-	109
Sensitivity analysis	
1) <i>Prorocentrum micans</i> grown on NH_4^+ , NO_3^- , and urea.....	115
2) <i>Amphidinium carterae</i> grown on NH_4^+ , NO_3^- , and urea.....	118
3) <i>Heterosigma carterae</i> grown on NH_4^+ , NO_3^- , and urea.....	118
4) <i>Heterosigma carterae</i> grown on NO_3^-	123

Discussion	
$\varepsilon(\text{NO}_3^-)$	126
$\varepsilon(\text{NH}_4^+)$	128
Effect of N deprivation.....	130
Conclusions	134
Future studies	135
References.....	136
Appendix 1.....	156

LIST OF TABLES

Table 1	Summary of experimental conditions. Nitrogen sources, species name, and average N starvation periods of triplicate batch cultures listed.	24
Table 2	Comparison of the order of N preference before and after re-addition of NH_4^+ , NO_3^- , and urea into triplicate batch cultures of <i>P. micans</i> , <i>A. carterae</i> , and <i>H. carterae</i> . Period I indicates the period when NH_4^+ , NO_3^- , and urea were all present in the medium. Period II indicates the period when NO_3^- and urea were present in the medium. Period III indicates the period when only urea was left in the medium.	31
Table 3.	Listing of variables and definitions used in the multiple N source uptake model.	104
Table 4	Variables and their values used in the multiple N source uptake model. <i>Prorocentrum micans</i> , <i>Amphidinium carterae</i> , and <i>Heterosigma carterae</i> were grown on multiple N sources (NO_3^- , NH_4^+ , and urea) under N-sufficient conditions. After 0 - 82 h of starvation, all three N sources were added simultaneously to the culture (i.e. N re-supply phase). <i>Heterosigma carterae</i> was grown on NO_3^- under NO_3^- -sufficient condition. After 52 h of N starvation, NO_3^- was added to the culture (i.e. N re-supply phase). Symbols are defined in Table 3.	106

LIST OF FIGURES

- Figure 1 Growth of *Prorocentrum micans* grown on NH_4^+ , NO_3^- , and urea under continuous light. Log plot of *in vivo* fluorescence versus time. Bars represent ± 1 S.D. (n=2-3). Error bars are smaller than symbols where not visible.32
- Figure 2 Nitrogen concentrations (urea as $\mu\text{g-at N L}^{-1}$) during the growth of *Prorocentrum micans* grown on NH_4^+ , NO_3^- , and urea under continuous light plotted against a) elapsed time and b) elapsed time since re-addition of NH_4^+ , NO_3^- , and urea at t=0 to previously N-starved cultures for 56 h. Thus (b) is an expanded time version of the N concentrations during the re-addition phase shown in (a). Cultures were N-starved between 130 and 186.5 h and then 42 μM NH_4^+ , 50 μM NO_3^- , and 47 $\mu\text{g-at N L}^{-1}$ urea were added at 186.5 h. Bars represent ± 1 S.D. (n=2-3). Error bars are smaller than symbols where not visible.33
- Figure 3 N uptake rates of triplicate, batch cultures of *Prorocentrum micans* grown on NH_4^+ , NO_3^- , and urea and under continuous light plotted against a) average time between sampling and b) average time between sampling since re-addition of NH_4^+ , NO_3^- , and urea at t=0 to previously N-starved cultures for 56 h. (b) is an expanded version of the re-addition phase of (a). Cultures were N starved between 130 and 186.5 h and NH_4^+ , NO_3^- , and urea were added at 186.5 h. Bars represent ± 1 S.D. (n=2-3). Error bars are smaller than symbols where not visible.36
- Figure 4 Relative N preference of NH_4^+ and NO_3^- relative to urea for *Prorocentrum micans* during the period I before (■) and after (□) N starvation. The relative preference for urea is fixed at 1, both before and after N starvation.38
- Figure 5 Relative N preference of urea relative to NO_3^- for *Prorocentrum micans* during the period II before (■) and after (□) N starvation. The relative preference for urea is fixed at 1, both before and after N starvation.38
- Figure 6 Growth of *Amphidinium carterae* grown on NH_4^+ , NO_3^- , and urea under continuous light. Log plot of *in vivo* fluorescence versus time. Bars represent ± 1 S.D. (n=2-3). Error bars are smaller than symbols where not visible.39

- Figure 7 Nitrogen concentrations (urea as $\mu\text{g-at N L}^{-1}$) during the growth of *Amphidinium carterae* grown on NH_4^+ , NO_3^- , and urea under continuous light plotted against a) elapsed time and b) elapsed time since re-addition of NH_4^+ , NO_3^- , and urea at $t=0$ to previously N-starved cultures for 75 h. Thus (b) is an expanded time version of the N concentrations during the re-addition phase shown in (a). Cultures were N-starved between 119 and 193.5 h and then 29 $\mu\text{M NH}_4^+$, 30 $\mu\text{M NO}_3^-$, and 30 $\mu\text{g-at N L}^{-1}$ urea were added at 193.5 h. Bars represent ± 1 S.D. ($n=2-3$). Error bars are smaller than symbols where not visible.41
- Figure 8 N uptake rates of triplicate, batch cultures of *Amphidinium carterae* grown on NH_4^+ , NO_3^- , and urea and under continuous light plotted against a) average time between sampling and b) average time between sampling since re-addition of NH_4^+ , NO_3^- , and urea at $t=0$ to previously N-starved cultures for 75 h. (b) is an expanded version of the re-addition phase of (a). Cultures were N-starved between 119 and 193.5 h and NH_4^+ , NO_3^- , and urea were added at 193.5 h. Bars represent ± 1 S.D. ($n=2-3$). Error bars are smaller than symbols where not visible.43
- Figure 9 Relative N preference of NH_4^+ and urea relative to NO_3^- for *Amphidinium carterae* during the period I before (■) and after (□) N starvation. The relative preference for urea is fixed at 1, both before and after N starvation.45
- Figure 10 Relative N preference of urea relative to NO_3^- for *Amphidinium carterae* during the period II before (■) and after (□) N starvation. The relative preference for urea is fixed at 1, both before and after N starvation.45
- Figure 11 Growth of *Heterosigma carterae* grown on NH_4^+ , NO_3^- , and urea under continuous light. Log plot of *in vivo* fluorescence versus time. Bars represent ± 1 S.D. ($n=2-3$). Error bars are smaller than symbols where not visible.47
- Figure 12 Nitrogen concentrations (urea as $\mu\text{g-at N L}^{-1}$) during the growth of *Heterosigma carterae* grown on NH_4^+ , NO_3^- , and urea under continuous light plotted against a) elapsed time and b) elapsed time since re-addition of NH_4^+ , NO_3^- , and urea at $t=0$ to previously N-starved culture for 0 h. Thus (b) is an expanded time version of the N concentrations during the re-addition phase shown in (a). 31 $\mu\text{M NH}_4^+$, 41 $\mu\text{M NO}_3^-$, and 38 $\mu\text{g-at N L}^{-1}$ were added at 175 h. Bars represent ± 1 S.D. ($n=2-3$). Error bars are smaller than symbols where not visible.48

- Figure 13 N uptake rates of triplicate, batch cultures of *Heterosigma carterae* grown on NH_4^+ , NO_3^- , and urea and under continuous light plotted against a) average time between sampling and b) average time between sampling since re-addition of NH_4^+ , NO_3^- , and urea at $t=0$ to previously N-starved cultures for 0 h. (b) is an expanded version of the re-addition phase of (a). NH_4^+ , NO_3^- , and urea were added at 175 h. Bars represent ± 1 S.D. ($n=2-3$). Error bars are smaller than symbols where not visible.51
- Figure 14 Relative N preference of NH_4^+ and NO_3^- relative to urea for *Heterosigma carterae* during the period I before (■) and after (□) N starvation. The relative preference for NO_3^- is fixed at 1, both before and after N starvation.53
- Figure 15 Relative N preference of urea relative to NO_3^- for *Heterosigma carterae* during the period II before and after N starvation. The relative preference for urea is fixed at 1, both before (■) and after (□) N starvation.55
- Figure 16 Growth of *Heterosigma carterae* grown on NO_3^- under continuous light. Log plot of *in vivo* fluorescence versus time. Bars represent ± 1 S.D. ($n=2-3$). Error bars are smaller than symbols where not visible.56
- Figure 17 NO_3^- concentrations during the growth of *Heterosigma carterae* grown on NO_3^- under continuous light plotted against a) elapsed time and b) elapsed time since re-addition of NO_3^- at $t=0$. Thus (b) is an expanded time version of the N concentrations during the re-addition phase shown in (a). Cultures were NO_3^- -starved between 64 and 116 h and then 88 μM NO_3^- was added at 116 h. Bars represent ± 1 S.D. ($n=2-3$). Error bars are smaller than symbols where not visible.57
- Figure 18 NO_3^- uptake rates of triplicate, batch cultures of *Heterosigma carterae* grown on NO_3^- and under continuous light plotted against a) average time between sampling and b) average time between sampling since re-addition of NO_3^- at $t=0$ to previously N-starved cultures for 51.5 h. (b) is an expanded version of the re-addition phase of (a). Cultures were NO_3^- starved between 64 and 115 h and then NO_3^- was added at 116 h. Bars represent ± 1 S.D. ($n=2-3$). Error bars are smaller than symbols where not visible.59
- Figure 19 Growth of *Heterosigma carterae* grown on NO_3^- and under a 14:10 L:D cycle. Log plot of *in vivo* fluorescence versus time. Stippled

- areas indicate dark periods. Bars represent ± 1 S.D. ($n=2-3$). Error bars are smaller than symbols where not visible.60
- Figure 20 NO_3^- concentrations during the growth of *Heterosigma carterae* on NO_3^- and under a 14:10 L:D cycle plotted against a) elapsed time and b) elapsed time after the re-addition of $73 \mu\text{M}$ NO_3^- at 215 h to N-starved *Heterosigma carterae* for 96 h. Thus (b) is an expanded time version of the N concentrations during the re-addition phase shown in (a). Cultures were NO_3^- -starved from 119 h to 215 h. Stippled areas indicate dark periods. Bars represent ± 1 S.D. ($n=2-3$). Error bars are smaller than symbols where not visible.62
- Figure 21 NO_3^- uptake rates of triplicate, batch cultures of *Heterosigma carterae* grown on NO_3^- and under a 14:10 L:D cycle plotted against a) average time between sampling and b) average time between sampling since re-addition of NO_3^- at $t=0$ to previously N-starved cultures for 96 h. (b) is an expanded version of the re-addition phase of (a). Cultures were NO_3^- starved between 119 and 215 h and then NO_3^- was added at 215 h. Stippled areas indicate dark periods. Bars represent ± 1 S.D. ($n=2-3$). Error bars are smaller than symbols where not visible.64
- Figure 22 Growth of *Heterosigma carterae* on NH_4^+ under continuous light, culture 1. Log plot of *in vivo* fluorescence versus time.66
- Figure 23 NH_4^+ concentrations during the growth of *Heterosigma carterae* grown on NH_4^+ under continuous light, culture 1, plotted against a) elapsed time and b) after the re-addition of NH_4^+ at $t=0$ to N-starved cells for 33 h. Thus (b) is an expanded time version of the N concentrations during the re-addition phase shown in (a). Culture was NH_4^+ -starved between 65 and 98 h and then $77 \mu\text{M}$ NH_4^+ was added at 98 h.67
- Figure 24 NH_4^+ uptake rates of a batch culture of *Heterosigma carterae* grown on NH_4^+ and under continuous light, culture 1, plotted against a) average time between sampling and b) average time between sampling since re-addition of NH_4^+ at $t=0$ to previously N-starved culture for 33 h. (b) is an expanded version of the re-addition phase of (a). Culture was NH_4^+ -starved between 65 and 98 h and then NH_4^+ was added 98 h.68
- Figure 25 Growth of *Heterosigma carterae* on NH_4^+ under continuous light, cultures 2 and 3. Log plot of *in vivo* fluorescence versus time.

- Bars represent ± 1 S.D. ($n=1-2$). Error bars are smaller than symbols where not visible.70
- Figure 26 NH_4^+ concentrations during the growth of *Heterosigma carterae* grown on NH_4^+ under continuous light, cultures 2 and 3, plotted against a) elapsed time and b) elapsed time after the re-addition of NH_4^+ at $t=0$, to N-starved cells for 18 h. Thus (b) is an expanded time version of the N concentrations during the re-addition phase shown in (a). Cultures were NH_4^+ -starved between 88 and 106 h and then $74 \mu\text{M}$ NH_4^+ was added at 106 h. Bars represent ± 1 S.D. ($n=1-2$). Error bars are smaller than symbols where not visible.71
- Figure 27 NH_4^+ uptake rates of duplicate, cultures of *Heterosigma carterae* grown on NH_4^+ and under continuous light, culture 2+3, plotted against a) average time between sampling and b) average time between sampling since re-addition of NH_4^+ at $t=0$ to previously N-starved for 18 h. (b) is an expanded version of the re-addition phase of (a). Cultures were NH_4^+ -starved between 88 and 106 h and then NH_4^+ was added at 106 h. Bars represent ± 1 S.D. ($n=1-2$). Error bars are smaller than symbols where not visible.73
- Figure 28 Growth of *Heterosigma carterae* grown on various N sources and light conditions. Log plot of *in vivo* fluorescence versus time. ...78
- Figure 29 Time series of $[\text{NO}_3^-]$ (●), $[\text{NH}_4^+]$ (○) and [urea] (▼) during the growth of *Prorocentrum micans* grown on NO_3^- , NH_4^+ , and urea under continuous light. Culture was N-starved between 105 and 186.5 h and then $36.6 \mu\text{g-at N L}^{-1}$ NH_4^+ , $48.7 \mu\text{g-at N L}^{-1}$ NO_3^- , and $49.4 \mu\text{g-at N L}^{-1}$ urea were added at 186.5 h. The best fits for the concentrations were determined by the dissolved N data using the equation: $y = a*(1-\text{EXP}(b*(x-c)))$ where a is an initial N concentration, b is a co-efficient number, and c is the time when N reached 0, and are indicated by the solid lines.102
- Figure 30 Time series of PN (▲) and $\delta^{15}\text{N}_{\text{PN}}$ (●) during the growth of *Prorocentrum micans* grown on NO_3^- , NH_4^+ , and urea under continuous light. Culture was N-starved between 105 and 186.5 h and then $36.6 \mu\text{g-at N L}^{-1}$ NH_4^+ , $48.7 \mu\text{g-at N L}^{-1}$ NO_3^- , and $49.4 \mu\text{g-at N L}^{-1}$ urea were added at 186.5 h. The $\delta^{15}\text{N}_{\text{PN}}$ as predicted by the multiple N source uptake model is shown by the solid line. The 3 dotted lines indicate times when $[\text{NH}_4^+]$, $[\text{NO}_3^-]$ and [urea] fits, determined by the dissolved N data to the concentration data in Fig. 29, reached 0, respectively.103

- Figure 31 Time series of $[\text{NO}_3^-]$ (●), $[\text{NH}_4^+]$ (○) and [urea] (▼) during the growth of *Amphidinium carterae* grown on NO_3^- , NH_4^+ , and urea under continuous light. Culture was N-starved between 119 and 193.5 h and then $29.6 \mu\text{g-at N L}^{-1} \text{NH}_4^+$, $34.3 \mu\text{g-at N L}^{-1} \text{NO}_3^-$, and $31.2 \mu\text{g-at N L}^{-1}$ urea were added at 193.5 h. The best fits for the concentrations were determined by the dissolved N data using the equation: $y = a*(1-\text{EXP}(b*(x-c)))$ where a is an initial N concentration, b is a co-efficient number, and c is the time when N reached 0, and are indicated by the solid lines. 107
- Figure 32 Time series of PN (▲) and $\delta^{15}\text{N}_{\text{PN}}$ (●) during the growth of *Amphidinium carterae* grown on NO_3^- , NH_4^+ , and urea under continuous light. Culture was N-starved between 119 and 193.5 h and then $29.6 \mu\text{g-at N L}^{-1} \text{NH}_4^+$, $34.3 \mu\text{g-at N L}^{-1} \text{NO}_3^-$, and $31.2 \mu\text{g-at N L}^{-1}$ urea were added at 193.5 h. The $\delta^{15}\text{N}_{\text{PN}}$ as predicted by the multiple N source uptake model is shown by the solid line. The 3 dotted lines indicate times when $[\text{NH}_4^+]$, $[\text{NO}_3^-]$ and [urea] fits, determined by the dissolved N data to the concentration data in Fig. 31, reached 0, respectively. 108
- Figure 33 Time series of $[\text{NO}_3^-]$ (●), $[\text{NH}_4^+]$ (○) and [urea] (▼) during the growth of *Heterosigma carterae* grown on NO_3^- , NH_4^+ , and urea under continuous light. Culture was added $32.2 \mu\text{g-at N L}^{-1} \text{NH}_4^+$, $41.2 \mu\text{g-at N L}^{-1} \text{NO}_3^-$, and $37 \mu\text{g-at N L}^{-1}$ urea at 175 h. The best fits for the concentrations were determined by the dissolved N data using the equation: $y = a*(1-\text{EXP}(b*(x-c)))$ where a is an initial N concentration, b is a co-efficient number, and c is the time when N reached 0, and are indicated by the solid lines. 110
- Figure 34 Time series of PN (▲) and $\delta^{15}\text{N}_{\text{PN}}$ (●) during the growth of *Heterosigma carterae* grown on NO_3^- , NH_4^+ , and urea under continuous light. Nitrogen additions at 175 h to the culture were $32.2 \mu\text{g-at N L}^{-1} \text{NH}_4^+$, $41.2 \mu\text{g-at N L}^{-1} \text{NO}_3^-$, and $37 \mu\text{g-at N L}^{-1}$ urea. The $\delta^{15}\text{N}_{\text{PN}}$ as predicted by the multiple N source uptake model is shown by the solid line. The 3 dotted lines indicate times when $[\text{NH}_4^+]$, $[\text{NO}_3^-]$ and [urea] fits, determined by the dissolved N data to the concentration data in Fig. 33, reached 0, respectively. 111
- Figure 35 Time series of $[\text{NO}_3^-]$ during the growth of *Heterosigma carterae* grown on NO_3^- under continuous light. Culture was N-starved between 64 and 115.5 h and then $85.6 \mu\text{g-at N L}^{-1} \text{NO}_3^-$ was added at 115.5 h. The best fits for the concentrations were determined by the dissolved N data using the equation: $y = a*(1-\text{EXP}(b*(x-c)))$ where a is an initial N concentration, b is a co-

- efficient number, and c is the time when N reached 0, and are indicated by the solid lines.112
- Figure 36 Time series of $PN(\blacktriangle)$ and $\delta^{15}N_{PN}(\bullet)$ during the growth of *Heterosigma carterae* grown on NO_3^- under continuous light. Culture was N-starved between 64 and 115.5 h and then $85.6 \mu\text{g-at N L}^{-1} NO_3^-$ was added at 115.5 h. The $\delta^{15}N_{PN}$ as predicted by the N source uptake model is shown by the solid line. The dotted line indicates times when $[NO_3^-]$ fits, determined by the dissolved N data to the concentration data in Fig. 35, reached 0.113
- Figure 37 Response of the model to changes in a) $\varepsilon(NH_4^+)$, b) $\varepsilon(NO_3^-)$, and c) PN_i in the N-sufficient condition for *Prorocentrum micans* grown on three N sources. The solid line represents the response of the model using the base values indicated in Table 4.116
- Figure 38 Response of the model to changes in $\varepsilon(NH_4^+)$ in the N re-supply phase for *Prorocentrum micans* grown on three N sources. The solid line represents the response of the model using the base variables indicated in Table 4.117
- Figure 39 Response of the model to changes in a) $\varepsilon(NH_4^+)$ and b) $\varepsilon(NO_3^-)$ in the N-sufficient condition for *Amphidinium carterae* grown on three N sources. The solid line represents the response of the model using the base values indicated in Table 4.119
- Figure 40 Response of the model to changes in $\varepsilon(NH_4^+)$ in the N-sufficient condition for *Amphidinium carterae* grown on three N sources. The solid line represents the response of the model using the base values indicated in Table 4.120
- Figure 41 Response of the model to changes in a) $\varepsilon(NH_4^+)$ and b) $\varepsilon(NO_3^-)$ in the N re-supply phase for *Heterosigma carterae* grown on three N sources. The solid lines represent the response of the model using the base variables indicated in Table 4.121
- Figure 42 Response of the model to change in $\varepsilon(NH_4^+)$ in the N re-supply phase for *Heterosigma carterae* grown on three N sources. The solid line represents the response of the model using the base values indicated in Table 4.122
- Figure 43 Response of the model to changes in $\varepsilon(NO_3^-)$ in the N-sufficient condition for *Heterosigma carterae* grown on three N sources. The solid line represents the response of the model using the base values indicated in Table 4.124

Figure 44 Response of the model to changes in $\epsilon(\text{NO}_3^-)$ in the N re-supply phase for *Heterosigma carterae* grown on three N sources. The solid lines represent the response of the model using the base variables indicated in Table 4. 125

ACKNOWLEDGMENTS

I would like to express my sincere gratitude to Dr. Paul J. Harrison for all his help in providing direction, encouragement, helpful advice, laboratory space, and funds for the experiments, as well as in reviewing this thesis. I would also like to thank Dr. Nathalie Waser for her direction on isotope fractionation analysis and helpful comments on this thesis. I would like to also thank Dr. F. J. R. Taylor for giving me a chance to study phytoplankton, providing cozy laboratory space with nice laboratory mates, such as Tonny Wagey and Juan Saldarriaga, a partial funding, and his comments on the thesis. I appreciate Dr. Al Lewis for helping me out from several emergencies and providing attention. Finally, I would like to thank Allen Milligan, Mingxing Guo, and Zhiming Yu for answering each of my questions in the laboratory and Bente Nielsen and Joe Needoba for helping with the isotope analysis.

INTRODUCTION

overview

Nitrogen (N) limitation determines the amount of primary production by phytoplankton in most coastal (Ryther & Dunstan 1971) and oceanic waters (Goldman *et al.* 1979). This has been expressed in terms of Liebig's "law of the minimum". The element in the lowest concentration relative to the other elemental requirements limits the production (Liebig 1840) and N is considered the principle limiting nutrient in the ocean. There are two kinds of primary production which are characterized by the form of N used. One is new production which is supported by allochthonous N sources such as NO_3^- which is mixed into surface waters from the NO_3^- -rich deep ocean, N_2 -fixation, riverine inflow and precipitation. Allochthonous N is defined as the encounter to the system for the first time. The other form of primary production is regenerated production. NH_4^+ , urea, and amino acids are regenerated N sources. These N sources are released by death, cell lysis, grazing, viral attack (Suttle *et al.* 1990), and animal excretion. The concentration of regenerated N in coastal regions fluctuates. The maximum natural concentration is $\sim 5 \mu\text{M}$ and concentrations $< 0.5 \mu\text{M}$ are frequently found (McCarthy 1980; Sharp 1983; Antia *et al.* 1991).

Among new and regenerated N, NO_3^- , NH_4^+ and urea ($\text{CO}(\text{NH}_2)_2$) are the three most abundant forms of N in the ocean that are used by phytoplankton. Marine phytoplankton in the nutrient-depleted layer of the ocean may experience rapid N supply by upwelling of NO_3^- (Walsh *et al.* 1978) or animal excretion of NH_4^+ and possibly urea (Dugdale 1967).

Ammonium (NH_4^+)

Atmospheric precipitation of NH_4^+ is important for N supply into the ocean (Buijsman *et al.* 1991). NH_4^+ , however, can be released by biological activities such as zooplankton excretion, bacterial decomposition, and schooling fish. Regenerated NH_4^+ contributed a significant portion of the primary production in the study of the spring bloom in the New York Bight (Conway & Whitledge 1979). In this study NH_4^+ utilization as a percentage of NH_4^+ plus NO_3^- utilization was 59% for the inshore areas and 70% at the shelf-break. The shelf-break had less N compared to the inshore water and primary production depended more on regenerated N.

Nitrate (NO_3^-)

NO_3^- is the most abundant form of N in coastal regions (Sharp 1983) and the most important N source in a highly productive ocean (Harrison *et al.* 1987). The abundance of NO_3^- shows seasonal trends. Surface NO_3^- concentrations of coastal waters increase during winter ($> 20 \mu\text{g-at N L}^{-1}$) and gradually decrease due to the utilization by phytoplankton during the spring bloom.

Urea ($\text{CO}(\text{NH}_2)_2$)

Urea contains two atoms of N and therefore $1 \mu\text{M urea} = 2 \mu\text{g-at L}^{-1}$ or $2 \mu\text{mol L}^{-1}$. The concentration of urea also largely depends on biological processes such as excretion by marine organisms, especially fish. Atmospheric precipitation also supplies urea to the marine system (Timperley *et al.* 1985).

Turley (1986) reported the highest urea concentration ($23 \mu\text{M}$) in the southern German Bight. Eutrophicated waters periodically exceed $3 \mu\text{M}$ urea. (Remsen 1971; Remsen *et al.* 1972; Berman 1974; Steinmann 1976; Satoh & Hanya 1981; Ignatiades 1986).

Physiology

There are two steps in the utilization of N by phytoplankton. The first step is uptake which is the actual transport of the particular form of N across the cell membrane. The second step is assimilation. In the second process, NO_3^- , NO_2^- , and urea are reduced to NH_4^+ and are incorporated into amino acids during cellular metabolic processes (Lobban *et al.* 1985). The ambient N concentration, the relative abundance of different N forms, the physiological status of the phytoplankton, the availability of light, and temperature influence both uptake and assimilation of N by phytoplankton.

Uptake

NH_4^+ can be taken up by facilitated diffusion with the indirect expenditure of cellular metabolic energy. This diffusion needs carriers to bind NH_4^+ at the outer membrane and assist the passage across the membrane to the inner surface. Ion channels which are macromolecular pores that traverse the cell membrane, have been invoked to explain the high transport rates that occur down an electrochemical-potential gradient (Hedrich & Schroeder 1989). NH_4^+ may also be taken up by active transport processes.

NO_3^- is actively taken up and hence this process requires energy.

Carriers move NO_3^- across the membrane against an electrochemical potential gradient. External concentrations of NO_3^- are in the micromolar NO_3^- range while intracellular concentrations are in the millimolar range. This large concentration difference between the inside and outside of the cell makes passive diffusion along an electrochemical gradient less important (Reed 1990). Active transport typically is much slower than channel-mediated transport because it is possible to transport only $10^3 - 10^5$ ions per second by active transport. In contrast, channels may allow 10^6 ions per second (Lobban & Harrison 1994).

Urea is an uncharged molecule and therefore it diffuses through the cell membrane. However, phytoplankton have an active transport system and are capable of accumulating urea intracellularly. Light stimulates urea uptake and proton ionophores inhibit the uptake of urea. Thus, urea transport by phytoplankton requires ATP. Urea uptake does not directly require light (Syrett 1981). However, the production of ATP for membrane transport (Falkowski 1975) and the assimilation of urea occur during photosynthesis and this makes it appear that urea uptake depends on light.

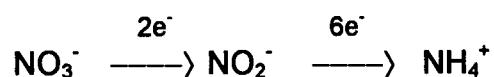
Light intensity and N uptake show a hyperbolic relationship with N uptake showing saturation at high light intensities (Eppley & Rogers 1970). In the ocean, light availability depends on the season, latitude, day/night cycle, and attenuation with depth. Phytoplankton in the ocean experience various light intensities in a daily periodic fashion. Malone *et al.* (1975) reported the periodicity of N uptake by various species in culture. The maximum N uptake

occurs during the day and the minimum uptake occurs at night (MacIsaac 1978; Fisher *et al.* 1982; Cochlan *et al.* 1991).

Assimilation

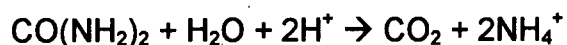
NH_4^+ can be directly assimilated into amino acids, usually as glutamine. Incorporation of NH_4^+ into amino acids occurs in the chloroplast. Glutamate dehydrogenase (GDH) which has a low affinity for NH_4^+ , is used when the internal pool of NH_4^+ is high. On the other hand, glutamate synthetase (GS) has a high affinity for NH_4^+ and is used when the internal pool has low NH_4^+ concentration. Glutamine oxoglutarate aminotransferase (GDF) follows the reaction by GS. The control of NH_4^+ assimilation is often assumed to be rate-limiting for N incorporation (Syrett 1981).

NO_3^- must first be reduced to NO_2^- by nitrate reductase using NADH or NAD(P)H as the electron donor. Nitrate reductase has been isolated and purified from many microalgae (Syrett 1981; Tischner *et al.* 1989; Solomonson & Barber 1990). The electron donor is usually NADH. However, NAD(P)H must be the electron donor in some phytoplankton (Lee 1980; Syrett 1981; Solomon & Barber 1990). Secondly, the product, NO_2^- , needs to be reduced to NH_4^+ by nitrite reductase with the help of ferredoxin as the electron donor. These steps follow the equation below:



Therefore, growth on NO_3^- requires extra energy. In addition to the high energy cost during the assimilation step, the energy cost for NO_3^- uptake is higher than that for NH_4^+ (Falkowski 1975; Turpin & Bruce 1990). Since cells grown on NO_3^- require an extra cost in reduction, the demand is increased for reducing power relative to ATP (Turpin & Bruce 1990). Both a higher photosynthetic quotient (Cleveland *et al.* 1989), and lower growth rate (Paasche 1971; Ward & Wetzel 1980; Rhee & Lederman 1983) occur. Several studies, however, reported that growth rates on NO_3^- were not significantly different from those on NH_4^+ (Conover 1975; Syrett 1981; Thompson *et al.* 1989). Phytoplankton grown on NO_3^- might compensate for their higher reductant requirements by adjustments in their biochemical composition, rather than by reducing their growth rates (Thompson *et al.* 1989). The reason why uptake of NO_3^- is affected by photoperiod is due to the diel periodicity in activity and synthesis of the nitrate reductase enzyme (Syrett 1981). NO_3^- -sufficient cells showed more pronounced diel periodicity of NO_3^- uptake than N-limited cells.

When urea is transported into the cell, it is broken down enzymatically using urease or urea carboxylase and converted to NH_4^+ as the final N product (Syrett 1981, 1988). The equation for this reaction is:



This assimilation requires energy. In terms of reductant, urea assimilation is similar to NH_4^+ .

Kinetic parameters

A hyperbolic function of the concentration of the limiting nutrient (similar to the Michaelis-Menten equation for enzyme kinetics) expresses the rate of steady-state N uptake by phytoplankton (Eppley & Coatsworth 1968). K_s is the half-saturation constant that represents the substrate concentration at which the uptake rate is half its maximum. Spatial and seasonal abundance of a particular species partially depends on the value of these N uptake parameters (MacIsaac & Dugdale 1972). For example, species that possess a lower K_s have an advantage because they take up N faster than other species at low N concentrations. Frequently the uptake rate varies with time in the case of NH_4^+ limitation (Probyn & Chapman 1982; Rosenberg *et al.* 1984; Thomas & Harrison 1987) and NO_3^- limitation (Thomas & Harrison 1987). A short incubation period can solve these problems by estimating the maximal uptake rate (Harrison *et al.* 1989).

Starvation and rapid uptake

Rapid uptake of NH_4^+ by N-starved phytoplankton is an example of the effect of cellular physiological state on N uptake (Glibert & Goldman 1981). NH_4^+ uptake was facilitated by starvation and showed much more rapid uptake of NH_4^+ by N-starved phytoplankton than by the N-replete phytoplankton (Suttle & Harrison 1988). Rapid uptake of NO_3^- , however, did not consistently occur after N starvation (Price & Harrison 1988). Increased urea uptake rates were also not observed after N starvation (Bekheet & Syrett 1979; Price & Harrison 1988).

Generally, the effect of N starvation causes phytoplankton to take up NH_4^+ at rates in excess of those rates required to meet their ordinary N demands during balanced growth.

Ecology

Culture and field studies exhibit the uptake interactions between the various forms of N (Antia *et al.* 1991). The utilization of different forms might affect algal growth, species composition, and species succession (Harrison & Turpin 1982). This is because limiting nutrients have selective roles due to the nutrient uptake kinetics of the different species. For example, species that are capable of rapid uptake of a transient supply of NH_4^+ and urea (in a patch) would have an advantage because such cells need only to be exposed to an intermittent pulse of NH_4^+ in order to acquire their daily ration of N for growth (McCarthy & Goldman 1979).

Interactions

1) NH_4^+ and NO_3^-

The interaction of NO_3^- and NH_4^+ in uptake has been well studied. Commonly, NH_4^+ inhibits NO_3^- uptake due to its preferential uptake over NO_3^- as a N source. *Chlorella vulgaris* that was grown with NH_4^+ and NO_3^- ceased NO_3^- assimilation after the addition of NH_4^+ (Syrett & Morris 1963). These cells started to take up NO_3^- immediately after NH_4^+ was used up in the medium. *Chlamydomonas reinhardtii* also showed a similar phenomenon (Thacker & Syrett

1972a,b; Florencio & Vega 1983). Not only phytoplankton, but also macroalgae such as *Gracilaria foliifera* and *Neogardhiella baileyi* preferred NH_4^+ over NO_3^- as a N source (D'Elia & deBoer 1978). The presence of NO_3^- did not decrease NH_4^+ uptake by these macroalgae.

The NH_4^+ concentration affected the degree of inhibition in NO_3^- uptake in the blue-green alga *Anabaena cylindrica* (Ohmori *et al.* 1977). In a lab study with *Dunaliella tertiolecta* and in a field investigation with *Skeletonema costatum*, NH_4^+ inhibited NO_3^- uptake (Conway 1977). This inhibition of NO_3^- uptake usually occurred above a certain range of NH_4^+ concentration. Oyster-pond microalgae, however, showed a long-term elevated NO_3^- uptake even in the presence of high NH_4^+ concentration (Collos *et al.* 1989). The maximum NO_3^- uptake by these microalgae occurred when NH_4^+ concentrations ranged between 10 and 30 μM and this maximum coincided with the maximum NH_4^+ uptake rate or with the start of a decrease in NH_4^+ uptake rate. NO_3^- uptake, then decreased and reached a secondary maximum rate again at low NH_4^+ concentrations.

2) Effect of the starvation on interaction between NH_4^+ and NO_3^-

N-deficient *Skeletonema costatum* showed strongly inhibited carrier-mediated NO_3^- uptake without affecting diffusion (Serra *et al.* 1978). The N-deficient batch culture of the same species enhanced NO_3^- uptake rate and accumulated a large NO_3^- internal pool after the addition of a mixture of NH_4^+ and NO_3^- (DeManche & Curl 1979). NO_3^- uptake ceased following this initial NO_3^- uptake and NO_3^- assimilation was inhibited until the ambient NH_4^+ was

taken up. At this point, NO_3^- uptake and assimilation commenced. In contrast, in the kelp, *Laminaria groenlandica*, NO_3^- uptake was suppressed for 30 min after NO_3^- and NH_4^+ were added back together to the N-starved macroalga (Harrison *et al.* 1986).

3) Effect of light limitation on the interaction between NH_4^+ and NO_3^-

Syrett and Morris (1963) used two different irradiances in investigating the preference of NO_3^- and NH_4^+ . The pattern of the inhibition of NO_3^- uptake by NH_4^+ , however, did not show any difference between high and low irradiance. However, the higher irradiance promoted the process because NH_4^+ disappeared faster and NO_3^- uptake commenced earlier in the time course.

4) Interactions between NH_4^+ and urea

The first study of the interaction between inorganic N (NH_4^+ and NO_3^-) and organic N (urea) was done by Lui and Roels (1970). NH_4^+ repressed the rate of urea uptake by the chrysomonad *Ochromonas malhamensis* in their study. Later, Horrigan and McCarthy (1982) showed that N-replete *Thalassiosira pseudonana* did not decrease urea uptake during the interaction with $10\ \mu\text{M}$ NH_4^+ for the first minute. In addition, urea uptake increased 5 min after these cells were exposed to NH_4^+ . *Skeletonema costatum*, however, showed urea uptake inhibition by NH_4^+ (Horrigan & McCarthy 1982). This inhibition required 30 min exposure to NH_4^+ . According to another report by Lund (1987), inhibition of urea uptake occurred immediately after exposure to NH_4^+ . Both *Thalassiosira pseudonana*

and *Skeletonema costatum* showed increased urea uptake inhibition by NH_4^+ under N-deplete conditions.

The extent of inhibition of urea uptake may be a function of NH_4^+ concentration, the N status of the cells and the species (Molloy & Syrett 1988a; 1988b). NH_4^+ at 350 μM strongly inhibited urea uptake by *Chlorella emersonii*, but not by *Phaeodactylum tricornutum*. Urea uptake at $\text{NH}_4^+ > 500 \mu\text{M}$ was strongly inhibited, particularly for *Phaeodactylum tricornutum* that was N-starved for 48 h. In contrast, 4 mM NH_4^+ was sufficient to inhibit urea uptake if the cells were N-replete. The addition of urea also depressed NH_4^+ uptake by *Phaeodactylum tricornutum* (Molloy & Syrett 1988a). The uptake rate of urea-grown cells decreased to near zero when such cells were cultured and resuspended in 5 mM NH_4^+ for 24 h (Rees & Syrett 1979). Probably, NH_4^+ suppressed the development of the urea uptake mechanism in *Phaeodactylum tricornutum*.

5) Interactions between NO_3^- and urea

Urea inhibited NO_3^- uptake in most experiments. In particular, such inhibition clearly occurred under dark and N-starved conditions (Molloy & Syrett 1988b). Nitrate reductase activity of the diatom, *Cyclotella cryptica* decreased due to the presence of urea (Liu & Hellebust 1974). 1 mM urea inhibited NO_3^- uptake in the prasinophyte *Platymonas* (Ricketts 1988). However, 1 mM of NO_3^- totally inhibited urea uptake (Ricketts 1988). These observations agree with the

general idea that urea suppresses NO_3^- uptake, but at a lower level than NH_4^+ (Grand *et al.* 1967; McCarthy & Eppley 1972).

Interestingly, NO_3^- -sufficient cells showed enhanced uptake rates of both urea and NH_4^+ (Horrigan & McCarthy 1982). Later, however, Price and Harrison (1988) reported that NO_3^- -replete *Thalassiosira pseudonana* did not exhibit an enhanced rate of urea uptake. Lund (1987), however, reported urea did not suppress NO_3^- uptake by *Skeletonema costatum*. On the other hand, NO_3^- suppressed urea uptake by the same species. In general, urea uptake is a constitutive property of phytoplankton growing on NO_3^- as the sole N source.

In the presence of NH_4^+ , NO_3^- , and urea, NH_4^+ are preferentially taken up, followed by NO_3^- and urea (Dugdale & Goering 1967; Paasche & Kristiansen 1982; Levasseur *et al.* 1990). Phytoplankton prefer NH_4^+ (more reduced form) over NO_3^- and urea (more oxidized forms) because NH_4^+ does not require a supply of electrons for reduction in the assimilation process which means less energy is required (Dugdale & Goering 1967; Eppley *et al.* 1973; McCarthy *et al.* 1977).

6) Field study

In a field study of the interactions among NH_4^+ , NO_3^- , and urea, all three N sources were taken up simultaneously in a natural spring phytoplankton assemblage from oyster ponds (Robert & Maestrini 1986). The urea uptake rate in this study, however, increased almost 10-fold with depletion of both NH_4^+ and NO_3^- . Interestingly, algal species composition changed within this assemblage.

Inorganic N (NH_4^+ and NO_3^-) promoted diatoms. On the other hand, urea supported the growth of dinoflagellates. Simultaneous uptake of urea and other N sources by phytoplankton communities were reported in other field studies (McCarthy & Eppley 1972; Price *et al.* 1985).

Isotopic fractionation

N uptake and assimilation by phytoplankton is associated with N isotopic fractionation. The two naturally occurring stable isotopes of N are qualitatively similar in chemical behavior. Their reaction, however, occurs at slightly different rates and generally, ^{14}N reacts more quickly than ^{15}N due to lighter atomic mass. The isotopic composition of the product of a reaction could be affected by that of the substrate even though the difference in reaction rate is small. The product has the same isotopic composition as the original substrate if the reaction is complete. On the other hand, if the reaction is not complete, the resulting product pool is depleted in ^{15}N relative to the original substrate. This is one of the important fractionation processes in the biogeochemical cycle of N in the ocean.

Isotope expression

The relative abundance of the stable isotopes of N is expressed as a ratio. For example, $^{15}\text{N}/^{14}\text{N} = 0.00677$. The isotope ratio of a sample is measured relative to a standard. The δ value expresses this relative difference and is defined as

$$\delta \text{ in } \text{‰} = (R_{\text{sample}} - R_{\text{standard}}) / (R_{\text{standard}}) \times 1000$$

where R is the isotope ratio with the most abundant isotope in the denominator.

Isotope fractionations

Variations in relative isotope abundance are derived from the preferential reaction of one of the isotopes. Fractionation occurs during physicochemical processes. The fractionation factor (α) expresses the degree of segregation of one isotope as a result of a particular process and α is defined as:

$$\alpha = R_{\text{products}} / R_{\text{reactants}}$$

This equation can be expressed as:

$$(\alpha - 1) 1000 \approx \delta_{\text{products}} - \delta_{\text{reactants}}$$

and α is dependent on the environmental conditions.

The isotopic composition of the product varies as a result of the extent of reaction. This process is referred to as Rayleigh distillation. The effect of Rayleigh distillation on the isotopic composition of the remaining reactant is expressed by $R_f/R_0 = F^{(\alpha-1)}$ where f is the fraction of remaining reactant. R_f is the value of the reactant at a particular f. R_0 refers to the value when f = 1, which indicates any reactant that is not removed.

ϵ (i.e. the per mil enrichment factor of the substrate relative to the product) is typically ≥ 0 and expressed as:

$$\epsilon = (\alpha - 1) \times 1000$$

Rayleigh equation (Mariotti *et al.* 1981) provides the magnitude of fractionation for a single-step, unidirectional reaction:

$$\delta^{15}\text{N}_{\text{product}} = \delta^{15}\text{N}_{\text{substrate, } t=0} - \epsilon^* - f/(1 - f) * \ln f$$

A positive ϵ indicates that the light isotope accumulates more quickly than the heavy one.

Montoya and McCarthy (1995) reported interesting results in which four flagellates, such as *Isochrysis galbana*, *Pavlova lutheri*, *Dunaliella tertiolecta*, and *Chroomonas salina* showed a lower fractionation factor (1 - 3‰) for NO_3^- uptake and diatoms such as *Skeletonema costatum* and *Thalassiosira weissflogii* had higher fractionation factors (9 - 12‰). These authors suggested that the mobility of flagellates might result in a smaller diffusion zone around the cell, which would reduce the potential of a fractionating step during the uptake for NO_3^- across the outer cell membrane.

Nitrogen isotope fractionation by phytoplankton

Recently the use of natural stable isotopes of N has provided a new way to examine the relationships between N sources and primary production (Francois *et al.* 1992; Calvert *et al.* 1992; Farrell *et al.* 1995). The isotope fractionation in various oceanic regimes can differ in terms of N availability, N source and species composition. The sedimentary $^{15}\text{N}/^{14}\text{N}$ ratio underlying nutrient-rich oceanic regimes can be used as a tracer of past relative NO_3^- utilization and under certain assumptions, of past productivity (Calvert *et al.* 1992; Farrell *et al.* 1995). Low particulate $^{15}\text{N}/^{14}\text{N}$ ratios of bulk sedimentary

organic matter and NO_3^- -rich waters and vice versa showed correspondence (Francois *et al.* 1992; Altabet & Francois 1994; Farrell *et al.* 1995). This correspondence results from the isotopic fractionation during the incorporation of NO_3^- by phytoplankton. However, the factors which control fractionation by phytoplankton require further investigation (Goericke *et al.* 1994).

The isotopic fractionation associated with the uptake of NO_3^- , NO_2^- , and NH_4^+ has been studied in the laboratory (Wada & Hattori 1978; Wada 1980; Montoya & McCarthy 1995; Pennock *et al.* 1996). The degree of isotopic fractionation during N uptake by the diatom *Phaeodactylum tricornutum* clearly depended on the culture conditions (Wada & Hattori 1978). The isotope fractionation factor for NO_3^- uptake by light-limited *Phaeodactylum tricornutum* was inversely related to the specific growth rate of the cells (Wada & Hattori 1978). The same results were obtained by Wada (1980) in the study of fractionation factors for NH_4^+ uptake by the diatom *Chaetoceros* sp. Field studies on fractionation factors for the uptake of NH_4^+ and NO_3^- by phytoplankton agreed with those from culture studies (Altabet & McCarthy 1985; Cifuentes *et al.* 1989; Montoya *et al.* 1991). The isotopic fractionation factor shows species differences. The diatom, *Thalassiosira weissflogii* exhibited a decline in the magnitude of the isotopic fraction factor for NO_3^- uptake with growth rate (Montoya & McCarthy 1995). Other tested species did not vary consistently with growth rate. These results suggest that the net isotopic fractionation during growth on NO_3^- is insensitive to growth rate. These authors concluded that the net isotopic fractionation may vary with photon flux density, which is supported

by the earlier studies by Wada (1980). Recently, Pennock *et al.* (1996) reported that fractionation was independent of the NO_3^- concentration. The NH_4^+ -grown diatoms, however, showed a dependency on the NH_4^+ concentration and fractionation increased as the NH_4^+ concentration increased.

N utilization by dinoflagellates and flagellates

Like diatoms, dinoflagellates can use NH_4^+ , NO_3^- , and urea. As in other phytoplankton, NO_3^- and urea must be converted to NH_4^+ before incorporation into amino acids (Parsons & Harrison 1983). Dinoflagellates can store NO_3^- internally. Internal concentrations of inorganic N were 1.8 mM NO_3^- and 8.2 mM NH_4^+ in NO_3^- and NH_4^+ -grown *Amphidinium carterae* (Dortch *et al.* 1984). When the same species was grown on NH_4^+ , the internal pool was 92 mM.

The activity of nitrate reductase depends on the presence of NO_3^- (Dortch & Maske 1982). Hersey and Swift (1976) reported the highest activity of nitrate reductase in *Amphidinium carterae* was twice as high at mid-day as at night. Some dinoflagellates did not exhibit this difference in laboratory and field studies (Packard & Blasco 1974; Eppley & Harrison 1975; Harrison 1976).

Some dinoflagellates and flagellates migrate vertically downward to take up NO_3^- at night below the nutricline and upward during the day for photosynthesis. These species possess high dark respiration activity that may account for this uptake activity. In addition, these cells used NADH (predominantly respiratory) rather than NADPH (chiefly from photosynthesis) for reduction of NO_3^- (Eppley *et al.* 1969a). Nitrate reductase activity was less

under low light condition than under high light condition (MacIsaac 1978). The same authors reported little or no rhythmicity of nitrate reductase activity. However, migrating species such as *Gymnodinium sanguineum* (Dortch & Maske 1982) and *Gonyaulax polyedra* (Eppley *et al.* 1969b) did take up and reduce NO_3^- in low light or darkness.

Dinoflagellates possess both enzyme pathways, GDH and GS/GOGAT, for NH_4^+ incorporation. *Amphidinium carterae*, however, exhibited no GDH (Turpin & Harrison 1978). Such species might have an advantage in an NH_4^+ -limited environment because GS has a higher affinity for NH_4^+ than GDH (Falkowski & Rivkin 1976).

The species studied

1) *Amphidinium carterae*

Amphidinium carterae Hulburt is a temperate naked marine dinoflagellate which occurs in shallow waters (Hulburt 1957). The average cell volume of *Amphidinium carterae* is $152 \mu\text{m}^3$ (Needoba 1995). A growth rate of 0.76 d^{-1} was reported for this species grown under a 14:10 L:D cycle at 20°C when $50 \mu\text{M}$ NH_4^+ was given to the culture at the beginning of the light period (Wheeler *et al.* 1983.) Some species of the genus *Amphidinium* have been associated with red tides and high concentrations have been reported to discolor sands in subtidal areas (Martin 1929; Herdman 1924a,b). Halstead (1965) described this species as a toxic dinoflagellate. Cells of *Amphidinium carterae* are toxic to fish and to mice (Thurberg & Sasner 1973). Because this toxin inhibited heart activities of

several marine animals, an acetylcholine analog was considered to be present in this organisms (Wangersky & Guillard 1960). Ikawa and Sasner (1975) identified toxins such as acrylycholine and choline o-sulfate in *Amphidinium carterae*. Seasonal fish kills by *Amphidinium carterae* blooms in the Sado estuary in Portugal was suspected (Sampayo 1985). Cyst formation has been reported and cysts remain healthy under a wide range of conditions (Sampayo 1985). Encysted stages survive conditions that would destroy the corresponding motile stage, enabling this species to repeatedly occur every year.

2) *Heterosigma carterae*

The raphidophyte *Heterosigma carterae* is a marine naked unicellular biflagellate phototrophic flagellate (Yamochi 1983; Yokote *et al.* 1985). The classification of this organism was reviewed by Taylor (1992) and renamed from *Heterosigma akashiwo*. The cells were 8 - 25 μm in length and 6 - 15 μm in width (Hara 1990). The growth rate of this species was $< 0.8 \text{ d}^{-1}$ under a 14:10 L:D photoperiod of $160 \mu\text{mol photon m}^{-2} \text{ s}^{-1}$ at 20°C with $100 \mu\text{M}$ of each N source (Hoe Chang & Page 1995). A growth rate of 0.9 d^{-1} was reported when the culture was grown at 18°C on NH_4^+ of 75% ESAW ; NH_4^+ and NO_3^- quotas grown on the same condition ranged from 46 to 47 and from 43.3 to 53 pg cell^{-1} respectively during the exponential phase (Wood & Flynn 1995). *Heterosigma carterae* has been identified as a major causative organism of noxious brown tide blooms in western Canada (Taylor & Haigh 1993), temperate and subtropical embayments in Japan (Yamochi 1989), Korea (Park 1989),

Singapore (Chang 1993), New Zealand (Larsen & Moestrup 1992), England (Larsen & Moestrup 1989), western areas of North America (Tomas 1982) and Bermuda (Tomas 1978). *Heterosigma carterae* possesses toxins that causes massive fish kills such as salmon, yellowtails, sea bass and other fish in cages (Larsen & Moestrup 1989; Hallegraeff 1991; Honjo 1992). Four neurotoxic components of *Heterosigma carterae* were identified (Khan *et al.* 1997).

This species is known to exhibit diel vertical migration (Nagasaki *et al.* 1996). There are several characteristics in the termination process of *Heterosigma carterae* brown tides. The population ceases diel vertical migration in situ and the brown tide disappears suddenly (Nagasaki *et al.* 1996). There is a size transition such that smaller-sized cells dominate toward the end of a simulated brown tide in outdoor tanks (Honjo & Tabata 1985). Lytic activities of the viruses suggest that they can be involved in regulating the bloom dynamics. Virus-like particles (VPLs) from infected *Heterosigma carterae* were isolated and showed strain-specific infection to *Heterosigma carterae* (Nagasaki & Yamaguchi 1997). *Heterosigma carterae* is known to possess benthic stages, including cysts, in the life cycle (Tomas 1978). This stage plays an important role as a seed population for brown tides. Cysts excyst between 10 and 15°C (French *et al.* 1995).

3) *Prorocentrum micans*

Prorocentrum micans is a common constituent of coastal phytoplankton (Reid *et al.* 1985). Non-toxic blooms of *Prorocentrum micans* have been

reported in several coastal waters (Sweeney 1975; Cassie 1981; Avaria 1982; Hata *et al.* 1982; Pybus 1984). The cells were measured 35 - 70 μm in length and 20 - 50 μm in width (Horiguchi 1990). Growth rates of 0.59 - 0.99 d^{-1} were reported for this species grown in f/2 medium under continuous light and 19°C (Costas 1990). The minimum cell quota for N was estimated to be 0.74×10^{-12} mol cell⁻¹ (Wang *et al.* 1996). A distinct phototactic response is characteristic to these species. The accumulation of *Prorocentrum micans* occurs in surface waters (Harvey 1966) and in the upper layer of the water column (Hattori *et al.* 1983). Therefore, they are exposed to a wide range in the intensity and quality of solar radiation. UV-absorbing compounds and yellow xanthophyll, and diadinoxanthin might protect cells by screening them from harmful radiation (Vernet *et al.* 1989). However, these UV absorbing compounds did not prevent photoinhibition and a decrease in chlorophyll per cell and a decrease in activities of Rubisco (Lesser 1996). Diel migration is another important characteristic of this species. Eppley and Harrison (1975) reported the ability to migrate through the thermocline on a diel basis. *Prorocentrum micans* migrated 6.3 m at a speed of 0.85 m h^{-1} (Edler & Olsson 1985). However, at this speed, *Prorocentrum micans* could not cross the halocline to reach NO_3^- -rich water in Laholm Bay in Sweden.

Objectives

The main objectives of this thesis were as follows:

- 1) Determine the impact of N deprivation on preference of three forms of N (NH_4^+ , NO_3^- and urea) by an ecologically important raphidophyte (*Heterosigma carterae*) and two dinoflagellates, *Amphidinium carterae* and *Prorocentrum micans*, isolated from British Columbia coastal waters.
- 2) Investigate responses by N-replete and N-deplete marine phytoplankton on N uptake.
- 3) Determine interactions between NO_3^- uptake and light by *Heterosigma carterae*.
- 4) Predict $\delta^{15}\text{N}$ of particulate N using the multiple N source uptake model by assuming the sum of the Rayleigh contributions associated with the incorporation of each N source.

MATERIALS AND METHODS

Culture methods - *Amphidinium carterae* Hulbert (NPCC 629), *Heterosigma carterae* Hulbert (NPCC 522R), *Prorocentrum micans* Ehrenberg (NPCC33) were obtained from the Northeast Pacific Culture Collection (NPCC), Department of Earth and Ocean Sciences, University of British Columbia. These cultures were grown on artificial seawater (ESAW) following the recipe of Harrison *et al.* (1980) as modified by Price *et al.* (1987). The medium contained a combination of three N sources, NO_3^- , NH_4^+ , and urea, which varied in concentration depending on the experiment (Table 1). The initial NO_3^- and NH_4^+ concentrations in the medium ranged from 64 to 76 μM for Experiment 1 (Exp. 1), 2 (Exp. 2), and 3 (Exp. 3). Urea concentration ranged 14 to 22 μM since a molecule of $\text{CO}(\text{NH}_2)_2$ contains 2 atoms of N. The initial concentration of N for Experiment 4 (Exp. 4) and 5 (Exp. 5) ranged from 78 to 79 and from 77 to 83 μM respectively. The initial NH_4^+ concentration of Experiment 6 (Exp. 6) ranged from 70 to 78 μM . The N:P ratio in the medium was 4:1 to ensure that N was limiting biomass during stationary phase. Bicarbonate (NaHCO_3) was initially 2 mM and was added occasionally to the cultures to prevent C limitation and keep the concentration near 2 mM as in ESAW. The pH of the medium initially ranged from 8.2 to 8.4 and increased to 8.8 to 8.9 during the stationary phase for Exp. 1 and Exp. 4. HCl (6N) was occasionally added to prevent an increase in pH due to carbon uptake during growth for all experiments except Exp. 2. Culture medium was filter sterilized (0.22 μm Millipore) and transferred into 1-liter

Table 1 Summary of experimental conditions. Nitrogen sources, species name, and average N starvation periods of triplicate batch cultures listed.

Experiment	Species	N Source	Light Condition	Starvation Period (h)	Added Back N Source
1	<i>Prorocentrum micans</i>	NH ₄ ⁺ NO ₃ ⁻ urea	continuous light	56	NH ₄ ⁺ NO ₃ ⁻ urea
2	<i>Amphidinium carterae</i>	NH ₄ ⁺ NO ₃ ⁻ urea	continuous light	75	NH ₄ ⁺ NO ₃ ⁻ urea
3	<i>Heterosigma carterae</i>	NH ₄ ⁺ NO ₃ ⁻ urea	continuous light	0	NH ₄ ⁺ NO ₃ ⁻ urea
4	<i>Heterosigma carterae</i>	NO ₃ ⁻	continuous light	51.5	NO ₃ ⁻
5	<i>Heterosigma carterae</i>	NO ₃ ⁻	light:dark cycle light	96	NO ₃ ⁻
6	<i>Heterosigma carterae</i>	NH ₄ ⁺	continuous light	33 18	NH ₄ ⁺ (culture 1) NH ₄ ⁺ (culture 2+3)

sterilized flasks, inoculated with the stock culture and placed in a cold room at $17.0 \pm 0.5^\circ\text{C}$. The cultures were gently stirred by hand twice a day. Autoclaving the flasks and inoculating the culture under the flow hood minimized bacterial contamination. The cultures were continuously illuminated with $170 - 185 \mu\text{mol photons m}^{-2} \text{s}^{-1}$ for all experiments except Exp. 5 which was grown on a 14L:10D cycle.

The cells were acclimated to the N substrate in 1-L flasks for at least 6 days and when samples were first collected, the cells had been growing exponentially for a minimum of about three generations. After inoculation, the cultures were grown first in N-sufficient conditions. Then, they experienced N starvation for 0 - 101 h, and all three N sources were added back into the medium for Exp. 1, 2, and 3 (Table 1). Only NO_3^- was added back for Exp. 4 and 5. Only NH_4^+ was added back for Exp. 6. Trace metals, vitamins, and macronutrients (Si, P, Fe, Bo, Se, and C) were added to the culture after N starvation so that their concentrations were the same as in ESAW. The experiment was designed to contrast a normal exponential growth (i.e. phase 1) and growth following the addition of N after a N starvation period. (i.e. phase 2).

Growth conditions were designed to correspond to eutrophic and oligotrophic and/or temporarily N-depleted surface oceans. Therefore, dinoflagellates and the raphidophyte were grown under both-N-sufficient and N-depleted conditions. The N-sufficient phase simulated bloom conditions and coastal environments where the concentration of dissolved N is large relative to its biological uptake. On the other hand, the N re-supply phase was designed to

simulate oligotrophic oceans where new and regenerated N is supplied to the N-depleted surface ocean during episodic events.

Biomass, particulate N and nutrient analysis - Samples for nutrients and particulate matter were mostly collected at relatively high cell densities at time intervals ranging up to 268.4 h. $\delta^{15}\text{N}$ analysis required a minimum of 1.5 $\mu\text{mol N}$. The growth rate, μ , was calculated from the following relationship:

$$\mu = \ln (F2/F1) / (t2-t1)$$
 where F2 and F1 are the *in vivo* fluorescence values at time 2 (t2) and time 1 (t1) during log phase. Fluorescence was measured on Turner Designs model 10 fluorometer. Particulate nitrogen (PN) samples were collected by vacuum filtration at 0.5 atm onto pre-combusted (450°C) glass-fiber filters (GF/F) measured with a FisonsTM automated CHN analyzer (model: NA 1500) on-line with the mass spectrometer which was used for ^{15}N isotope analysis. The precision of each PN analysis was 1 - 2%. Aliquots of phytoplankton culture (30 to 480 ml) were withdrawn from the flasks at designated time intervals. The filtrate was used for NO_3^- , NH_4^+ and urea analyses. Manual NO_3^- analyses were made using a spongy cadmium method (Jones 1984). NH_4^+ was analyzed according to Slawyk & MacIsaac (1972) and urea was measured manually according to the diacetyl monoxime method (Price & Harrison 1987).

Rate measurements - Previously acid-washed polypropylene bottles were used to collect the samples and were rinsed once with the sample. The rate of

decrease of dissolved N concentration was calculated from the slope of external N concentration against time. This N disappearance rate is expressed as $\mu\text{g-at urea N L}^{-1} \text{ h}^{-1}$ or $\mu\text{M h}^{-1}$. To indicate the change in the preference for the three N sources, comparison of the phases of the uptake rate was calculated by using the ratio of each disappearance rate.

Uptake rate - Uptake rate was calculated using the following equation:

$$V = (C_0 - C_1) / N \cdot t$$

when C_0 and C_1 are the concentrations ($\mu\text{g-at N L}^{-1}$) of N at the beginning and end of the time period. N is the cell density (cells L^{-1}), t is the time period of uptake (h) and V is the uptake rate ($\mu\text{g-at } 10^{-6} \text{ cells}^{-1} \text{ h}^{-1}$). Cell density was calculated from the fluorescence value which corresponded with the cell numbers at a particular time. Fluorescence and cell numbers were assumed to change in a linear relationship.

Nitrogen isotope analysis - N isotope abundance was determined with a VG PRISMTM mass spectrometer. Particulate samples were prepared by rolling a GF/F filter in tin foil and compressing the foil into small pellets. Then, they were combusted in a stream of oxygen at an oven temperature of 1020°C. Results are expressed in the delta notation:

$$\delta^{15}\text{N} = (R_{\text{sample}} / R_{\text{std}} - 1) \times 1000 \quad - (1)$$

where R is the $^{15}\text{N}/^{14}\text{N}$ ratio and the standard (std) is N_2 gas (NBS-14). The $\delta^{15}\text{N}$ of N1 and N2 standard, i.e. $(\text{NH}_4)_2\text{SO}_4$, was 1.34 and 20.85‰ relative to NBS-14

respectively. It was 0.54 and 20.05‰ relative to air. Internationally air is accepted as the standard. However, in the present studies, $\delta^{15}\text{N}$ relative to NBS-14 is used as a standard because absolute values are not critical for this study. The difference between the $\delta^{15}\text{N}$ of PN and the source is important other than the absolute value of either of them as explained below. The precision of $\delta^{15}\text{N}$ of the N source was 0.17‰ (\pm SD of replicate pairs, $n = 44$ pairs). The $\delta^{15}\text{N}$ of the three N sources was: 3.82 ± 0.18 ‰ (mean \pm 1SE, $n = 12$) for NaNO_3 , -0.34 ± 0.20 ‰ (mean \pm 1SE, $n = 2$) for NH_4Cl , and 0.06 ± 0.12 ‰ (mean \pm 1SE, $n = 3$) for $\text{CO}(\text{NH}_2)_2$. Correction for carry-over of ^{15}N -enriched NO_3^- from the inoculum (0.5 mM NO_3^-) to the culture medium was estimated to be small (i.e., < 0.2 ‰) due to the small volume of inoculum which was used. A small ^{15}N enrichment might be introduced during culture dilution.

Calculations of the fractionation factor - The isotope fractionation factor α was calculated using the accumulated product equation (Mariotti *et al.* 1981). Note that contrary to the definition adopted by Mariotti *et al.* (1981), α is typically ≥ 1 and ϵ (i.e. the per mil enrichment factor of the substrate relative to the product) is typically ≥ 0 ; with $\epsilon = (\alpha - 1) \times 1000$. In a closed system, as in a batch culture, the $\delta^{15}\text{N}$ of the first accumulated product is given by:

$$\delta^{15}\text{N}_{\text{PNO}} = \delta^{15}\text{N}_{\text{DNO}} - \epsilon \quad - (2)$$

where PN_0 and DN_0 are the initial particulate N and dissolved N, respectively.

Provided that ϵ was constant during the consumption of the substrate, ϵ was then derived from the accumulated product equation:

$$\delta^{15}N_{PN} = \delta^{15}N_{(DN)0} - \epsilon \cdot -f \ln f / (1-f) \quad - (3)$$

where f is the fraction of unreacted substrate at any time during exponential growth. A curve of $\delta^{15}N_{PN}$ versus F (F is defined as $[-f/(1-f)] \ln f$) was fitted with a linear function. In order to be applicable for equation (2), only data in log phase were analyzed for the calculation of ϵ . The reason for this is it was only during this phase that N incorporation could be approximated by a one step unidirectional reaction. It means conversion of DN to PN. Once DN is exhausted, cell lysis will start and release various forms of N.

Multiple N source uptake model - A model simulates the $\delta^{15}N_{PN}$ which results from batch culture growth on multiple N sources. The model was designed to test if $\delta^{15}N_{PN}$ can be described as the sum of the Rayleigh contributions associated with the incorporation of each N source. The dependent expressions for concentration of NH_4^+ , NO_3^- , and urea are determined by the fits of the dissolved N data. The $\delta^{15}N_{PNt}$ is described as follows:

$$\delta^{15}N_{PNt} = (\delta^{15}N_{PN} \cdot \sum PN_X + \delta^{15}N_{PNI} \cdot PN_i) / (\sum PN_X + PN_i)$$

Part I

RESULTS

During batch culture experiments, N was used up and then cells were N-starved for up to 96 h before they were re-supplied with N. The first period when NH_4^+ , NO_3^- , and urea were all in the medium together is termed before I (bef. I) and the period after N re-supply is termed after I (aft. I). When only NO_3^- and urea were present in the medium (i.e. NH_4^+ was already taken up), this period is termed before II (bef. II) and after N re-supply, after II (aft. II). When only urea was left in the medium, this period is termed before III (bef. III) and after III (aft. III). The order of N uptake preference was not changed in any experiments by N starvation (Table 2). However, the degree of preference of each N source changed. This will be illustrated in the following sections.

***Prorocentrum micans* grown on and re-supplied with NH_4^+ , NO_3^- , and urea (Experiment 1)**

The growth curve of *Prorocentrum micans* is shown in Fig. 1. The growth rate, μ calculated from 33 to 149 h was 0.30 d^{-1} . This growth rate was the lowest among the three species used in the present study. The cell number was 940,000 cells L^{-1} at the fluorescence value of 9.4, which was used for the calculation of uptake rates (i.e. 1 fluorescence value corresponds to 100,000 cells L^{-1}).

The N concentration in the medium during the entire incubation period and after the re-addition of N sources is shown in Figs. 2a and 2b respectively.

Table 2 Comparison of the order of N preference before and after re-addition of NH_4^+ , NO_3^- , and urea into triplicate batch cultures of *P. micans*, *A. carterae*, and *H. carterae*. Period I indicates the period when NH_4^+ , NO_3^- , and urea were all present in the medium. Period II indicates the period when NO_3^- and urea were present in the medium. Period III indicates the period when only urea was left in the medium.

N sources in medium	Period I			Period II		Period III	
	NH_4^+ NO_3^- Urea			NO_3^- Urea		Urea	
	Order			Order			
	1st	2nd	3rd	1st	2nd		
<i>Prorocentrum micans</i> before N starvation	NH_4^+	NO_3^-	Urea	NO_3^-	Urea	Urea	
after N starvation	NH_4^+	NO_3^-	Urea	NO_3^-	Urea	Urea	
	Order			Order			
	1st	2nd	3rd	1st	2nd		
<i>Amphidinium carterae</i> before N starvation	NH_4^+	NO_3^-	Urea	NO_3^-	Urea	Urea	
after N starvation	NH_4^+	NO_3^-	Urea	NO_3^-	Urea	Urea	
	Order			Order			
	1st	2nd	3rd	1st	2nd		
<i>Heterosigma carterae</i> before N starvation	NH_4^+	NO_3^-	Urea	NO_3^-	Urea	Urea	
after N starvation	NH_4^+	NO_3^-	Urea	NO_3^-	Urea	Urea	

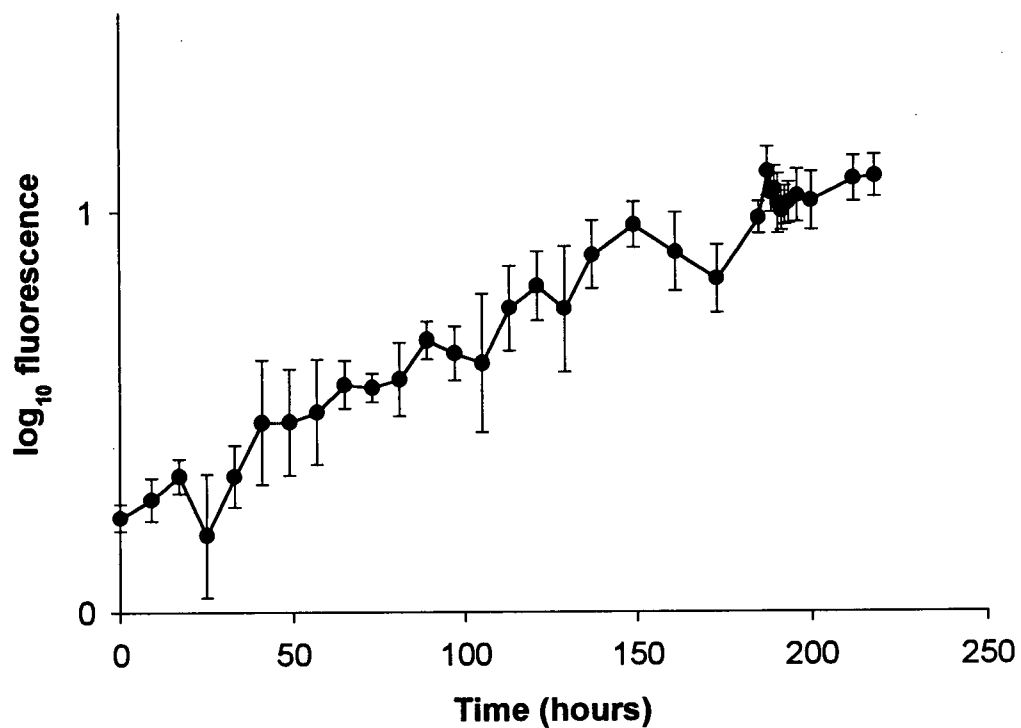


Figure 1 Growth of *Prorocentrum micans* grown on NH_4^+ , NO_3^- , and urea under continuous light. Log plot of *in vivo* fluorescence versus time. Bars represent ± 1 S.D. ($n=2-3$). Error bars are smaller than symbols where not visible.

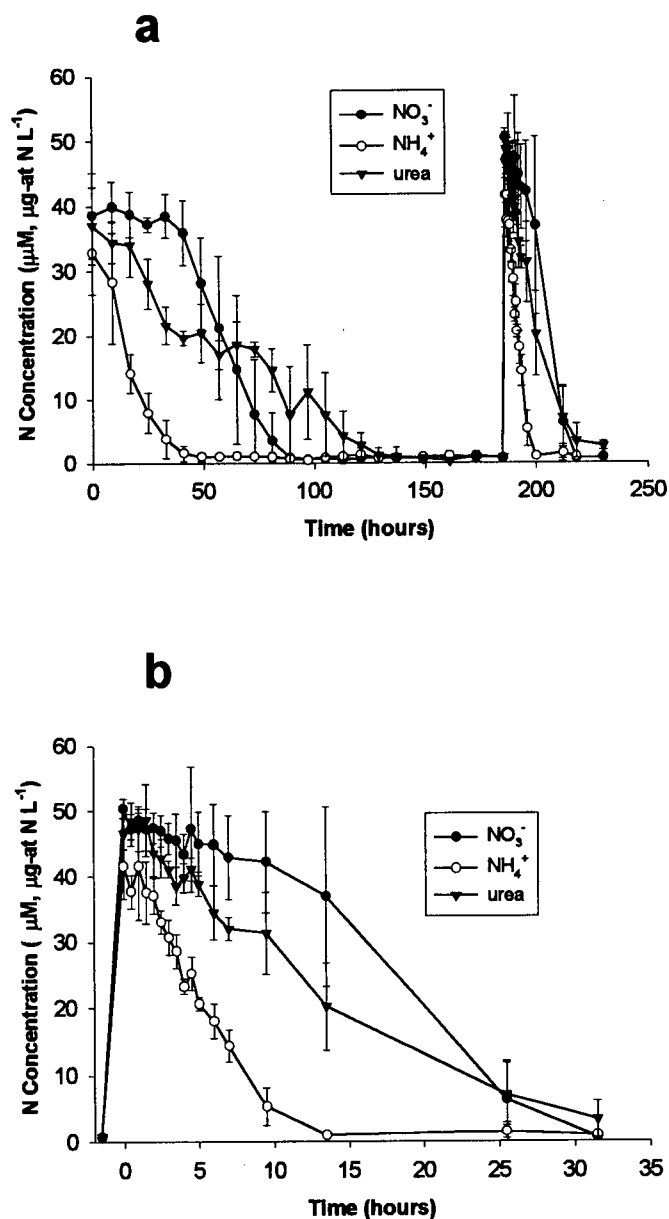


Figure 2 Nitrogen concentrations (urea as $\mu\text{g-at N L}^{-1}$) during the growth of *Prorocentrum micans* grown on NH_4^+ , NO_3^- , and urea under continuous light plotted against a) elapsed time and b) elapsed time since re-addition of NH_4^+ , NO_3^- , and urea at $t=0$ to previously N-starved cultures for 56 h. Thus (b) is an expanded time version of the N concentrations during the re-addition phase shown in (a). Cultures were N-starved between 130 and 186.5 h and then $42 \mu\text{M}$ NH_4^+ , $50 \mu\text{M}$ NO_3^- , and $47 \mu\text{g-at N L}^{-1}$ urea were added at 186.5 h. Bars represent ± 1 S.D. (n=2-3). Error bars are smaller than symbols where not visible.

NH_4^+ disappeared from the medium within 49 h at a rate of $0.97 \mu\text{mol L}^{-1} \text{h}^{-1}$. NH_4^+ showed a slow disappearance rate of $0.29 \mu\text{mol L}^{-1} \text{h}^{-1}$ between 0 and 9 h, followed by a faster rate at $2.5 \mu\text{mol L}^{-1} \text{h}^{-1}$ (9 - 17 h) and $0.64 \mu\text{mol L}^{-1} \text{h}^{-1}$ (17 - 33 h). During that period (bef. I), urea was also taken up at a rate of $0.34 \mu\text{g-at N L}^{-1} \text{h}^{-1}$. Between 0 and 17 h, there was a slow uptake of $0.18 \mu\text{g-at N L}^{-1} \text{h}^{-1}$ followed by a much faster rate of $0.77 \mu\text{g-at N L}^{-1} \text{h}^{-1}$. However, NO_3^- showed little uptake during this period. The disappearance rate of NO_3^- during this period (I) was $0.21 \mu\text{mol L}^{-1} \text{h}^{-1}$. In particular, NO_3^- was taken up at a very slow rate of $0.07 \mu\text{mol L}^{-1} \text{h}^{-1}$ for the first 41 h. After NH_4^+ was $< 1 \mu\text{M}$, the NO_3^- disappearance rate increased to $0.57 \mu\text{mol L}^{-1} \text{h}^{-1}$. Between 41 and 81 h, NO_3^- disappeared at a rate of $0.81 \mu\text{mol L}^{-1} \text{h}^{-1}$. During this period (bef. II), the disappearance of urea was $0.27 \mu\text{g-at N L}^{-1} \text{h}^{-1}$. Between 33 and 65 h, very little urea was taken up and the disappearance rate was $0.06 \mu\text{g-at N L}^{-1} \text{h}^{-1}$. When NO_3^- was $< 1 \mu\text{M}$, the disappearance rate of urea increased to $0.14 \mu\text{g-at N L}^{-1} \text{h}^{-1}$. Between 81 and 137 h, the urea disappearance rate was $0.30 \mu\text{g-at N L}^{-1} \text{h}^{-1}$.

After 56 h of N starvation, the three N sources were re-supplied. For the first 2 h immediately after the re-supply of the three N sources, all three N sources remained almost at their initial concentrations. NH_4^+ disappeared from the medium within 13.5 h and the disappearance rate of NH_4^+ during the first 2 h was $2.2 \mu\text{mol L}^{-1} \text{h}^{-1}$ and was followed by a faster rate of $5.5 \mu\text{mol L}^{-1} \text{h}^{-1}$ (2 - 5 h). The concentration of urea again decreased together with NH_4^+ , but at a rate of

65% of that of NH_4^+ during the period (aft. I). Between 1 - 1.5 h after the re-supply of N, the disappearance rate of urea was negative ($-1.3 \mu\text{g-at N L}^{-1} \text{h}^{-1}$). NO_3^- was not used until the concentration of NH_4^+ was $< 1 \mu\text{M}$. Between 0 and 5 h, the disappearance rate of NO_3^- was $1.1 \mu\text{mol L}^{-1} \text{h}^{-1}$. Once NH_4^+ disappeared from the culture, the disappearance of NO_3^- exceeded that of urea for the following 18 h (aft. II). The disappearance rates of NO_3^- and urea were $2.1 \mu\text{mol L}^{-1} \text{h}^{-1}$ and $0.93 \mu\text{g-at N L}^{-1} \text{h}^{-1}$ respectively during this period (aft. II). Especially, between 13.5 and 25.5 h, the disappearance rate of NO_3^- was $2.5 \mu\text{mol L}^{-1} \text{h}^{-1}$. On the other hand, urea was taken up more slowly than NO_3^- at $1.5 \mu\text{g-at N L}^{-1} \text{h}^{-1}$ between 4 and 25.5 h.

Uptake rates are plotted versus the average time between sampling for the entire incubation period (Fig. 3a). The maximum NH_4^+ uptake rate ($0.009 \mu\text{g-at } 10^{-6} \text{cells}^{-1} \text{h}^{-1}$) by N-replete cells occurred during the 9 - 17 h interval. After the re-supply of the three N sources, the maximum NH_4^+ uptake rate ($0.007 \mu\text{g-at } 10^{-6} \text{cells}^{-1} \text{h}^{-1}$) during the aft. I period occurred during the 3 - 4 h interval. (Fig. 3b). The maximum NO_3^- uptake rate ($0.003 \mu\text{g-at } 10^{-6} \text{cells}^{-1} \text{h}^{-1}$) occurred during the 41 - 49 h interval, which coincided with the exhaustion of NH_4^+ . Subsequently, the average uptake rate during the 49 - 89 h interval was $0.002 \mu\text{g-at } 10^{-6} \text{cells}^{-1} \text{h}^{-1}$. NO_3^- uptake rate was $0.009 \mu\text{g-at } 10^{-6} \text{cells}^{-1} \text{h}^{-1}$ for the aft. I period and $0.002 \mu\text{g-at } 10^{-6} \text{cells}^{-1} \text{h}^{-1}$ for the aft. II period. The maximum uptake rate of urea ($0.004 \mu\text{g-at } 10^{-6} \text{cells}^{-1} \text{h}^{-1}$) by N-replete cells occurred during the 25

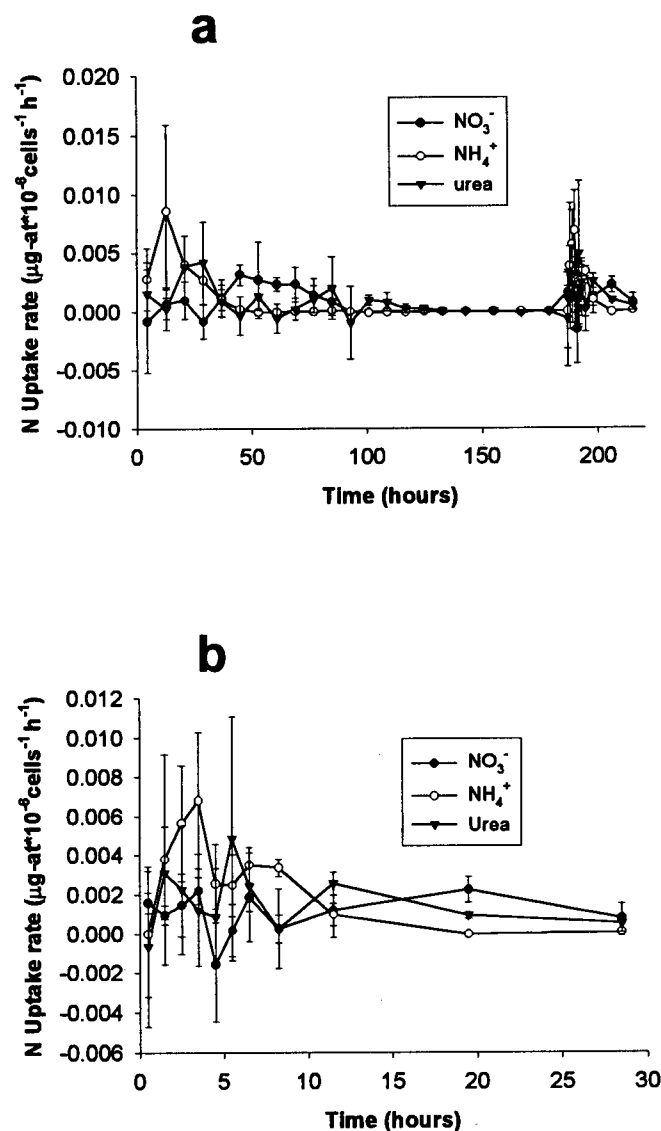


Figure 3 N uptake rates of triplicate, batch cultures of *Prorocentrum micans* grown on NH_4^+ , NO_3^- , and urea and under continuous light plotted against a) average time between sampling and b) average time between sampling since re-addition of NH_4^+ , NO_3^- , and urea at $t=0$ to previously N-starved cultures for 56 h. (b) is an expanded time version of the re-addition phase of (a). Cultures were N-starved between 130 and 186.5 h and NH_4^+ , NO_3^- , and urea were added at 186.5 h. Bars represent ± 1 S.D. ($n=2-3$). Error bars are smaller than symbols where not visible.

- 33 h interval during the bef. I period, and was $0.002 \mu\text{g-at } 10^6 \text{ cells}^{-1} \text{ h}^{-1}$. While NO_3^- uptake was high during the bef. II period, the uptake rate of urea was $0.005 \mu\text{g-at } 10^6 \text{ cells}^{-1} \text{ h}^{-1}$ and 34% of NO_3^- uptake. After N starvation and the re-addition of the three N sources, the maximum urea uptake ($0.005 \mu\text{g-at } 10^6 \text{ cells}^{-1} \text{ h}^{-1}$) occurred during 25 - 33 h. Surge uptake of any of the N sources was not observed.

The purpose of the present experiments was to determine the effect of N starvation on the preference for the three N sources, NH_4^+ , NO_3^- , and urea. Therefore, the relative disappearance rates were also calculated and expressed as ratios (Figs. 4 and 5). Before N starvation and while the three N sources (from 0 to 49 h) were present in the medium, the ratio of the disappearance and uptake rates of each N was $\text{NH}_4^+:\text{NO}_3^-:\text{urea} = 1.9:0.6:1$. Preference for urea over NH_4^+ and NO_3^- during the aft. I period increased during N starvation. Preference for NH_4^+ and NO_3^- relative to urea decreased and the ratio was 1.5:0.5:1 after N starvation. Period II was also compared. Before N starvation (from 49 to 97 h), the ratio of the disappearance rate of $\text{NO}_3^-:\text{urea}$ was 2.1:1 compared to 2.0:1 after N starvation and not significantly different.

***Amphidinium carterae* grown on and re-supplied with NH_4^+ , NO_3^- , and urea (Experiment 2)**

The growth curve of *Amphidinium carterae* is given in Fig. 6. The growth rate (μ) was 0.76 d^{-1} calculated from 59 to 143 h. When the fluorescence value

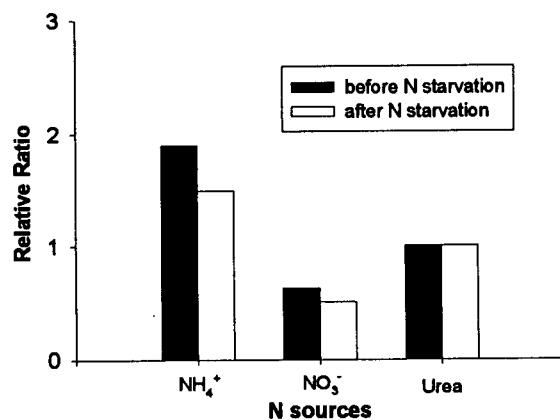


Figure 4 Relative N preference of NH_4^+ and NO_3^- relative to urea for *Prorocentrum micans* during the period I before (■) and after (□) N starvation. The relative preference for urea is fixed at 1, both before and after N starvation.

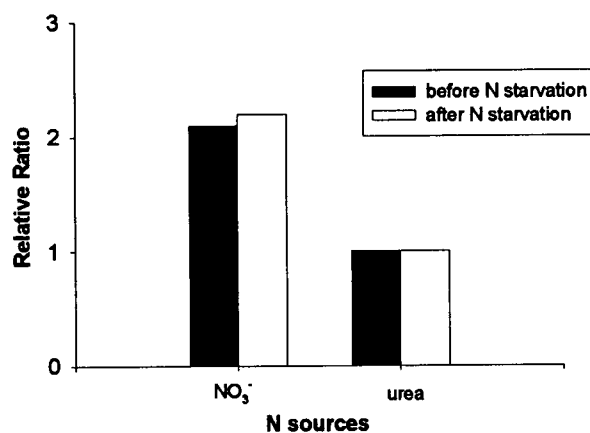


Figure 5 Relative N preference of urea relative to NO_3^- for *Prorocentrum micans* during the period II before (■) and after (□) N starvation. The relative preference for urea is fixed at 1, both before and after N starvation.

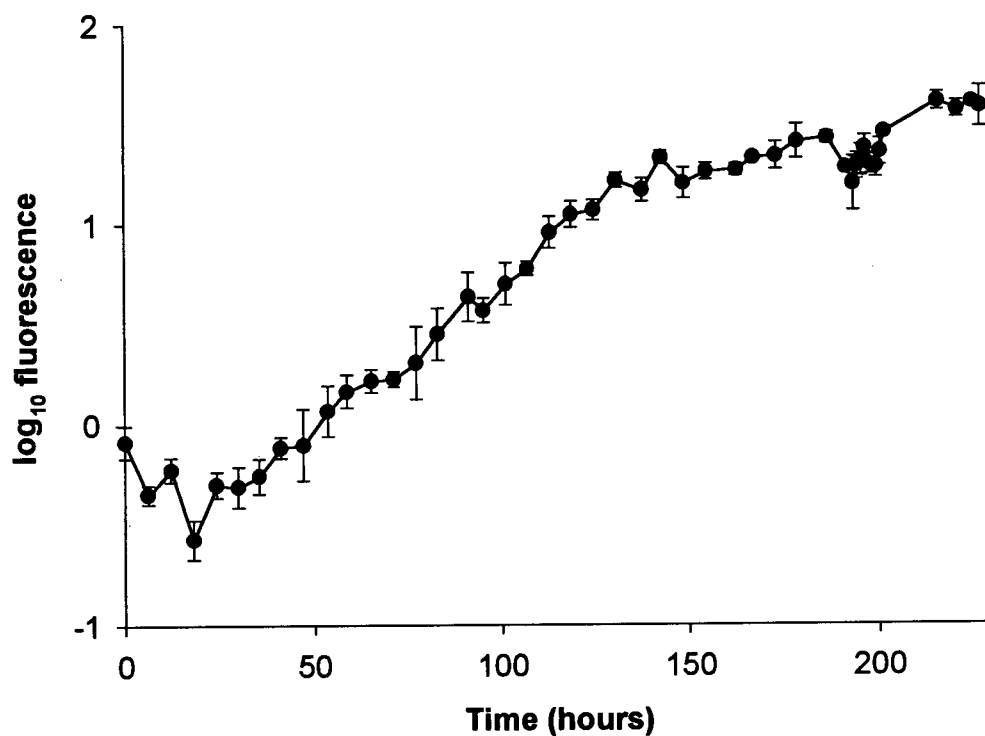


Figure 6 Growth of *Amphidinium carterae* grown on NH_4^+ , NO_3^- , and urea under continuous light. Log plot of *in vivo* fluorescence versus time. Bars represent ± 1 S.D. ($n=2-3$). Error bars are smaller than symbols where not visible.

was 18, the cell number was 345,600 cells L⁻¹, which was used for the calculation for the uptake rate (i.e. 1 fluorescence value corresponds to 19,200 cells L⁻¹).

N concentration in the medium is shown for the entire incubation period (Fig. 7a) and after the re-addition of N sources (Fig. 7b). Generally the values for separate cultures agreed well. First, NH₄⁺ disappeared from the medium within 71 h during the bef. I period at a rate of 0.48 μmol L⁻¹ h⁻¹. During this period, the concentration of both NO₃⁻ and urea remained at almost their initial concentrations. The disappearance rate for the period (bef. I) was -0.01 μmol L⁻¹ h⁻¹ for NO₃⁻ and 0.07 μg-at N L⁻¹ h⁻¹ for urea. The negative value for the NO₃⁻ disappearance rate may be due to the efflux of NO₃⁻. The disappearance rates for NO₃⁻ and urea were 0.01 μmol L⁻¹ h⁻¹ and 0.11 μg-at N L⁻¹ h⁻¹ respectively between 0 and 77 h. When the concentration of NH₄⁺ was < 1 μM, NO₃⁻ and urea were both taken up at the rate of 0.77 μmol L⁻¹ h⁻¹ and 0.46 μg-at N L⁻¹ h⁻¹ respectively during bef. II period. Between 15 and 21 h, the disappearance rates of NO₃⁻ and urea were 0.79 μmol L⁻¹ h⁻¹ and 0.61 μg-at N L⁻¹ h⁻¹. Finally, urea was the only N source in the medium and disappeared within the following 11 h (bef. III) at a rate of 0.48 μg-at N L⁻¹ h⁻¹.

After the cells were N-starved for 75 h and then re-supplied with the three sources of N, NH₄⁺ decreased quickly after the re-supply, and the disappearance rate was 10.1 μmol L⁻¹ h⁻¹ during the first 2.7 h (aft. I). Focusing only on the initial 0 to 15 min and 20 to 120 min periods, the rates were 29.8 and 9.2

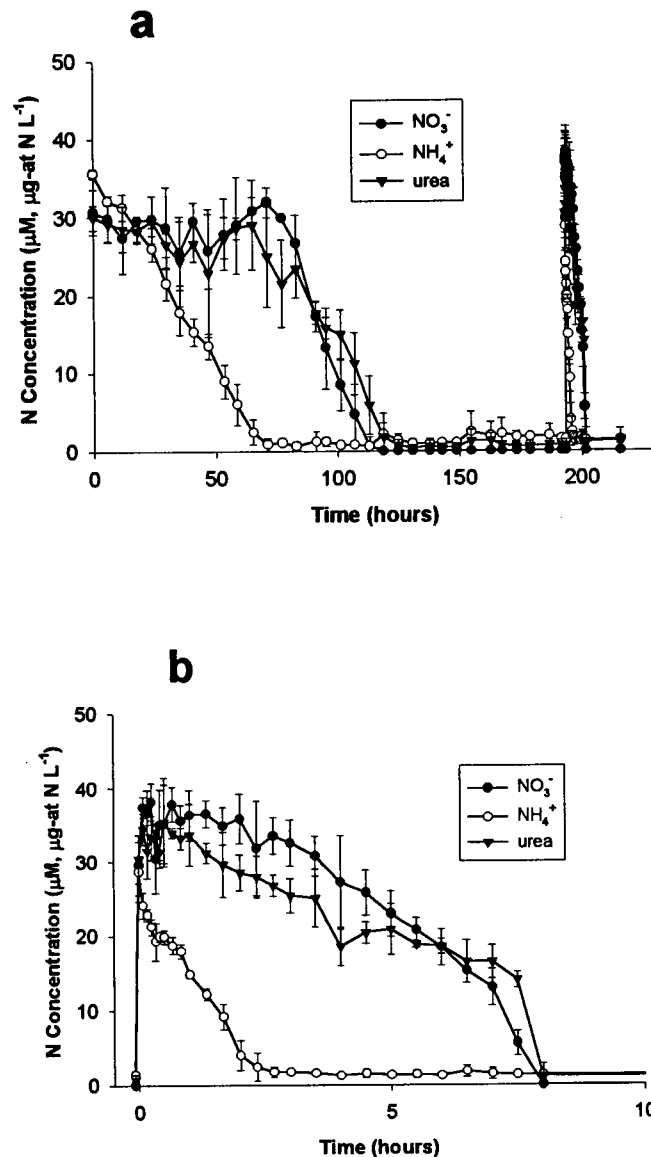


Figure 7 Nitrogen concentrations (urea as $\mu\text{g-at N L}^{-1}$) during the growth of *Amphidinium carterae* grown on NH_4^+ , NO_3^- , and urea under continuous light plotted against a) elapsed time and b) elapsed time since re-addition of NH_4^+ , NO_3^- , and urea at $t=0$ to previously N-starved cultures for 75 h. Thus (b) is an expanded time version of the N concentrations during the re-addition phase shown in (a). Cultures were N-starved between 119 and 193.5 h and then 29 μM NH_4^+ , 30 μM NO_3^- , and 30 $\mu\text{g-at N L}^{-1}$ urea were added at 193.5 h. Bars represent ± 1 S.D. (n=2-3). Error bars are smaller than symbols where not visible.

$\mu\text{mol L}^{-1} \text{h}^{-1}$ respectively. The concentration of NO_3^- and urea increased during the first 5 min after the re-addition of the three N sources. NO_3^- increased from 29.6 to 37.4 μM and urea increased from 30.4 to 34.5 $\mu\text{g-at N L}^{-1}$. Between 0 and 40 min, efflux of NO_3^- and urea occurred at rates of $-12.3 \mu\text{mol L}^{-1} \text{h}^{-1}$ and $-5.3 \mu\text{g-at N L}^{-1} \text{h}^{-1}$ respectively. During the rapid decrease in NH_4^+ concentration (aft. I), NO_3^- and urea concentrations both remained almost constant. However, urea started to decrease slightly before NO_3^- started to decline. The decrease in urea started when NH_4^+ was 18 μM , while NO_3^- started to decrease when NH_4^+ was 4 μM . When NH_4^+ was present in the medium (aft. II), the disappearance rate of urea was $0.68 \mu\text{g-at N L}^{-1} \text{h}^{-1}$ and $-0.74 \mu\text{g-at N L}^{-1} \text{h}^{-1}$ for NO_3^- . Between 50 min and 7 h, the observed rates were $3.7 \mu\text{mol L}^{-1} \text{h}^{-1}$ for NO_3^- and $2.7 \mu\text{g-at N L}^{-1} \text{h}^{-1}$ for urea. Once the concentration of NH_4^+ in the medium reached 1.7 μM , the disappearance rate of NO_3^- was $6.6 \mu\text{mol L}^{-1} \text{h}^{-1}$ and that of urea was $4.9 \mu\text{g-at N L}^{-1} \text{h}^{-1}$. After the concentration of NO_3^- reached 5.6 μM , both NO_3^- and urea decreased rapidly.

The maximum uptake of NH_4^+ ($0.08 \mu\text{g-at } 10^6 \text{cells}^{-1} \text{h}^{-1}$) for N-replete cells occurred during the 24 - 30 h interval (Fig. 8a). After the re-addition of three N sources, the maximum NH_4^+ uptake rate ($0.005 \mu\text{g-at } 10^6 \text{cells}^{-1} \text{h}^{-1}$) occurred during the initial 0 - 0.5 h interval (Fig. 8b). Uptake rates of NO_3^- during the bef. I period fluctuated widely ($-0.05 - 0.03 \mu\text{g-at } 10^6 \text{cells}^{-1} \text{h}^{-1}$) including negative uptake, indicating efflux. Uptake rate of NO_3^- during the initial 0 - 5 h interval was $-0.033 \mu\text{g-at } 10^6 \text{cells}^{-1} \text{h}^{-1}$. The maximum NO_3^- uptake rates (0.027

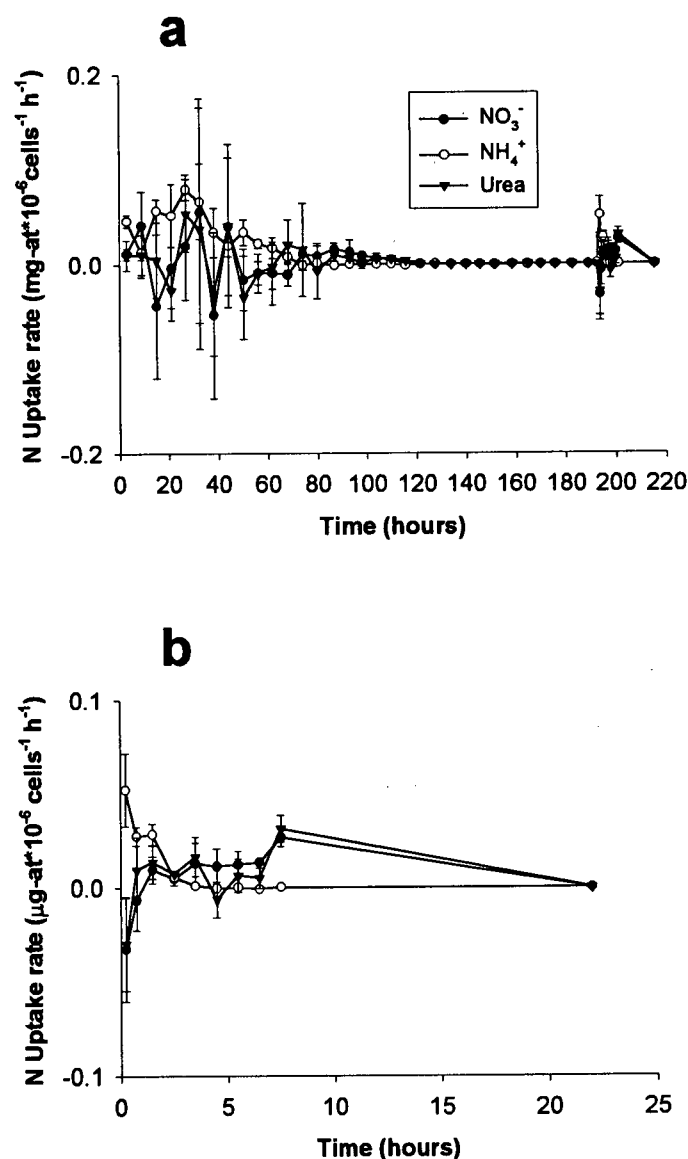


Figure 8 N uptake rates of triplicate, batch cultures of *Amphidinium carterae* grown on NH_4^+ , NO_3^- , and urea and under continuous light plotted against a) average time between sampling and b) average time between sampling since re-addition of NH_4^+ , NO_3^- , and urea at $t=0$ to previously N-starved cultures for 75 h. (b) is an expanded version of the re-addition phase of (a). Cultures were N-starved between 119 and 193.5 h and NH_4^+ , NO_3^- , and urea were added at 193.5 h. Bars represent ± 1 S.D. ($n=2-3$). Error bars are smaller than symbols where not visible.

$\mu\text{g-at } 10^{-6}\text{cells}^{-1} \text{ h}^{-1}$) after the re-addition of N sources occurred during 6 - 8 h intervals when only NO_3^- and urea were in the medium. Urea uptake during the bef. I period also fluctuated, and ranged from -0.031 to 0.055 $\mu\text{g-at } 10^{-6}\text{cells}^{-1} \text{ h}^{-1}$. Then, it became stable during the bef. II with an average urea uptake rate of 0.005 $\mu\text{g-at } 10^{-6}\text{cells}^{-1} \text{ h}^{-1}$ between 71 - 113 h. Very low uptake (-0.030 $\mu\text{g-at } 10^{-6}\text{cells}^{-1} \text{ h}^{-1}$) occurred immediately after the re-addition of N sources (0 - 5 h), as the lowest NO_3^- uptake occurred during the same period. Urea uptake rate during the aft. I period was 0.004 $\mu\text{g-at } 10^{-6}\text{cells}^{-1} \text{ h}^{-1}$ and only 13% of NH_4^+ uptake. Uptake rate of urea during aft. II (2.3 - 8 h) was 0.011 $\mu\text{g-at } 10^{-6}\text{cells}^{-1} \text{ h}^{-1}$ and 76% of NO_3^- uptake and reached a maximum uptake rate (0.031 $\mu\text{g-at } 10^{-6}\text{cells}^{-1} \text{ h}^{-1}$) during the last interval of aft. II (6 - 8 h). Surge uptake of any of the N sources was not observed.

The ratio of the disappearance and uptake rates was calculated to find the N preference (Figs. 9 and 10). Before N starvation, the uptake ratio of $\text{NH}_4^+:\text{NO}_3^-:\text{urea}$ was 6.9:-0.2:1, during the period that the three N sources existed in the medium (bef. I). After N starvation, the uptake ratio for that same period (aft. I) was 7.5:-1.1:1. The negative ratio for NO_3^- indicates NO_3^- efflux. The order of preference, NH_4^+ , urea, and NO_3^- remained the same after N deprivation. However, the relative preference of NH_4^+ over NO_3^- and urea increased after N deprivation. The preference of NH_4^+ relative to urea increased by 8.4%. The uptake of urea was faster than NO_3^- after N starvation, which indicated that urea was preferably used by starved cells in period I. The

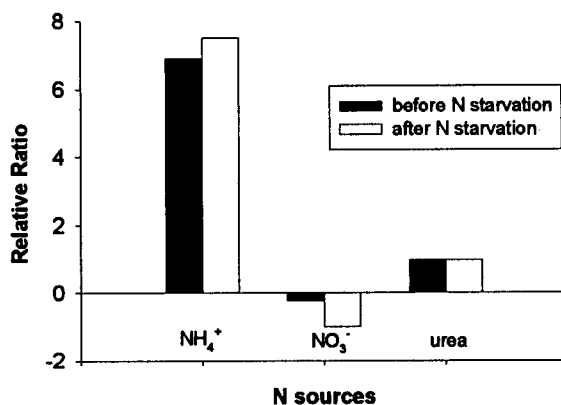


Figure 9 Relative N preference of NH_4^+ and urea relative to NO_3^- for *Amphidinium carterae* during the period I before (■) and after (□) N starvation. The relative preference for urea is fixed at 1, both before and after N starvation.

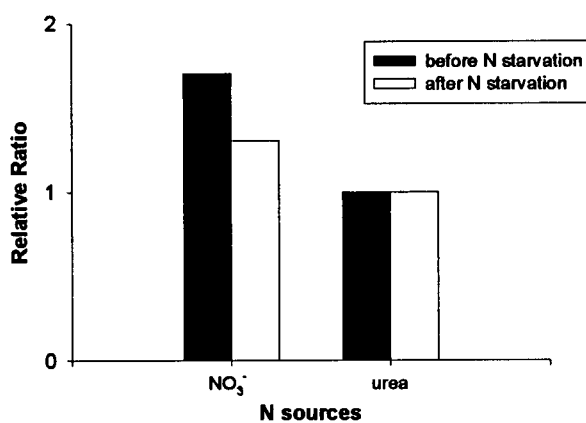


Figure 10 Relative N preference of urea relative to NO_3^- for *Amphidinium carterae* during the period II before (■) and after (□) N starvation. The relative preference for urea is fixed at 1, both before and after N starvation.

relative preference of NO_3^- over urea dropped dramatically by 5-fold. During the period when only NO_3^- and urea were present in the medium (II), the ratios of disappearance rates of NO_3^- and urea were 1.7:1 before N starvation and 1.3:1 after N starvation. Again, the order of preference was not changed. However, after N deprivation, the relative preference of NO_3^- over urea decreased by 20%. N-starved *Amphidinium carterae* cells showed enhanced urea utilization ability over NO_3^- in periods I and II.

***Heterosigma carterae* grown on and re-supplied with NH_4^+ , NO_3^- , and urea (Experiment 3)**

The growth curve of *Heterosigma carterae* is given in Fig. 11. The growth rate was 0.56 d^{-1} calculated from 0 to 108 h. When the fluorescence values were 19.4 and 23.2, cell numbers were 457,080 and 520,640 cells L^{-1} respectively. The maximum cell density was 911,040 cells L^{-1} at the fluorescence value of 45. The calculation of cell density for *Heterosigma carterae* depended on these measured values in this study. The equation for the calculation of cell density was obtained from the change in the linear regression (cell density = $21755 \times [\text{fluorescence value}] - 27046$; except for the fluorescence values < 1.24).

The N concentration in the medium is shown for the entire incubation period (Fig. 12a) and after re-supply of the three N sources (Fig. 12b).

Generally, the values for separate cultures agreed well. Before N starvation, NH_4^+ disappeared from the culture medium first. The disappearance rates of

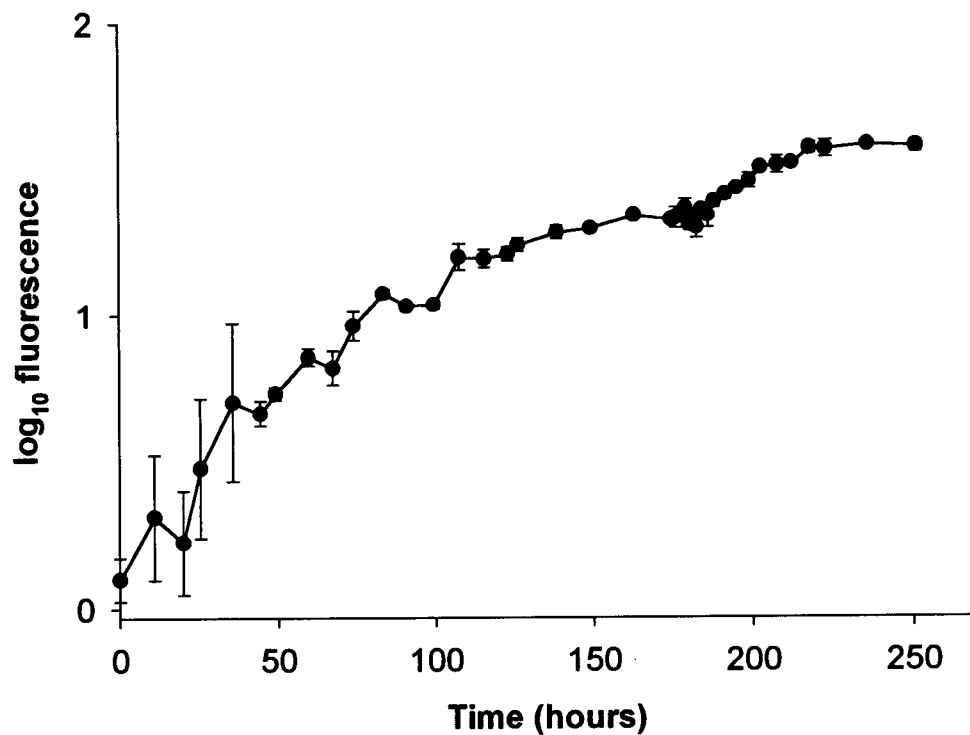


Figure 11 Growth of *Heterosigma carterae* grown on NH_4^+ , NO_3^- , and urea under continuous light. Log plot of *in vivo* fluorescence versus time. Bars represent ± 1 S.D. ($n=2-3$). Error bars are smaller than symbols where not visible.

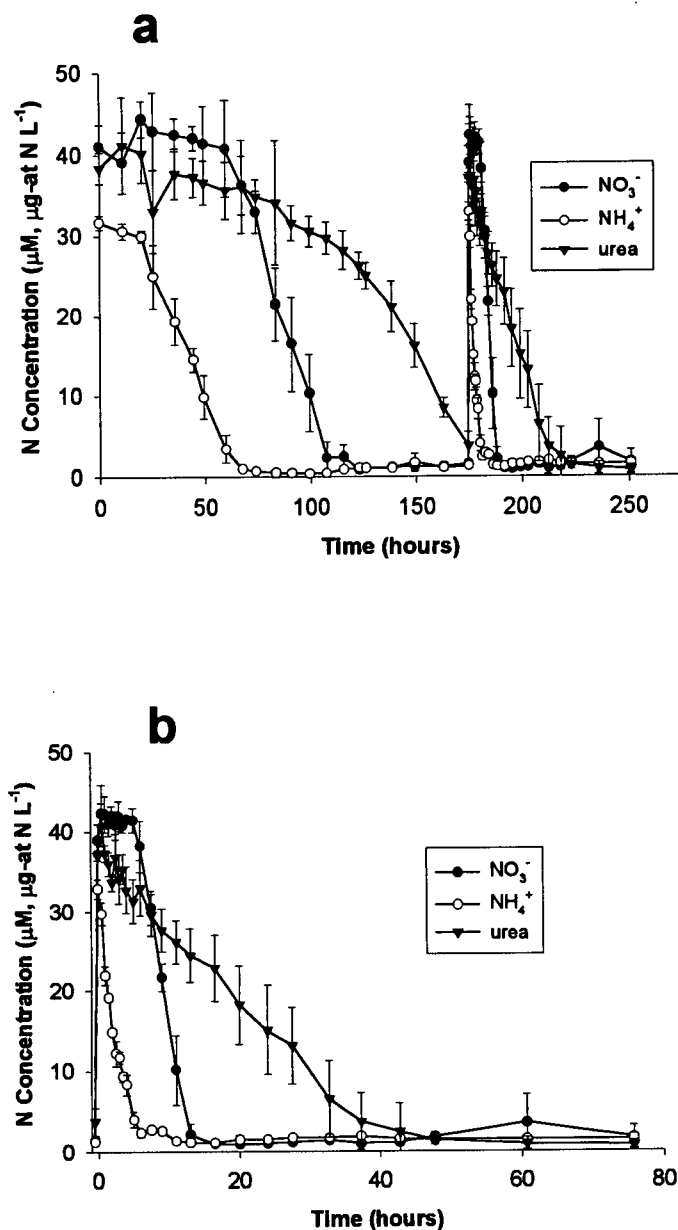


Figure 12 Nitrogen concentrations (urea as $\mu\text{g-at N L}^{-1}$) during the growth of *Heterosigma carterae* grown on NH_4^+ , NO_3^- , and urea under continuous light plotted against a) elapsed time and b) elapsed time since re-addition of NH_4^+ , NO_3^- , and urea at $t=0$ to previously N-starved culture for 0 h. Thus (b) is an expanded time version of the N concentrations during the re-addition phase shown in (a). $31 \mu\text{M}$ NH_4^+ , $41 \mu\text{M}$ NO_3^- , and $38 \mu\text{g-at N L}^{-1}$ were added at 175 h. Bars represent ± 1 S.D. ($n=2-3$). Error bars are smaller than symbols where not visible.

NH_4^+ between 0 and 20 h and 20 and 62 h were only $0.09 \mu\text{mol L}^{-1} \text{h}^{-1}$ and $0.57 \mu\text{mol L}^{-1} \text{h}^{-1}$ respectively. While NH_4^+ was primarily used (bef. I), both NO_3^- and urea remained near their initial concentrations. During this period (bef. I), the disappearance rates of NH_4^+ , NO_3^- , and urea were $0.47 \mu\text{mol L}^{-1} \text{h}^{-1}$, $0.005 \mu\text{mol L}^{-1} \text{h}^{-1}$, and $0.05 \mu\text{g-at N L}^{-1} \text{h}^{-1}$ respectively. Especially low disappearance rates of $0.005 \mu\text{mol L}^{-1} \text{h}^{-1}$ for NO_3^- and 0.05h^{-1} for urea were observed between 0 and 60 h and between 0 and 67.5 h respectively. The low NO_3^- uptake was due to the increase in the NO_3^- concentration during the first 12 h. Urea uptake showed less influence by NH_4^+ in Exp. 1 and 2, and its concentration decreased more than NO_3^- . However, once the concentration of NH_4^+ reached $3.4 \mu\text{M}$ (bef. II), NO_3^- rapidly decreased within 63 h at a rate of $0.63 \mu\text{mol L}^{-1} \text{h}^{-1}$. The disappearance rate of NO_3^- between 67.5 and 107.5 h increased to $0.85 \mu\text{mol L}^{-1} \text{h}^{-1}$. During the period when NO_3^- and urea both existed in the medium (bef. II), the disappearance rate of urea was $0.15 \mu\text{g-at N L}^{-1} \text{h}^{-1}$. Between 67.5 and 123 h, the rate of urea disappearance was $0.18 \mu\text{g-at N L}^{-1} \text{h}^{-1}$. Cells took up urea very slowly even after urea became the only N source in the culture medium. The disappearance rate of urea during bef. III period was $0.43 \mu\text{g-at N L}^{-1} \text{h}^{-1}$ and it was $0.44 \mu\text{g-at N L}^{-1} \text{h}^{-1}$ between 123 and 163 h. Since urea did not completely disappear from the culture medium, *Heterosigma carterae* did not experience true N starvation.

After the re-supply of the three N sources, NH_4^+ was immediately used up within 6 h (aft. I) at a disappearance rate of $5.1 \mu\text{mol L}^{-1} \text{h}^{-1}$. At the end of NH_4^+

uptake (6 - 13 h), the rate slowed to $0.17 \mu\text{mol L}^{-1} \text{h}^{-1}$. During the same period (aft. I), NO_3^- remained nearly constant and urea was slightly used at a disappearance rate of $0.68 \mu\text{g-at N L}^{-1} \text{h}^{-1}$. Again, in the presence of the three N sources, NH_4^+ strongly influenced on NO_3^- uptake. The disappearance rates of NO_3^- from 0 to 5 h, from 5 to 6 h, and from 11 to 15 h were -0.50, 3.2, and $5.1 \mu\text{mol L}^{-1} \text{h}^{-1}$ respectively. Once NH_4^+ concentration became $< 2.4 \mu\text{M}$, NO_3^- was quickly used up within the following 10.5 h (aft. II). Urea showed different phases of uptake. From 0 to 16.5 h (when NO_3^- was primarily consumed) and from 16.5 to 27.5 h (after NO_3^- was consumed), both rates were almost the same and they were $0.86 \mu\text{g-at N L}^{-1} \text{h}^{-1}$ and $0.89 \mu\text{g-at N L}^{-1} \text{h}^{-1}$ respectively. Then, urea disappeared gradually.

The maximum NH_4^+ uptake rate ($0.008 \mu\text{g-at } 10^6 \text{cells}^{-1} \text{h}^{-1}$) of N-replete cells occurred during 20 - 25 h interval, followed by a decrease in uptake before it reached a roughly constant rate of $0.008 \mu\text{g-at } 10^6 \text{cells}^{-1} \text{h}^{-1}$ (Fig. 13a). Uptake rate during the bef. I period was 96-fold higher than NO_3^- and 10-fold higher than urea. In the N re-supply phase, the maximum uptake rate ($0.003 \mu\text{g-at } 10^6 \text{cells}^{-1} \text{h}^{-1}$) occurred during the initial 0 - 0.5 h interval (Fig 13b). NH_4^+ uptake rate was $0.009 \mu\text{g-at } 10^6 \text{cells}^{-1} \text{h}^{-1}$ (4 - 5 h) from $0.007 \mu\text{g-at } 10^6 \text{cells}^{-1} \text{h}^{-1}$ (2 - 4 h). NO_3^- uptake rate temporally decreased from 0.007 to $-0.03 \mu\text{g-at } 10^6 \text{cells}^{-1} \text{h}^{-1}$ during the initial 0 - 20 h interval, followed by a rapid increase in uptake until it reached a roughly constant rate of $0.0008 \mu\text{g-at } 10^6 \text{cells}^{-1} \text{h}^{-1}$ during the bef. I period. After the re-addition of

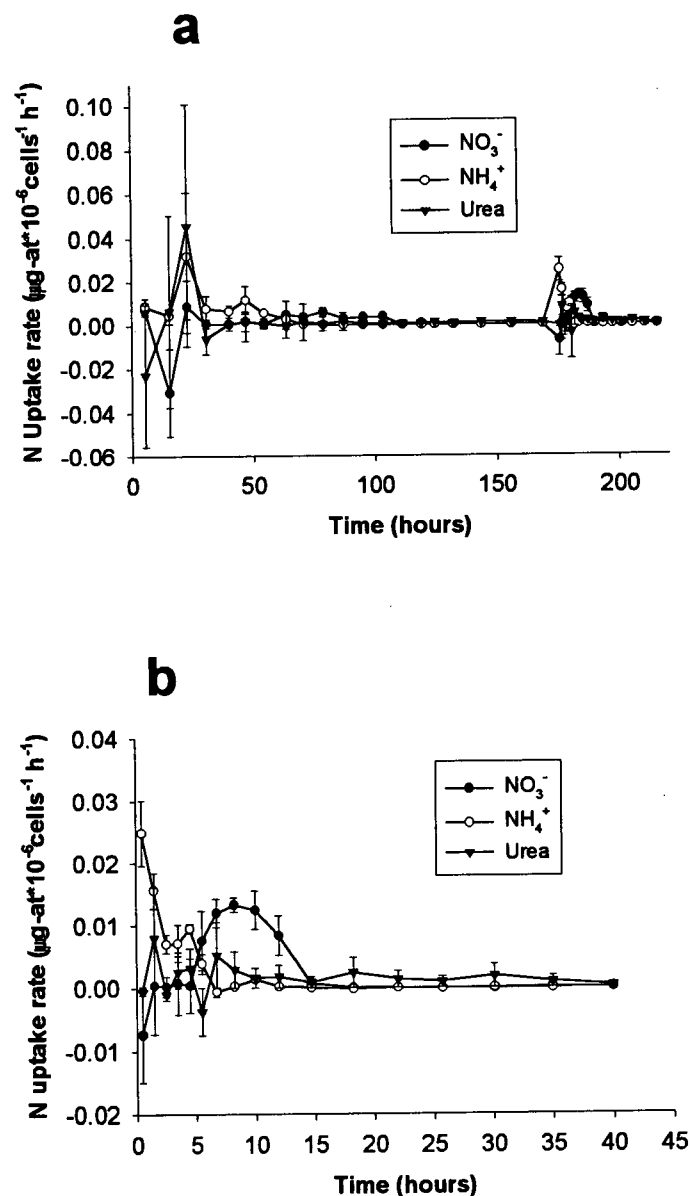


Figure 13 N uptake rates of triplicate, batch cultures of *Heterosigma carterae* grown on NH_4^+ , NO_3^- , and urea and under continuous light plotted against a) average time between sampling and b) average time between sampling since re-addition of NH_4^+ , NO_3^- , and urea at $t=0$ to previously N-starved cultures for 0 h. (b) is an expanded version of the re-addition phase of (a). NH_4^+ , NO_3^- , and urea were added at 175 h. Bars represent ± 1 S.D. ($n=2-3$). Error bars are smaller than symbols where not visible.

the three N sources, NO_3^- uptake showed a negative value of $-0.007 \mu\text{g-at } 10^{-6}\text{cells}^{-1} \text{ h}^{-1}$ during the initial 0 - 1 h interval, followed by uptake rates which were close to zero. Toward the completion of NH_4^+ uptake, NO_3^- uptake increased to $0.008 \mu\text{g-at } 10^{-6}\text{cells}^{-1} \text{ h}^{-1}$ (5 - 6 h) and maximum uptake rate ($0.013 \mu\text{g-at } 10^{-6}\text{cells}^{-1} \text{ h}^{-1}$) occurred during 7.5 - 10 h interval. The maximum uptake rate of urea ($0.046 \mu\text{g-at } 10^{-6}\text{cells}^{-1} \text{ h}^{-1}$) by N-replete cells occurred during the 20 - 25.5 h interval, followed by a rapid decrease in uptake to roughly $0.002 \mu\text{g-at } 10^{-6}\text{cells}^{-1} \text{ h}^{-1}$ in the next 25.5 - 175 h. Interestingly, during bef. III (urea was the only available N source) urea uptake rate was very low, and roughly $0.001 \mu\text{g-at } 10^{-6}\text{cells}^{-1} \text{ h}^{-1}$. In N re-supply phase, maximum urea uptake ($0.005 \mu\text{g-at } 10^{-6}\text{cells}^{-1} \text{ h}^{-1}$) occurred during 1 - 2 h interval. Evidence of any N surge uptake by N-deprived cells was not observed.

Before the re-supply of N, the order of preference among the three N sources was NH_4^+ , then urea, and lastly NO_3^- in period I. The ratio of NH_4^+ , NO_3^- , and urea uptake during this period (bef. I) was 10:0.1:1 before the re-supply of N (Fig. 14). *Heterosigma carterae* showed a strong preference for NH_4^+ before N starvation. After N starvation and the re-supply of the three N sources, the ratio changed to 7.5 (NH_4^+):0.2 (NO_3^-):1 (urea). During this period when three N sources existed in culture medium (aft. I), starved cells increased the relative preference of NO_3^- to urea unlike the previous experiments (Exp. 1 and 2). The preference for NO_3^- relative to NH_4^+ also increased. As the N-replete culture decreased utilization of NH_4^+ and urea compared to *Prorocentrum micans* and *Amphidinium carterae*, N limitation might facilitate the ability to take

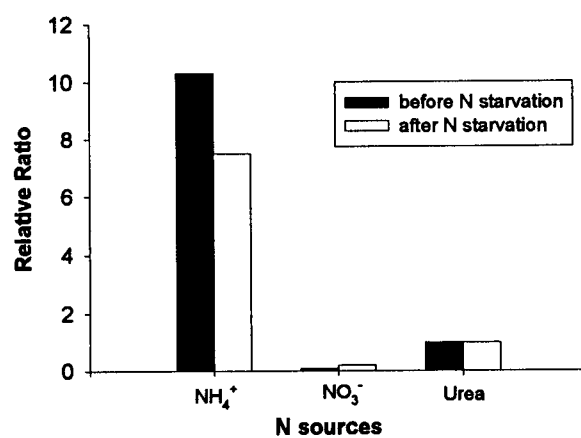


Figure 14 Relative N preference of NH_4^+ and NO_3^- relative to urea for *Heterosigma carterae* during the period I before (■) and after (□) N starvation. The relative preference for NO_3^- is fixed at 1, both before and after N starvation.

up NO_3^- . Otherwise, NH_4^+ may influence on urea to a greater degree than NO_3^- . Following the 10.5 h period (aft. II), the ratio of these N disappearance and uptake rates was $\text{NO}_3^-:\text{urea} = 3.7:1$ respectively (Fig. 15). The ratio of NO_3^- and urea utilization before N limitation was 4.2 :1. The preference of urea relative to NO_3^- was enhanced during this period (aft. II).

***Heterosigma carterae* grown on and re-supplied with NO_3^- under continuous light (Experiment 4)**

The growth curve is shown in Fig. 16. The average growth rate, μ , of the triplicate cultures was 1.0 d^{-1} calculated between 0 and 64 h. The relationship between fluorescence values and cell numbers is described in the results section of Exp. 3. The NO_3^- concentration in the medium is shown for the entire incubation period (Fig. 17a) and after the re-addition of NO_3^- (Fig. 17b). Generally the values for separate cultures agreed well. The NO_3^- concentration in the culture medium remained quite constant during the first 16 h before N starvation. The disappearance rate was $0.24 \mu\text{mol L}^{-1} \text{ h}^{-1}$. This corresponded to the lag phase in growth rate. The concentration of NO_3^- gradually decreased and reached near zero within 64 h. During this period, two evidently different uptake phases occurred. These two rates were $1.1 \mu\text{mol L}^{-1} \text{ h}^{-1}$ and $2.6 \mu\text{mol L}^{-1} \text{ h}^{-1}$ between 16 and 48 h, and 48 and 64 h respectively.

After cells experienced 48 h of N starvation and NO_3^- was re-added, NO_3^- was immediately taken up by cells at a rate of $2.2 \mu\text{mol L}^{-1} \text{ h}^{-1}$ between 0 and 2.5

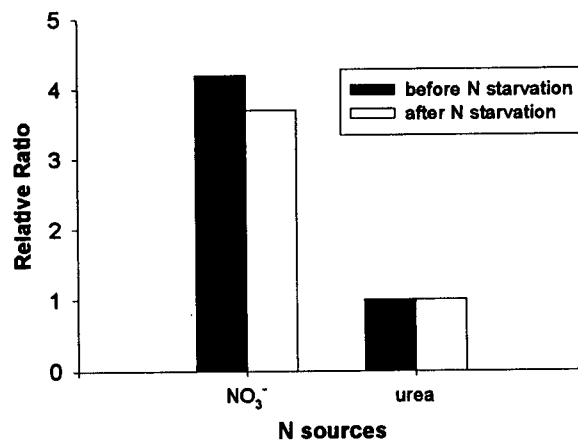


Figure 15 Relative N preference of urea relative to NO₃⁻ for *Heterosigma carterae* during the period II before and after N starvation. The relative preference for urea is fixed at 1, both before (■) and after (□) N starvation.

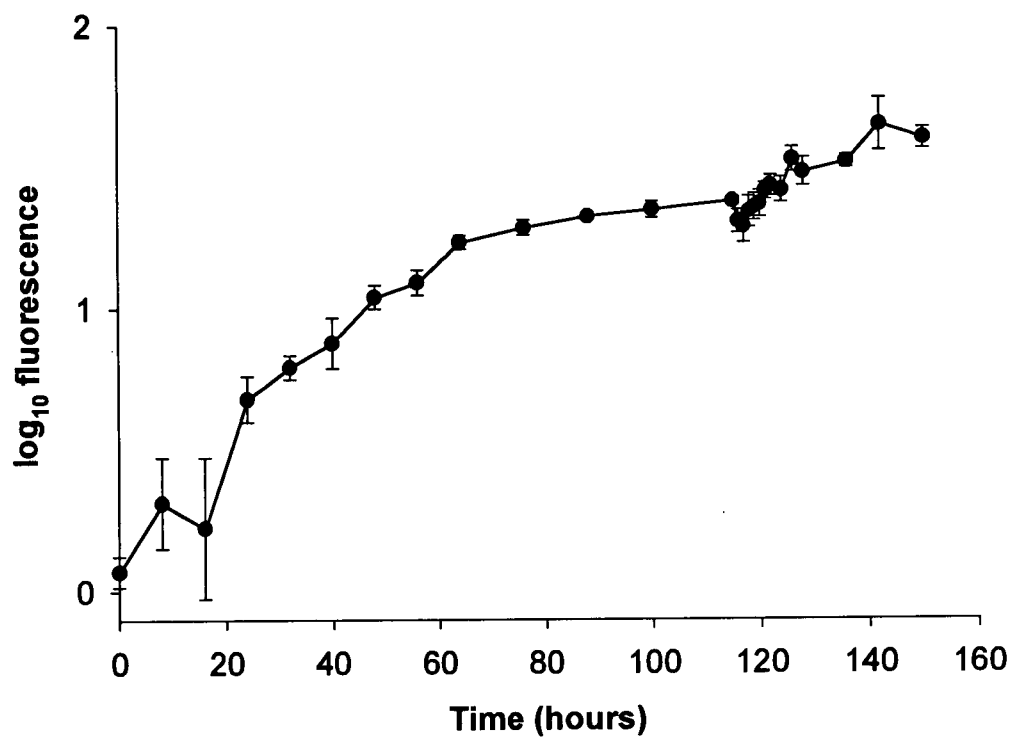


Figure 16 Growth of *Heterosigma carterae* grown on NO_3^- under continuous light. Log plot of *in vivo* fluorescence versus time. Bars represent ± 1 S.D. ($n=2-3$). Error bars are smaller than symbols where not visible.

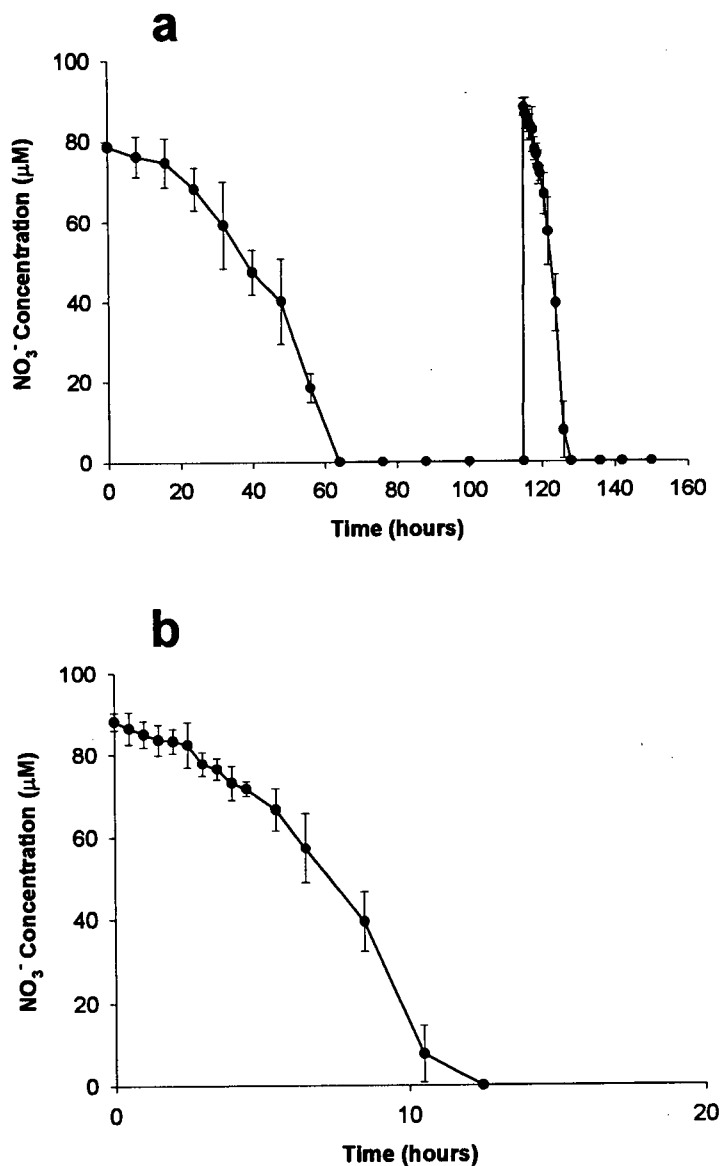


Figure 17 NO₃⁻ concentrations during the growth of *Heterosigma carterae* grown on NO₃⁻ under continuous light plotted against a) elapsed time and b) elapsed time since re-addition of NO₃⁻ at t=0. Thus (b) is an expanded time version of the N concentrations during the re-addition phase shown in (a). Cultures were NO₃⁻-starved between 64 and 116 h and then 88 μM NO₃⁻ was added at 116 h. Bars represent ± 1 S.D. (n=2-3). Error bars are smaller than symbols where not visible.

h. This was immediately followed by the increased rate of $5.3 \mu\text{mol L}^{-1} \text{h}^{-1}$ from 2.5 to 5.5 h and $11.8 \mu\text{mol L}^{-1} \text{h}^{-1}$ from 5.5 to 10.5 h.

NO_3^- uptake rates are plotted versus average time between sampling for the entire incubation period in Fig. 18a. Maximum NO_3^- uptake rate of $0.028 \mu\text{g-at } 10^6 \text{cells}^{-1} \text{h}^{-1}$ by N-replete cells occurred during 32 - 40 h interval, followed by an efflux of $-0.006 \mu\text{g-at } 10^6 \text{cells}^{-1} \text{h}^{-1}$ (40 - 48 h). After the re-addition of NO_3^- , uptake rate was relatively low, and ranged from 0.002 to $0.013 \mu\text{g-at } 10^6 \text{cells}^{-1} \text{h}^{-1}$ during the initial 0 - 4.5 h interval (Fig. 18b). Then the NO_3^- uptake rate increased to a maximum of $0.026 \mu\text{g-at } 10^6 \text{cells}^{-1} \text{h}^{-1}$ during the 8.5 - 10.5 h interval, followed by a rapid decrease in uptake ($0.006 \mu\text{g-at } 10^6 \text{cells}^{-1} \text{h}^{-1}$, 10.5 - 12.5 h) until the re-added NO_3^- was completely utilized. The maximum NO_3^- uptake rate of N-deplete cell was 91% of N-replete cells.

***Heterosigma carterae* grown on and re-supplied with NO_3^- under L:D cycle lights (Experiment 5)**

The growth curve is shown in Fig. 19. The average growth rate under a L:D cycle was 0.72 d^{-1} calculated from 49 to 105 h, which was lower than under continuous light (1.0 d^{-1}). Compared to continuous light, the growth curve was more variable, probably attributable to the L:D cycle. At most transit periods from light to dark, fluorescence increased except for the one transit period from 121 h (light) to 129 h (dark). On the other hand, a decrease in fluorescence

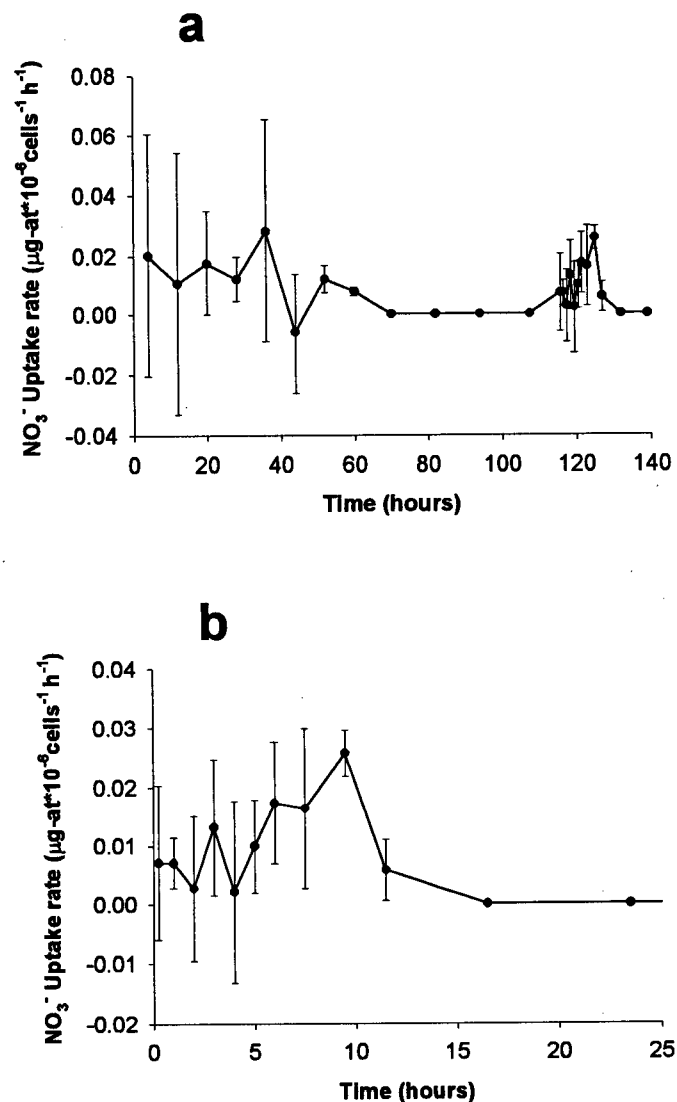


Figure 18 NO₃⁻ uptake rates of triplicate, batch cultures of *Heterosigma carterae* grown on NO₃⁻ and under continuous light plotted against a) average time between sampling and b) average time between sampling since re-addition of NO₃⁻ at t=0 to previously N-starved cultures for 51.5 h. (b) is an expanded version of the re-addition phase of (a). Cultures were NO₃⁻ starved between 64 and 115 h and then NO₃⁻ was added at 116 h. Bars represent ± 1 S.D. (n=2-3). Error bars are smaller than symbols where not visible.

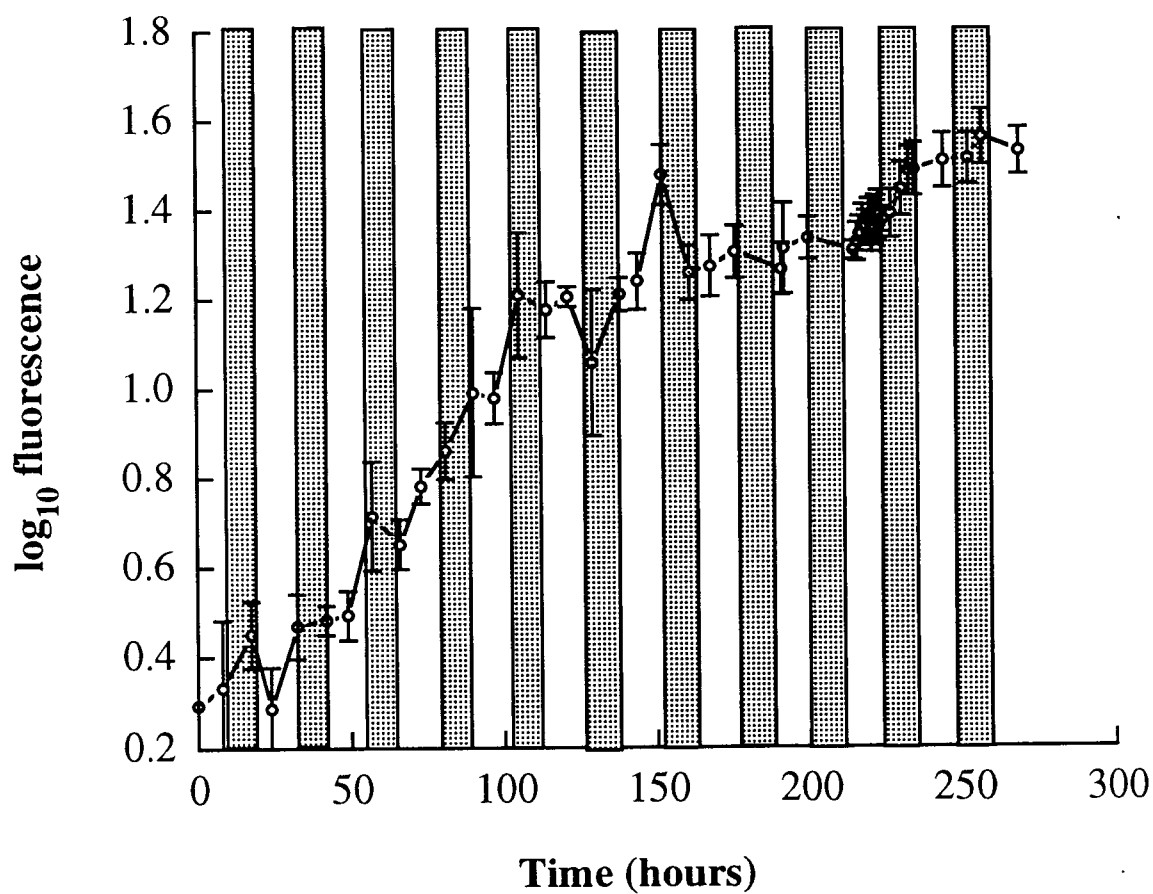


Figure 19 Growth of *Heterosigma carterae* grown on NO_3^- and under a 14:10 L:D cycle. Log plot of *in vivo* fluorescence versus time. Stippled areas indicate dark periods. Bars represent ± 1 S.D. (n=2-3). Error bars are smaller than symbols where not visible.

from the beginning to the end of dark period was observed between 57 – 66, 105 – 114, and 152 – 161 h. During the dark period, the fluorescence increased, which indicated that they had divided. The relationship between fluorescence values and cell numbers is described in the results section of Exp. 3.

The NO_3^- concentration is shown for the entire incubation period (Fig. 20a) and after N limitation (Fig. 20b). Generally, the values for separate cultures agreed well. The disappearance rate of NO_3^- was divided into three phases. They were $0.09 \mu\text{mol L}^{-1} \text{h}^{-1}$, $0.77 \mu\text{mol L}^{-1} \text{h}^{-1}$, and $1.1 \mu\text{mol L}^{-1} \text{h}^{-1}$ between 0 and 42 h, 42 and 81 h, and 81 and 114 h respectively. Overall, the concentration of NO_3^- fluctuated before the cells experienced N starvation. On the other hand, under continuous light, NO_3^- decreased more smoothly and the growth curve was also smooth. NO_3^- fluctuated for the first 42 h and then, when light was available, the concentration dropped rapidly from 76.9 to 63.4 μM during the following 15 h. Then, during the next dark period, the concentration of NO_3^- increased from 53.6 to 62.5 μM during the following 9 h of darkness. During the next two light periods and one dark period, NO_3^- decreased. This phenomenon was observed in all triplicate cultures and did not occur in cultures with continuous light before N starvation.

After N re-supply to the medium, all triplicate cultures showed an increase in the NO_3^- concentration. The average value of this increase was 11.7 μM (from 72.7 to 84.4 μM). This concentration remained above 80 μM for almost 3 h after the re-supply of NO_3^- . The efflux rate was $-1.0 \mu\text{mol L}^{-1} \text{h}^{-1}$ between 0

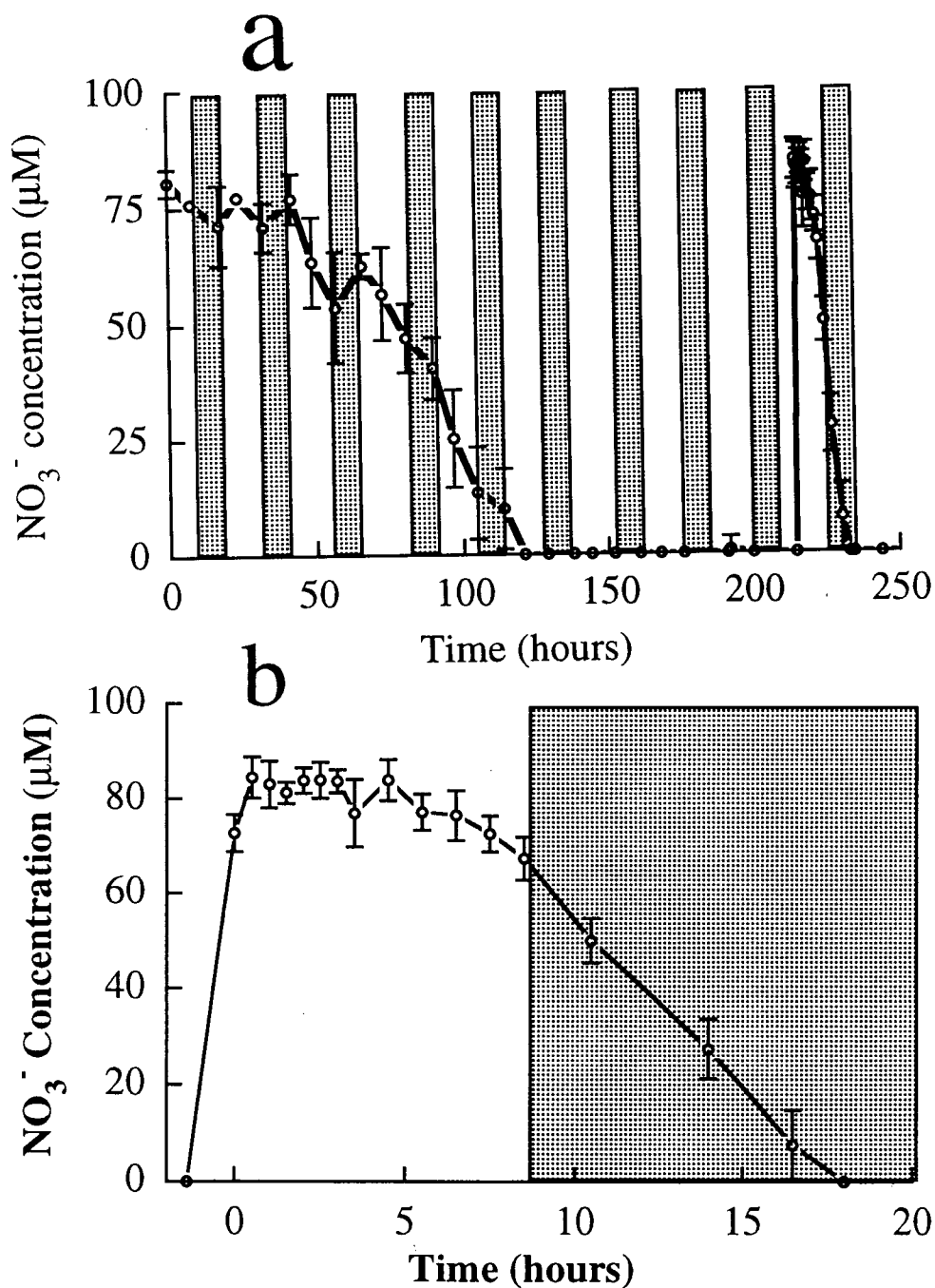


Figure 20 NO_3^- concentrations during the growth of *Heterosigma carterae* on NO_3^- and under a 14:10 L:D cycle plotted against a) elapsed time and b) elapsed time after the re-addition of 73 μM NO_3^- at 215 h to N-starved *Heterosigma carterae* for 96 h. Thus (b) is an expanded time version of the N concentrations during the re-addition phase shown in (a). Cultures were NO_3^- -starved from 119 h to 215 h. Stippled areas indicate dark periods. Bars represent ± 1 S.D. (n=2-3). Error bars are smaller than symbols where not visible.

and 4 h. Then the concentration of NO_3^- started to decline and the disappearance rates between 5 and 8 h and 8 and 15.5 h were $3.8 \mu\text{mol L}^{-1} \text{h}^{-1}$ and $6.0 \mu\text{mol L}^{-1} \text{h}^{-1}$ respectively. Finally, NO_3^- disappeared 62.5 h after the re-supply of NO_3^- . Compared to the continuous light culture, the concentration of NO_3^- hardly decreased after the re-supply of NO_3^- , while NO_3^- in the continuous light culture started to decrease immediately.

NO_3^- uptake rate in the N-replete phase fluctuated widely until it reached a maximum uptake rate ($0.048 \mu\text{g-at } 10^{-6}\text{cells}^{-1} \text{h}^{-1}$, 42 - 49 h) (Fig. 21a). Then uptake rate reached a roughly constant rate of $0.004 \mu\text{g-at } 10^{-6}\text{cells}^{-1} \text{h}^{-1}$ in the next 66 - 97 h interval. Uptake rates at the end of dark periods always dropped from their previous values, and negative values (i.e. efflux) of $-0.017 \mu\text{g-at } 10^{-6}\text{cells}^{-1} \text{h}^{-1}$ (32.5 - 42 h), $-0.013 \mu\text{g-at } 10^{-6}\text{cells}^{-1} \text{h}^{-1}$ (57 - 66 h) and very small values of $0.004 \mu\text{g-at } 10^{-6}\text{cells}^{-1} \text{h}^{-1}$ (81 - 90 h), $0.001 \mu\text{g-at } 10^{-6}\text{cells}^{-1} \text{h}^{-1}$ (105 - 114 h) occurred. The average NO_3^- uptake rate after the re-addition of NO_3^- was $-0.006 \mu\text{g-at } 10^{-6}\text{cells}^{-1} \text{h}^{-1}$ during the first 5 h of the light period (Fig. 21b). The maximum uptake rate ($0.023 \mu\text{g-at } 10^{-6}\text{cells}^{-1} \text{h}^{-1}$) occurred during the 9.5 - 12 h interval in the light period. Maximum uptake rate of the N-deplete cell was 49% of that of N-replete cells.

***Heterosigma carterae* grown on and re-supplied with NH_4^+ under continuous light (Experiment 6)**

Triplicate cultures were grown for this experiment. However, one culture had only $69.6 \mu\text{M } \text{NH}_4^+$ initially and consumed it very rapidly compared to the

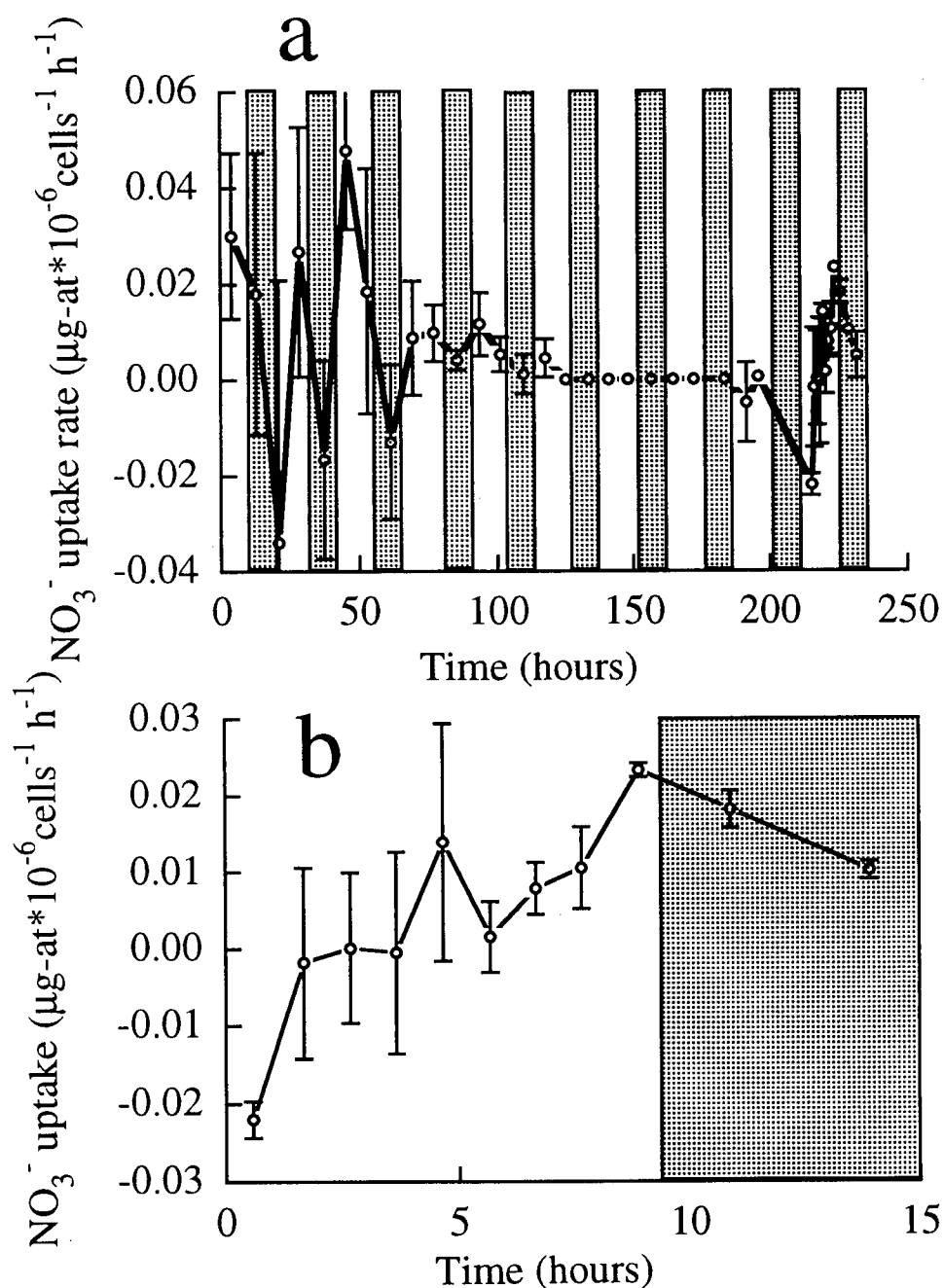


Figure 21 NO_3^- uptake rates of triplicate, batch cultures of *Heterosigma carterae* grown on NO_3^- and under a 14:10 L:D cycle plotted against a) average time between sampling and b) average time between sampling since re-addition of NO_3^- at $t=0$ to previously N-starved cultures for 96 h. (b) is an expanded version of the re-addition phase of (a). Cultures were NO_3^- -starved between 119 and 215 h and then NO_3^- was added at 215 h. Stippled areas indicate dark periods. Bars represent ± 1 S.D. ($n=2-3$). Error bars are smaller than symbols where not visible.

other two cultures which had 78.4 μM for their average initial concentration.

Therefore, the two results will be discussed separately.

The growth curve for culture 1 is shown in Fig. 22. The growth rate, μ , was 1.1 d^{-1} calculated from 0 to 58 h. The relationship between fluorescence values and cell numbers is described in the result section of Exp. 3.

The NH_4^+ concentration for culture 1 is shown in Fig. 23a and after the NH_4^+ re-addition in Fig. 23b. The NH_4^+ in the first culture disappeared from the culture medium within 65 h. During the first 8 h, the disappearance rate of NH_4^+ was $0.41 \mu\text{mol L}^{-1} \text{ h}^{-1}$, which was followed by an increased rate of $1.6 \mu\text{mol L}^{-1} \text{ h}^{-1}$ between 14 and 45 h. Then cells experienced 33 h of N starvation.

After the re-supply of NH_4^+ , the concentration of NH_4^+ only decreased from 77.2 to 70.4 μM within the following 2 h at a rate of $3.4 \mu\text{mol L}^{-1} \text{ h}^{-1}$. Then, within the next 1.5 h, the concentration dropped from 70.4 to 56.1 μM and the rate during this period was $28.6 \mu\text{mol L}^{-1} \text{ h}^{-1}$. Interestingly, the NH_4^+ concentration $> 50 \mu\text{M}$ remained for the following 5 h and resulted in this very slow NH_4^+ disappearance. The disappearance rates during this period were $1.7 \mu\text{mol L}^{-1} \text{ h}^{-1}$ and $0.41 \mu\text{mol L}^{-1} \text{ h}^{-1}$ between 2.5 and 4.5 h and 4.5 and 7.5 h respectively. NH_4^+ gradually started to disappear again at the rate of $4.1 \mu\text{mol L}^{-1} \text{ h}^{-1}$ between 7.5 and 14.5 h, after the 5 h period where little uptake occurred. It took 32.5 h to consume all the added NH_4^+ .

The maximum NH_4^+ uptake rate $0.031 \mu\text{g-at } 10^6 \text{ cells}^{-1} \text{ h}^{-1}$ of N-replete cells occurred during the 14 - 18 h interval (Fig. 24a). In the N re-addition

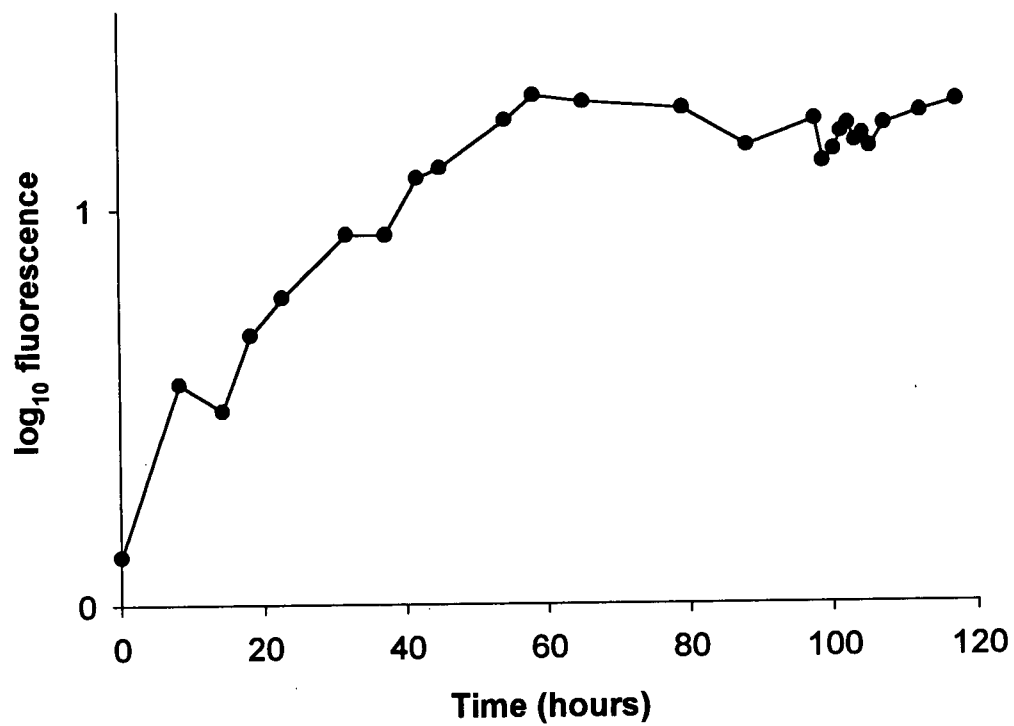


Figure 22 Growth of *Heterosigma carterae* on NH_4^+ under continuous light, culture 1. Log plot of *in vivo* fluorescence versus time.

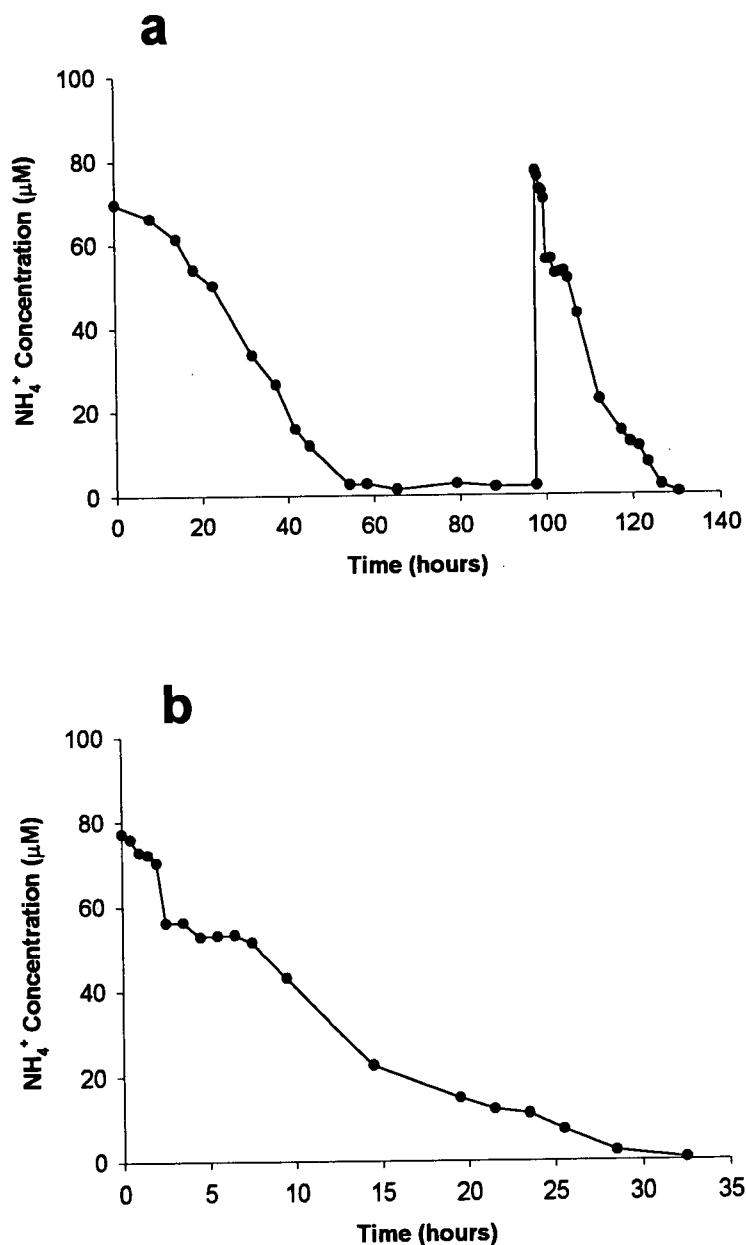


Figure 23 NH_4^+ concentrations during the growth of *Heterosigma carterae* grown on NH_4^+ under continuous light, culture 1, plotted against a) elapsed time and b) after the re-addition of NH_4^+ at $t=0$ to N-starved cells for 33 h. Thus (b) is an expanded time version of the N concentrations during the re-addition phase shown in (a). Culture was NH_4^+ -starved between 65 and 98 h and then $77 \mu\text{M}$ NH_4^+ was added at 98 h.

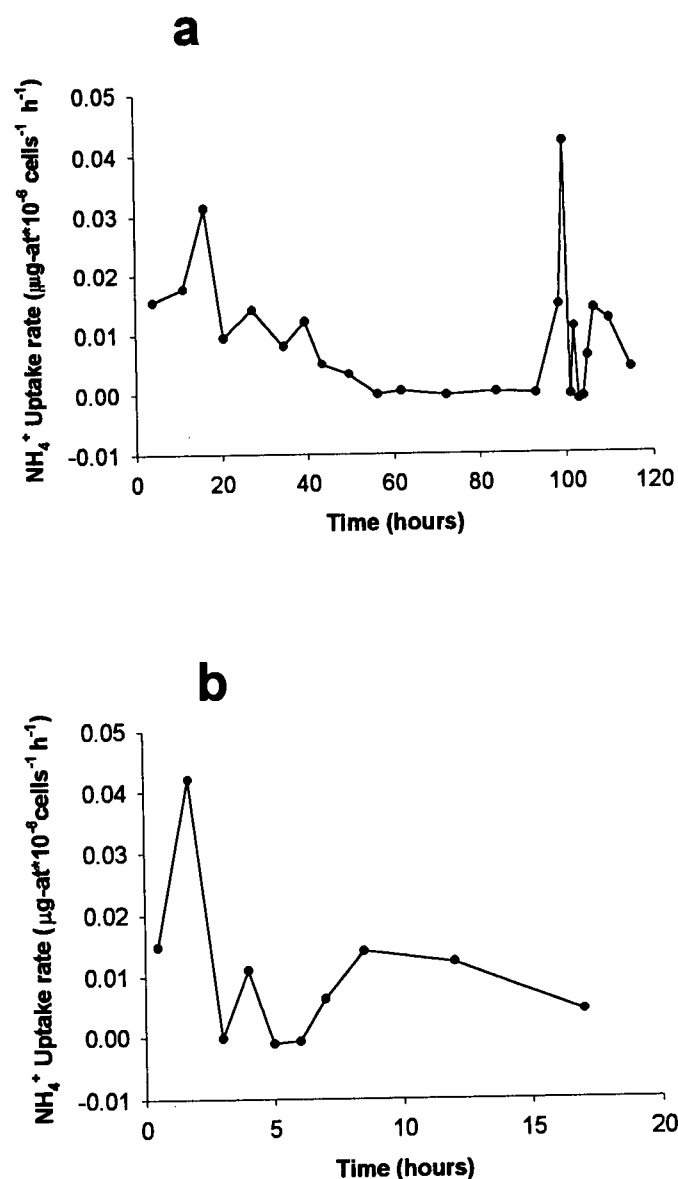


Figure 24 NH_4^+ uptake rates of a batch culture of *Heterosigma carterae* grown on NH_4^+ and under continuous light, culture 1, plotted against a) average time between sampling and b) average time between sampling since re-addition of NH_4^+ at $t=0$ to previously N-starved culture for 33 h. (b) is an expanded version of the re-addition phase of (a). Culture was NH_4^+ -starved between 65 and 98 h and then NH_4^+ was added at 98 h.

phase, maximum uptake ($0.042 \mu\text{g-at } 10^6\text{cells}^{-1} \text{ h}^{-1}$) occurred during the 1 - 2.5 h interval, followed by a rapid decrease in uptake and very low NH_4^+ uptake period (2.5 - 6.5 h) with an average rate of $0.002 \mu\text{g-at } 10^6\text{cells}^{-1} \text{ h}^{-1}$ (Fig. 24b).

Data from the other duplicate cultures agreed well with both growth 1.02 d^{-1} calculated 14 to 54 h and NH_4^+ disappearance rates (Figs. 25 and 26a). Before N starvation, the NH_4^+ concentration continued to decline without any lag period, which matched the log period of growth. The disappearance rates of NH_4^+ were $0.78 \mu\text{mol L}^{-1} \text{ h}^{-1}$ and $1.51 \mu\text{mol L}^{-1} \text{ h}^{-1}$ between 0 and 23 h and 23 and 54 h respectively.

After the re-addition of NH_4^+ to N-starved cells, NH_4^+ concentration hardly decreased for the following 1.5 h (Fig. 26b), which also occurred in culture 1. The disappearance rate between 0 and 1.5 h was $0.96 \mu\text{mol L}^{-1} \text{ h}^{-1}$. Following the lag period, NH_4^+ concentration rapidly dropped from 72.1 to 59.4 μM at a rate of $25.4 \mu\text{mol L}^{-1} \text{ h}^{-1}$. As in culture 1, the concentration of NH_4^+ almost did not decrease after the rapid disappearance of NH_4^+ . The disappearance rate from 2 to 4.5 h was $2.8 \mu\text{mol L}^{-1} \text{ h}^{-1}$. From 4.5 to 5.5 h, the rate increased to $13.0 \mu\text{mol L}^{-1} \text{ h}^{-1}$. Then, NH_4^+ started to disappear again gradually at a rate of $4.4 \mu\text{mol L}^{-1} \text{ h}^{-1}$ between 5.5 and 10.5 h and it took 24.5 h for the complete disappearance. NH_4^+ disappearance after the re-supply of NH_4^+ showed several steps. First, the concentration did not change and, then the concentration dramatically dropped followed by a slow decrease in NH_4^+ . This phenomenon was more distinct than that observed in the same species grown on NO_3^- and continuous light (Exp. 4).

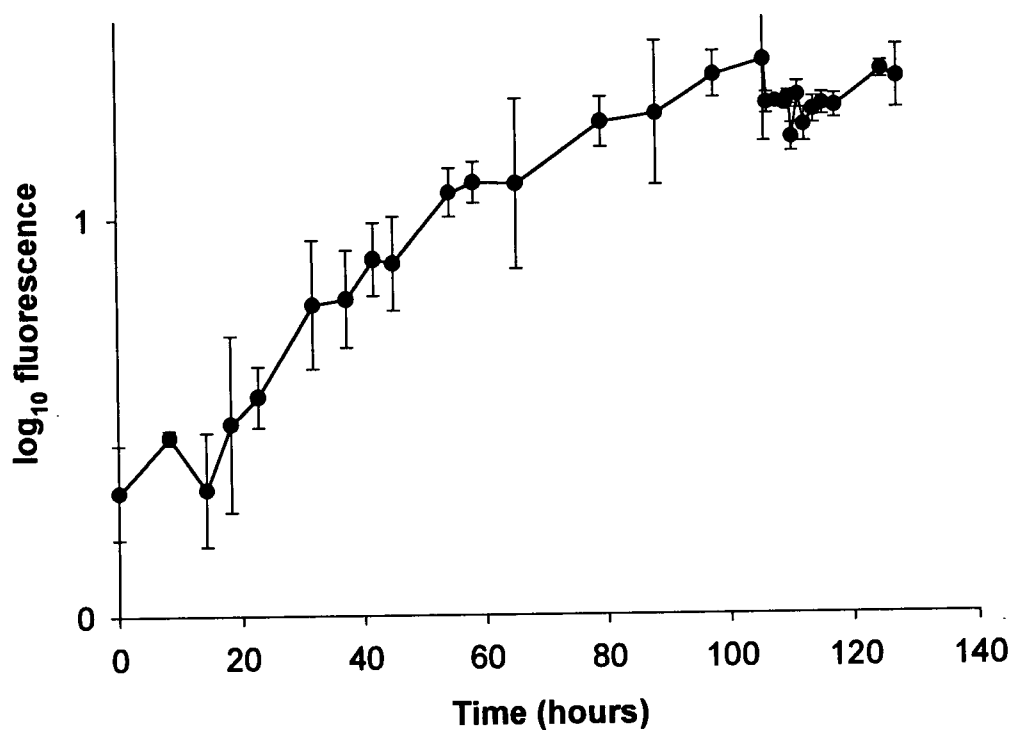


Figure 25 Growth of *Heterosigma carterae* on NH_4^+ under continuous light, cultures 2 and 3. Log plot of *in vivo* fluorescence versus time. Bars represent ± 1 S.D. ($n=1-2$). Error bars are smaller than symbols where not visible.

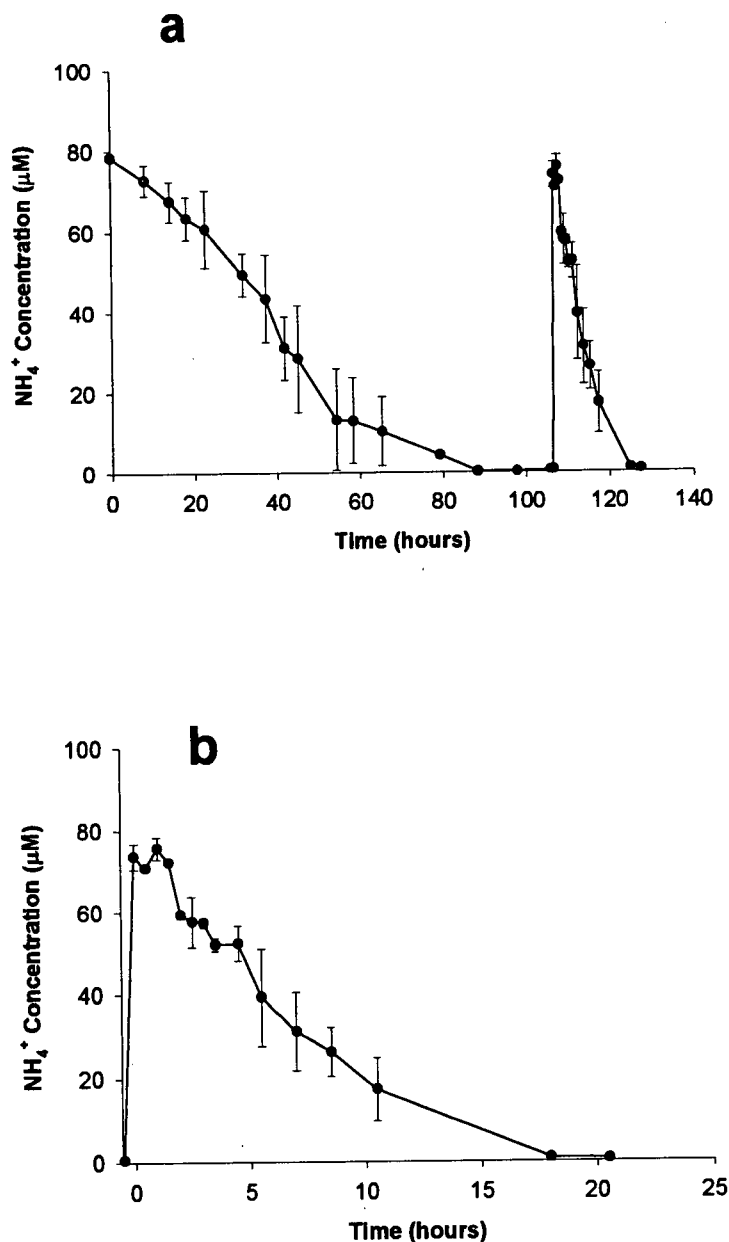


Figure 26 NH_4^+ concentrations during the growth of *Heterosigma carterae* grown on NH_4^+ under continuous light, cultures 2 and 3, plotted against a) elapsed time and b) elapsed time after the re-addition of NH_4^+ at $t=0$, to N-starved cells for 18 h. Thus (b) is an expanded time version of the N concentrations during the re-addition phase shown in (a). Cultures were NH_4^+ -starved between 88 and 106 h and then $74 \mu\text{M}$ NH_4^+ was added at 106 h. Bars represent ± 1 S.D. ($n=1-2$). Error bars are smaller than symbols where not visible.

A relatively high average NO_3^- uptake ($0.030 \mu\text{g-at } 10^{-6}\text{cells}^{-1} \text{ h}^{-1}$) for N-replete cells occurred during the initial 0 - 18 h interval (Fig. 27a). During the N-deplete phase, uptake rate fluctuated and even the NH_4^+ concentration in the medium did not change much (2.5 - 4.5 h) (Fig. 27b). The maximum NH_4^+ uptake rate ($0.034 \mu\text{g-at } 10^{-6}\text{cells}^{-1} \text{ h}^{-1}$) occurred during the 4.5 - 5.5 h interval.

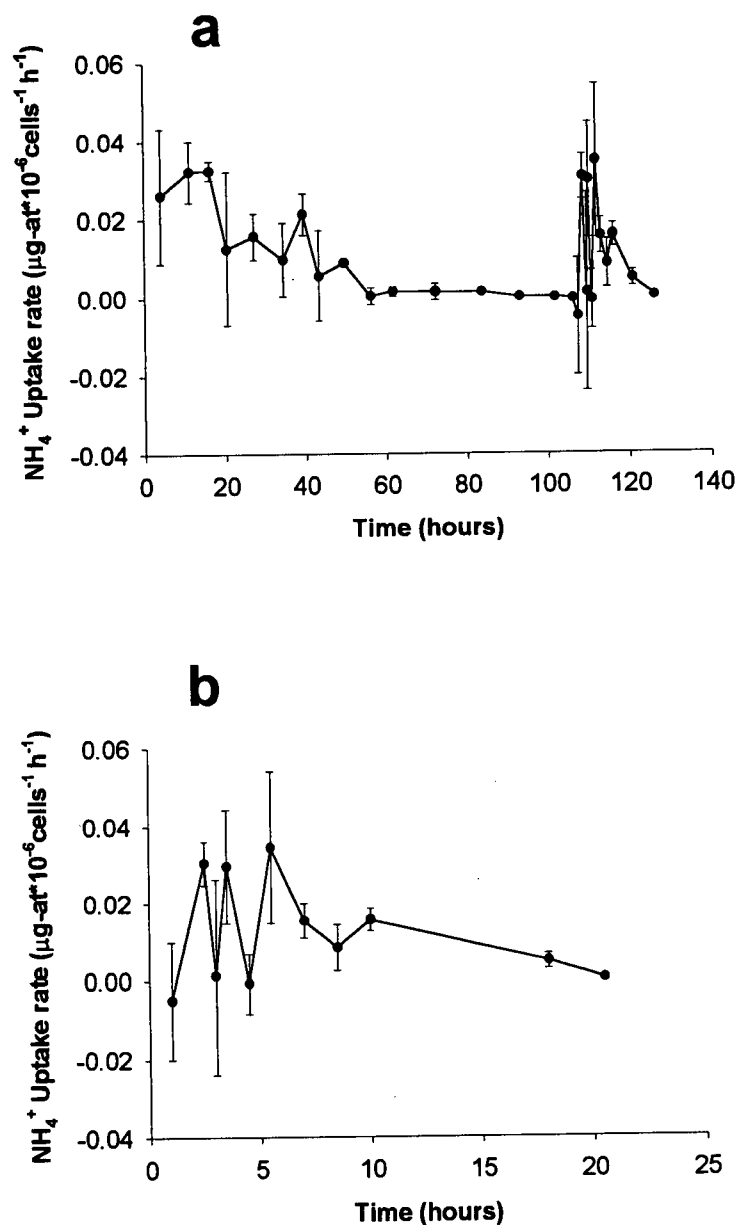


Figure 27 NH_4^+ uptake rates of duplicate, cultures of *Heterosigma carterae* grown on NH_4^+ and under continuous light, culture 2+3, plotted against a) average time between sampling and b) average time between sampling since re-addition of NH_4^+ at $t=0$ to previously N-starved for 18 h. (b) is an expanded version of the re-addition phase of (a). Cultures were NH_4^+ -starved between 88 and 106 h and then NH_4^+ was added at 106 h. Bars represent ± 1 S.D. ($n=1-2$). Error bars are smaller than symbols where not visible.

DISCUSSION

N Preference change

1) period I

In the present study, *Prorocentrum micans*, *Amphidinium carterae*, and *Heterosigma carterae* showed different degrees of N preference compared to the generally accepted pattern of preferring NH_4^+ and then NO_3^- , over urea (Dugdale & Goering 1967; Paasche & Kristiansen 1982; Levasseur *et al.* 1990). Urea uptake was higher than NO_3^- uptake in the presence of NH_4^+ . This result was different from previous field studies, where N utilization was 54% (NH_4^+), 26% (NO_3^-), and 5% (urea) (Maguer *et al.* 1995) and 48% (NH_4^+), 32% (NO_3^-), and 13% (urea) (L'Helguen *et al.* 1996).

N-replete *Prorocentrum micans* preferred NH_4^+ over NO_3^- and urea with an uptake ratio of 1.9:0.6:1 respectively. This species used the three N sources most evenly among the tested species. Urea utilization was seen at $> 14 \mu\text{M}$ NH_4^+ , which occurred in only *Prorocentrum micans* but not in the other species. N-depleted cells increased their urea preference relative to NO_3^- and NH_4^+ and the NO_3^- preference relative to NH_4^+ . However, the increase in the preference for urea was greater than NO_3^- .

The strong preference for NH_4^+ by *Heterosigma carterae* (Exp. 3) resulted in N preference ratios of 10 (NH_4^+):0.1 (NO_3^-):1 (urea) by N-replete cells. Such a strong preference for a particular N source was found only in this species. N-

replete cells did not use NO_3^- when $\text{NH}_4^+ > 1 \mu\text{M}$. On the other hand, urea was utilized more than NO_3^- . These results were in good agreement with the field study on several lakes in Brazil by Mitamura *et al.* (1995) who showed that the contribution of NO_3^- as N source was negligible compared to NH_4^+ and urea. N-deplete cells of *Heterosigma carterae* decreased their preference for NH_4^+ relative to both NO_3^- and urea. The preference for NH_4^+ relative to NO_3^- showed a 59% decrease, and urea preference relative to NO_3^- decreased 44%. This is the only species that decreased the preference for urea relative to NO_3^- after N deprivation. Consequently, N-deplete cells used the three N sources more indiscriminately than N-replete cells. However, the preference for NH_4^+ was still very high compared to the other species, before and after N deprivation.

Amphidinium carterae also showed a strong preference for NH_4^+ .

Interestingly, N-replete cells did not use NO_3^- at all when NH_4^+ was available. N-deplete cells enhanced the relative preference of NH_4^+ over both NO_3^- and urea and the consequence was a significant decrease in the relative preference for NO_3^- . This resulted in a wider range of the preferences for N sources than N-replete cells.

In general, the present study showed that influence by NH_4^+ affected NO_3^- to a greater extent than urea. For all three species, urea was more preferred than NO_3^- in the presence of NH_4^+ (bef. and aft. I).

The important new finding in the present study was the interactions of the three re-added N sources. Most reports of inhibition by N sources focused on only two N sources, NH_4^+ and NO_3^- . Therefore, previous reports of interactions

apply only partially to the present results. For example, the present results of the increased urea uptake relative to NH_4^+ after the re-addition of three N sources (Exp. 1 and 2) were the opposite of the results by Horrigan and McCarthy (1982) and Lund (1987). This discrepancy is considered due to the interaction of N sources, culture conditions, and different species (*Thalassiosira pseudonana* and *Skeletonema costatum*). Furthermore, the previously reported increased NO_3^- uptake by removing inhibition by NH_4^+ (MacIsaac & Dugdale, 1972) was not observed in my study, perhaps due to the enhanced urea uptake, when NH_4^+ was depleted in Exp. 1 and 2. However, the increased preference for urea over NH_4^+ and NO_3^- (Exp. 1 and 2) and over NH_4^+ (Exp. 3) observed during aft. I periods agreed with the results by Rees and Syrett (1979).

The increased urea preference by N-starved dinoflagellates in the present study is in agreement with the results of a recent study on a coccolithophore and a diatom by Waser *et al.* (1998a). In their study, using three N sources, NH_4^+ was utilized first, followed by the simultaneous uptake of NO_3^- and urea by N-replete *Thalassiosira pseudonana* and *Chaetoceros debilis*. N-replete *Emiliania huxleyi* took up N in the following order NH_4^+ , NO_3^- , and urea. However, N-deprived *Thalassiosira pseudonana* and *Emiliania huxleyi* used reduced N forms (NH_4^+ and urea) immediately after the re-supply of N sources and NO_3^- was used last. Interestingly, N-starved *Chaetoceros debilis* took up only urea after the re-addition of three N sources, and NH_4^+ was not immediately utilized. These observations suggest that increasing preference for urea in the interaction of the three N sources is a general phenomenon in several groups of marine

phytoplankton. However, the evidence that the raphidophyte *Heterosigma carterae* did not increase urea preference after N deprivation in the present study also suggests increasing urea preference is group or species specific.

2) Period II

During this period (II) of N uptake after N addition to N-starved cells, the preference for urea relative to NO_3^- increased 20 and 12% in *Amphidinium carterae* and *Heterosigma carterae* respectively; there was no change in the urea preference in *Prorocentrum micans*.

Further investigation is needed to determine why *Heterosigma carterae* developed a preference toward NO_3^- utilization after N starvation. *Heterosigma carterae* grown on three N sources could not use urea before and after N deficiency. *Heterosigma carterae* did not grow well on urea (Fig. 28). The growth rate of *Heterosigma carterae* on urea was 0.90 d^{-1} , (calculated from 0 to 3 d) and was not the lowest compared to growth on other N sources. However, maximum fluorescence of this culture with urea was 80% of Exp. 3 (three N sources), 78% of Exp. 4 (NO_3^- and continuous light), 79% of Exp. 5 (NO_3^- and L:D cycle), and 78% of Exp. 6 (NH_4^+ and continuous light). Therefore, to compensate for N deficiency which was exacerbated by the incapability of using urea, *Heterosigma carterae* might have increased its capability to take up NO_3^- during N deprivation.

Overall, the order of preference of N was not changed for each period. However, it was revealed that the order of N preference really depended on the

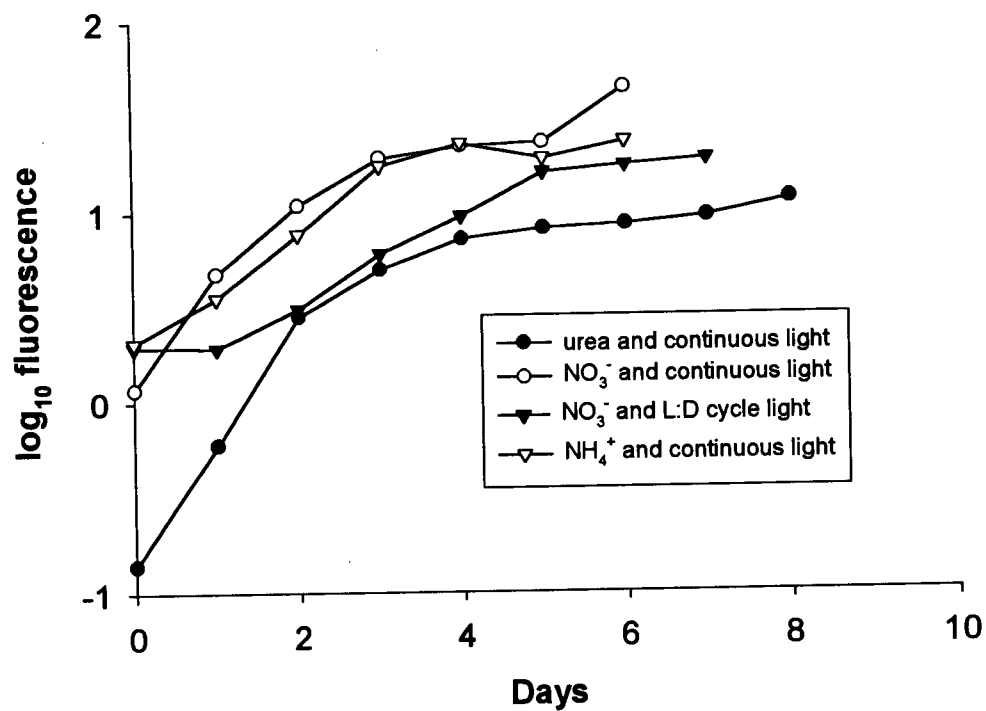


Figure 28 Growth of *Heterosigma carterae* grown on various N sources and light conditions. Log plot of *in vivo* fluorescence versus time.

combinations of N sources. In addition, the N physiological state affected the degree of N preference, which was shown by a significantly increased preference for urea relative to NH_4^+ and NO_3^- by N-starved *Prorocentrum micans* and *Amphidinium carterae*, and an increased NO_3^- preference of N-deprived *Heterosigma carterae*.

Cellular physiological state

1) Surge uptake

N-starved cells did not exhibit evident of faster NH_4^+ , NO_3^- and urea uptake than non-starved cells for all three species, except for *Heterosigma carterae* grown on NH_4^+ (culture 1). In addition, the fastest uptake of N occurred some time after the re-addition of N sources, except NH_4^+ uptake by N-starved *Amphidinium carterae* and *Heterosigma carterae* grown on three N sources.

Syrett (1953) and Harvey (1953) first demonstrated the effects of cellular physiological state on N uptake rates. Following these first results, a natural phytoplankton community and a batch culture were shown to exhibit rapid uptake of NH_4^+ after N deprivation (Conway *et al.* 1976; McCarthy & Goldman 1979; Goldman *et al.* 1981; Goldman & Glibert 1982; Dortch *et al.*, 1982; Wheeler *et al.* 1982; Harrison 1983; Suttle & Harrison 1988; Syrett & Peplinska 1988). However, this enhanced uptake rate decreased rapidly after the cells overcame the N deficiency (Fitzgerald 1968). In general, species specificity (Conway & Harrison 1977) and the duration of N deprivation (Parslow *et al.* 1984a) determine the magnitude of the surge uptake response. This enhanced uptake

rate of N could be an adaptive response for phytoplankton to take up regenerated NH_4^+ (McCarthy & Goldman 1979; Glibert & Goldman 1981; Goldman & Glibert 1982). Consequently, it allows phytoplankton to maintain relatively high growth rates in oligotrophic waters (Goldman *et al.* 1979; Goldman & Glibert 1982).

The apparent role of surge uptake for phytoplankton is to overcome the N deficiency and speed up the incorporation of N into macromolecules. Wheeler *et al.* (1982, 1983) suggested that growth is limited by the rate at which cellular metabolism can incorporate N into macromolecules.

2) Ammonium uptake in N-deplete phase

During the N re-supply period, the fastest uptake rate ($0.07 \mu\text{g-at } 10^6 \text{ cells}^{-1} \text{ h}^{-1}$) of NH_4^+ was observed between 3 and 4 h in *Prorocentrum micans*. However, in *Amphidinium carterae* and *Heterosigma carterae*, the fastest rates occurred during the initial interval after the re-addition of N sources. The former species required an acclimation period to take up the re-added NH_4^+ . Waser *et al.* (1998a) also reported a similar phenomenon in which NH_4^+ was taken up immediately after the three N sources by N-starved *Emiliana huxleyi* and *Thalassiosira pseudonana*, but not *Chaetoceros debilis*. Therefore, the capacity for surge uptake of NH_4^+ must be species specific.

Heterosigma carterae grown on NH_4^+ showed the maximum uptake rate of $0.042 \mu\text{g-at } 10^6 \text{ cells}^{-1} \text{ h}^{-1}$ in culture 1 and $0.33 \mu\text{g-at } 10^6 \text{ cells}^{-1} \text{ h}^{-1}$ (culture 2+3). Following the rapid uptake of NH_4^+ , uptake rate slowed for a short period in the

Heterosigma carterae culture. The NH_4^+ uptake rates during this period were 0.006 (2.5 - 4.5 h) in culture 1 and 0.014 $\mu\text{g-at } 10^6\text{cells}^{-1} \text{ h}^{-1}$ (2.5 - 4.5 h) in culture 2+3. The same phenomenon also occurred in *Prorocentrum micans* grown on three N sources. However, such a pattern was not as distinct as the pattern that occurred in cultures grown on only NH_4^+ (Exp. 6).

Freshwater phytoplankton (Suttle & Harrison 1988) and a picoplankter, *Micromonas pusilla* (Cochlan *et al.* 1991) exhibited the phenomenon of a short-term decrease in $^{15}\text{NH}_4^+$ uptake following surge uptake, which was similar to the results in the present study. This phenomenon could be explained by the short lag before the processing of NH_4^+ into amino acids, or a sudden loss of membrane potential due to the influx of cations (Suttle & Harrison 1988). Evidence that N-starved *Lemna gibba*, which was re-supplied with NH_4^+ suddenly lost membrane potential supports the later explanation (Ullrich *et al.* 1984). Since approximately 100 $\mu\text{g-at N L}^{-1}$ of N, with the combinations of NH_4^+ (cation), NO_3^- (anion), and uncharged urea were re-supplied to *Prorocentrum micans* (Exp. 1) and *Heterosigma carterae* (Exp. 3), membrane potential might have been lost, although the magnitude of influx of cations is less than in *Heterosigma carterae* supplied with only 100 $\mu\text{M NH}_4^+$.

The re-supply of NH_4^+ affects many cellular processes. During N deprivation, cultures continue accumulating polysaccharides by photosynthesis (Syrett 1981). Once these cultures are supplied with NH_4^+ , they take up NH_4^+ very rapidly and convert it to organic N compounds. Simultaneously, the accumulated polysaccharide disappears because it is converted into organic N

compounds (Syrett 1953; Hattori 1958; Reisner *et al.* 1960). Also, these polysaccharides are used for producing energy due to increased respiration during the rapid assimilation of NH_4^+ .

3) Nitrate uptake in N-deplete phase

NO_3^- was not rapidly taken up by N-starved *Heterosigma carterae* when it was the only N source (Exp. 4 and 5), and when it was one of three N sources with NH_4^+ and urea during period I (Exp. 1, 2, and 3). The concentration of NO_3^- began to decline only after 3 h (Exp. 1), 6 h (Exp. 2), 11 h (Exp. 3), 6 h (Exp. 4), and 2.5 h (Exp. 5). Previous uptake rates were quite low and they were 0.001 (Exp. 1), 0.002 (Exp. 2), 0.004 (Exp. 3), 0.006 (Exp. 4), and -0.011 $\mu\text{g-at } 10^6\text{cells}^{-1} \text{ h}^{-1}$ (Exp. 5). The difference in the period in which no NO_3^- uptake occurs may be species dependent (Conway & Harrison 1977), and vary with the duration of N starvation (Parslow *et al.* 1984a), and other environmental factors. Overall, N-starved cells needed an acclimation period to start to take up NO_3^- again. Maximum uptake rates ranged from 0.002 (*Prorocentrum micans*) to 0.025 $\mu\text{g-at } 10^6\text{cells}^{-1} \text{ h}^{-1}$ (*Heterosigma carterae* grown on NO_3^- under continuous light) and occurred some time after these low NO_3^- uptake periods.

In Exp. 1, 2, and 3, influence by NH_4^+ and urea could be responsible for the period of no NO_3^- uptake. When NH_4^+ decreased to a certain concentration, then NO_3^- started to decline. In Exp. 4 and 5, there must be another reason for *Heterosigma carterae* grown on NO_3^- . NO_3^- was not taken up as readily by the NO_3^- -starved culture of *Heterosigma carterae* compared to the reduced N form,

NH_4^+ by NH_4^+ -starved *Heterosigma carterae*. A reduction in the ability of NO_3^- uptake after N deprivation has been commonly reported (Collos 1980; Dortch *et al.* 1982). NO_3^- -starved phytoplankton usually require previous exposure to NO_3^- before NO_3^- uptake can occur (Dortch *et al.* 1982; Collos 1983; Parslow *et al.* 1984b). Starved cells achieve maximal NO_3^- uptake after an acclimation period (Collos 1983; Harrison *et al.* 1989). One of reasons for a reduction in the initial NO_3^- uptake is that long term NO_3^- deprivation might reduce the ability of NO_3^- uptake due to the loss of viability of cells. The decline in the ability to take up NO_3^- after short term N deprivation is also attributable to the loss of an active uptake system (Falkowski 1975) and to inactivation of nitrate reductase (Syrett 1981). Inactivation of nitrate reductase alone did not interfere with the initial uptake of NO_3^- since transient internal NO_3^- pools were observed in even N-starved cells (Dortch *et al.* 1984). Details will be discussed in the following "Interaction" section.

4) Urea uptake in N-deplete phase

In the present study, urea uptake after N-starvation and re-supply of urea was observed in the interaction of other N sources such as NO_3^- and NH_4^+ . Surge uptake of urea was not observed in any species. This agrees with the results of no evidence of urea surge uptake by N-starved cells (Bekheet & Syrett 1979; Price & Harrison 1988). Maximum urea uptake rates were 0.044, 0.014, and 0.008 $\mu\text{g-at } 10^{-6}\text{cells}^{-1} \text{ h}^{-1}$ for *Prorocentrum micans*, *Amphidinium carterae*, and *Heterosigma carterae* respectively. However, there are many reports that

urea uptake is enhanced by N deprivation (Rees & Syrett 1979; Horrigan & McCarthy 1981; Price & Harrison 1988). The enhancement of urea uptake is attributed to the removal of NH_4^+ originating from urea in the cell (Rees & Syrett 1979). Increased N-specific urea uptake might be due to a reduction in the cell N quota and retention of all of the urea-N by the N-starved cells.

N Interaction

The present study demonstrated that NO_3^- uptake by *Prorocentrum micans*, *Heterosigma carterae*, and *Amphidinium carterae* could not proceed in the presence of NH_4^+ concentrations as low as 1.6, 1.7, and 0.9 μM respectively before they experienced N deprivation. The three species started to take up NO_3^- only after NH_4^+ reached near zero. An interesting finding was that urea uptake rate exceeded NH_4^+ uptake rate in *Prorocentrum micans* culture during a short-term decrease in NH_4^+ uptake followed a period of rapid uptake in the N-deplete phase. Generally, NH_4^+ influence on urea uptake was weaker compared to that on NO_3^- and NO_3^- influenced on urea uptake when only those two N sources co-existed in the medium for all three species.

N-replete *Prorocentrum micans* (Exp. 1) showed less influence on NO_3^- uptake by both NH_4^+ and urea than *Amphidinium carterae* (Exp. 2) and *Heterosigma carterae* (Exp. 3). In addition, *Prorocentrum micans* used urea more favorably than *Amphidinium carterae* and *Heterosigma carterae* during the period (I), both before and after N starvation. Thus, this species could utilize the three N sources indiscriminately. In contrast, in *Amphidinium carterae*, NH_4^+

strongly influenced on both NO_3^- and urea uptake before N starvation, and only NH_4^+ was taken up preferentially. Both NO_3^- and urea remained near their initial concentration until the NH_4^+ concentration $< 1 \mu\text{M}$. Then, urea and NO_3^- were both taken up almost simultaneously. However, after they experienced N starvation, only urea started to decline in the medium when $> 18 \mu\text{M}$ NH_4^+ existed. On the other hand, NO_3^- was still not utilized at this NH_4^+ concentration. Therefore after N starvation, influence of urea uptake by NH_4^+ decreased but NO_3^- uptake was still influenced. In *Heterosigma carterae* (Exp. 3), NO_3^- was suppressed by NH_4^+ but not urea, before and after N starvation because once NH_4^+ disappeared from the culture medium, NO_3^- was taken up much faster than urea. However, NH_4^+ influence on NO_3^- uptake clearly decreased after N starvation.

Focusing on the interaction between NO_3^- and urea, NO_3^- influence on urea uptake during the aft. II period was slightly strengthened in *Prorocentrum micans*. In contrast, such an influence was weakened in N-deplete *Amphidinium carterae* and *Heterosigma carterae* cultures.

In general, species and nutritional state affect on interaction between NO_3^- and NH_4^+ (Syrett 1981; McCarthy 1981). Inhibition of NO_3^- uptake by NH_4^+ ranged from total suppression (Syrett & Morris 1963; McCarthy & Eppley 1972; Cresswell & Syrett 1979) to simultaneous and comparable rates of NH_4^+ and NO_3^- uptake in cultures (Caperon & Ziemann 1976; Conway 1977) and natural communities (Price *et al.* 1985, Collos *et al.* 1989). Higher concentrations of

NH_4^+ inhibited NO_3^- uptake, but stimulation of NO_3^- uptake has been reported to occur at low NH_4^+ concentrations (Yin 1988).

The mechanism of the inhibition of NO_3^- utilization needs further investigation. Regulatory action at the level of NO_3^- uptake (Eppley & Rogers 1970; Tischner & Lorenzen 1979) and NO_3^- reduction (Syrett & Morris 1963; Hipkin *et al.* 1980) have been suggested to influence NO_3^- uptake. To a certain extent, the effect of NH_4^+ on both mechanisms may be independent (Ullrich 1987). It is known that NO_3^- uptake stops very quickly when NH_4^+ is added and starts when the NH_4^+ has disappeared (Syrett & Morris 1963; Eppley *et al.* 1969a; Conway *et al.* 1976). This inhibition by NH_4^+ is too rapid to be accounted for by the inactivation of nitrate reductase. Probably, the primary and most rapidly acting effect of NH_4^+ on NO_3^- utilization is attributed to an inhibition of the NO_3^- uptake system. Then, this may be followed by the effects on NO_3^- metabolism through inhibition of nitrate reductase activity, by irreversible proteolytic breakdown (Hipkin *et al.* 1980), reversible inactivation (Pistorius *et al.* 1978), or suppression of its synthesis (Morris & Syrett 1963; Amy & Garrett 1974).

The rate of NO_3^- uptake is modulated in response to changes in pools of some organic product of NH_4^+ assimilation (Syrett 1981; Guerrero *et al.* 1981). Highly C-deficient cells did not show inhibition of NO_3^- uptake by NH_4^+ and these cells reduced NO_3^- to NH_4^+ (Syrett & Morris 1963; Thacker & Syrett 1972a; Ullrich 1987). Therefore, NH_4^+ itself may not be an inhibitor and an organic product of NH_4^+ assimilation is suspected to be an inhibitor.

NH_4^+ repressed urea uptake in *Thalassiosira pseudonana* (Lui & Roels 1970). Lund (1987) found that NH_4^+ immediately inhibited urea uptake by *Skeletonema costatum*, while Horrigan and McCarthy (1982) reported that urea uptake inhibition occurred after 30 min. When these two diatom species were N-depleted, NH_4^+ inhibited urea uptake to an even greater extent.

In general, urea suppresses NO_3^- uptake but at a lower level than NH_4^+ (Grant *et al.* 1967; McCarthy & Eppley 1972; Molly & Syrett 1988b). However, simultaneous uptake of urea and other N sources by phytoplankton communities (McCarthy & Eppley 1972; Price *et al.* 1985) and a normal uptake rate of NO_3^- in the presence of $10 \mu\text{g-at N L}^{-1}$ urea by *Skeletonema costatum* (Lund 1987) have been reported. Urea was taken up by a natural phytoplankton assemblage simultaneously with NO_3^- and NH_4^+ , with little influence on the uptake rates of NH_4^+ (Robert *et al.* 1986). Repression of nitrate reductase by urea, which was reported in studies on *Cyclotella cryptica* (Liu & Hellebust 1976) and *Chlorella* (Smith & Thompson 1968) is a possible explanation of the inhibition of NO_3^- uptake by urea.

Nutritional state affects the interaction between urea and other inorganic N sources. NO_3^- uptake inhibition by urea weakened after N starvation in the study of *Skeletonema costatum* (Lund 1987). On the other hand, Molly and Syrett (1988a) reported that urea increased the suppression of NO_3^- uptake. NH_4^+ suppression of urea uptake disappeared due to N starvation (Rees & Syrett 1979). Horrigan & McCarthy (1982) reported that urea and NH_4^+ uptake rates were enhanced even for NO_3^- -sufficient cells.

To conclude, the magnitude of the effect of the interaction of three N sources on uptake rates was species specific, and influenced by N starvation. As it was mentioned in the N preference section, the interaction among N sources was variable and depended on the N sources in the medium. Since NH_4^+ and urea are found in similar concentrations in the sea (Harrison 1992), it is important to consider urea in studies of N interactions.

Increased concentrations and efflux of N

An increase in the external N concentration during the initial interval after the re-addition of N sources occurred in the culture of *Prorocentrum micans* (three N), *Amphidinium carterae* (three N), *Heterosigma carterae* (three N), *Heterosigma carterae* (NO_3^-), and *Heterosigma carterae* (NH_4^+ , culture 2+3). In the *Amphidinium carterae* culture, an increase in the concentration of both NO_3^- and urea occurred. In Exp. 3 and 5, *Heterosigma carterae* excreted NO_3^- . Urea efflux during the initial interval was $-0.006 \mu\text{g-at } 10^6\text{cells}^{-1} \text{ h}^{-1}$ during 0 - 1 h (*Prorocentrum micans*), $-0.03 \text{ g-at } 10^6\text{cells}^{-1} \text{ h}^{-1}$ during 0 - 0.5 h (*Amphidinium carterae*), and $-0.0006 \mu\text{g-at } 10^6\text{cells}^{-1} \text{ h}^{-1}$ during 0 - 1 h (*Heterosigma carterae*) when these three N-starved species were re-supplied with three N sources. Effluxes of NO_3^- of $-0.007 \mu\text{g-at } 10^6\text{cells}^{-1} \text{ h}^{-1}$ (Exp. 3) and $-0.022 \mu\text{g-at } 10^6\text{cells}^{-1} \text{ h}^{-1}$ (Exp. 5), during the initial interval of the N re-supplied phase were observed in N-starved *Heterosigma carterae*.

The initial stage of urea uptake involves a rapid influx and probably an accumulation of an intracellular pool (Antia *et al.* 1991). Excretion of urea in the

form of dissolved organic N is not re-assimilated in the short term. Excretion into the culture medium of ^{14}C -labelled organic products derived from urea-C could explain the lower urea uptake rates (Antia *et al.* 1991).

Efflux of NO_3^- in Exp. 3 coincided with the high uptake rate of NH_4^+ . Therefore, NH_4^+ taken up by N-starved cells may be attributed to this efflux of NO_3^- . The efflux of NO_3^- of N-starved *Heterosigma carterae* in Exp. 5 occurred during the light period, although the N-replete culture showed several periods of efflux of NO_3^- during dark periods. Pujo-Pay *et al.* (1997) reported $< 10\%$ of the NO_3^- uptake was released as DON with the rate of 10.4 to 13.3 $\text{nmol N L}^{-1} \text{ h}^{-1}$. They mentioned the released DON was an important resource for some organisms.

NH_4^+ excretion occurred in NH_4^+ -grown *Heterosigma carterae* culture, and such a phenomenon has been reported often. NH_4^+ excretion was observed by axenic cultures of *Thalassiosira pseudonana* after the addition of 10 $\mu\text{g-at N L}^{-1}$ of urea (Price & Harrison 1988). NH_4^+ excretion also occurred in urea-grown *Phaeodactylum tricornutum* (Rees & Syrett 1979). Urea appears to be one of the sources of NH_4^+ excretion.

Ecology

Amphidinium carterae showed an enhanced preference for NH_4^+ relative to both NO_3^- and urea during the period I and preference for urea relative to NO_3^- during period II. *Prorocentrum micans* also enhanced its preference for urea rather than NO_3^- during N starvation, however, its preference for NH_4^+

decreased. In general, species that increase their preference for NH_4^+ or urea have a better chance to take up a transit N supply of regenerated N, which is mainly NH_4^+ and urea. However, the increased preference for NO_3^- relative to NH_4^+ and urea by *Heterosigma carterae* does not appear to offer an advantage for survival in a N-deplete environment. Nevertheless, N-deprived *Heterosigma carterae* still possessed a much stronger preference for NH_4^+ ($\text{NH}_4^+:\text{NO}_3^-:\text{urea} = 39:1:5.2$) compared to the other two species.

The reduction in the ability to take up NO_3^- and the increase in the ability to take up NH_4^+ may be an ecological acclimation by N-deprived phytoplankton in oligotrophic waters (Dortch *et al.* 1982). NO_3^- is recycled over a much longer time period and it is usually supplied continuously at low rates by eddy diffusion from deeper NO_3^- -rich waters (Dugdale 1967; Eppley *et al.* 1979). Sporadic NO_3^- supply by upwelling, frontal mixing, and internal waves occurs in the euphotic zone at very slow rates (Walsh *et al.* 1978; Pingree *et al.* 1978; Parsons *et al.* 1981; Cullen *et al.* 1983). These physical events also dilute the phytoplankton community in the euphotic zone. Therefore, the demand for the nutrient by phytoplankton decreases and NO_3^- remains in the euphotic zone for some time, which reduces the benefits for transient elevated uptake rates of NO_3^- (Parslow *et al.* 1984b). Compared to NO_3^- , NH_4^+ and urea are recycled rapidly within the euphotic zone and introduced to the system by animal excretion (Dugdale 1967). Maintaining a high uptake capability during N starvation results in metabolic costs (Raven 1986). Therefore, it is probably more beneficial for cells to have a high uptake capability for NH_4^+ and urea rather than NO_3^- because NH_4^+ and

urea are recycled N sources. Interestingly, annual phytoplankton production expressed as N production in well mixed water (Western English Channel) was mainly based on recycling of N forms such as NH_4^+ (54%), but not new N forms (Maguer *et al.* 1995).

To conclude, phytoplankton which are capable of assimilating NH_4^+ or urea rapidly after they are N starved may have an advantage for species succession and growth in the environment where N limitation is the primary stress. Therefore, *Amphidinium carterae* that increased the preference for NH_4^+ relative to NO_3^- (period I), and the preference for urea relative to NO_3^- (period II), can acclimate to N-deplete water, while *Prorocentrum micans* and *Heterosigma carterae* increased their preference for NO_3^- during period I or II.

Growth rate

Growth rates were 0.30 for *Prorocentrum micans* (three N sources), 0.76 for *Amphidinium carterae* (three N sources), 0.56 for *Heterosigma carterae* (three N sources), 1.0 for *Heterosigma carterae* (NO_3^- + continuous light), 0.72 for *Heterosigma carterae* (NO_3^- + L:D cycle), 1.1 for *Heterosigma carterae* (NH_4^+) (culture 1), and 1.02 d^{-1} for *Heterosigma carterae* (NH_4^+) (culture 2+3). *Prorocentrum micans* had the lowest growth rate (0.30 d^{-1}). *Prorocentrum micans* grown in f/2 medium under continuous light and $19 \pm 10^\circ\text{C}$ showed growth rates ranging from 0.59 to 0.99 d^{-1} in the study by Costas (1990). The temperature used in the present study (17°C) was lower than the 19°C in Costas' study and could partially account for the lower growth rate in

Prorocentrum micans. Growth rates of *Prorocentrum micans* were measured in a culture containing a mixture of other dinoflagellates (Fedorov & Il'yash 1991). *Prorocentrum micans* and other dinoflagellates such as *Glenodinium foliaceum*, *Excuviala cordata*, *Gymnodinium kovalevskii*, and *Olisthodiscus luteus* (*Heterosigma carterae*) were grown in Goldberg medium (Lanskaya 1971) under natural illumination at 20 - 22°C. The growth rate of *Prorocentrum micans* was 0.2 d⁻¹. When *Prorocentrum micans* was grown by itself without the interaction with other species, its growth rate was also low and < 0.5 d⁻¹, even though a relatively high temperature was used. These results are in agreement with this study, and indicate that *Prorocentrum micans* possesses a low growth rate. Fedorov and Il'yash (1991) concluded that *Prorocentrum micans* was able to increase its population density slowly but steadily by utilizing limited amounts of resources and classified it as a "patient" species.

Amphidinium carterae had the highest growth rate of 0.76 d⁻¹ among the other three species grown on three N sources (Exp. 2). This species also exhibited the same growth rate grown under a 14:10 L:D cycle at 20°C when 50 µM NH₄⁺ was given to the culture at the beginning of the light period (Wheeler *et al.* 1983). However, if the same concentration of NH₄⁺ was given at the beginning of the dark period, the growth rate increased to 1.4 d⁻¹. *Amphidinium carterae* has been used for many studies because it grows well in various culture conditions.

The growth rates of *Heterosigma carterae* ranged from 0.56 to 1.1 d⁻¹ depending on culture conditions. Since this is the first study for *Heterosigma*

carterae grown on three combined N sources, there are no comparable data on growth rates from the literature. However, growth rates on individual N sources are available. All growth rates were $< 0.8 \text{ d}^{-1}$ under 14:10 L:D photoperiod of $160 \mu\text{mol photon m}^{-2} \text{ s}^{-1}$ at 20°C with $100 \mu\text{M}$ of each N (Hoe Chang & Page 1995). Another study by Wood & Flynn (1995) reported 0.9 d^{-1} and 0.6 d^{-1} when grown on NH_4^+ and NO_3^- of 75% ESAW (Harrison *et al.* 1980) respectively in a 12:12 L:D cycle at 18°C . The growth rates of NO_3^- and NH_4^+ grown cells in the present study were generally higher than those of literature values.

Light : Dark cycle

1) Cell division and fluorescence number

An expected step-wise increase in fluorescence, which indicates synchronicity and phasing of growth to the L:D cycle, was not evident in *Heterosigma carterae* under the 14:10 L:D cycle (Exp. 5). Therefore, the occurrence of cell division at night could not be detected. However, the fluorescence increased much more smoothly in cultures under continuous light (Exp. 4). The growth rates for Exp. 4 and 5 were 1.00 d^{-1} (0 - 64 h) and 0.72 d^{-1} (49 - 105 h) respectively. Growth rate often varies with a 24 h periodicity and the timing of division depends on experimental conditions and species (Sweeney 1983).

2) Uptake diel periodicity

Diel periodicity of NO_3^- uptake occurred during log phase growth. N-replete *Heterosigma carterae* grown on NO_3^- under a L:D cycle showed high NO_3^- uptake rate during the light period and at the beginning of the dark period. At the end of dark period, uptake rates were dramatically decreased to negative values or values close to zero. During early log phase, a large decrease in uptake rate was not observed in the culture under continuous light (Exp. 4). This observation agreed with findings by Cochlan *et al.* (1991) who found that NO_3^- uptake rates were maximal during the light periods and decreased during the dark periods for *Micromonas pusilla*. The outdoor culture of *Chaetoceros* sp. which was grown on low N also exhibited cyclic variations in NO_3^- uptake with the maximum at night and the minimum during the day (Malone *et al.* 1975).

In the present study, after N starvation, NO_3^- uptake occurred during the dark period. The uptake rate of N-deplete cells in the dark was $0.017 \mu\text{g-at } 10^6 \text{ cells}^{-1} \text{ h}^{-1}$ and higher than that of N-replete cells. This agrees with the finding that *Pavlova lutheri* grown on low N showed an increase in the relative importance of potential nighttime N uptake (Laws & Wong 1978).

N availability has been considered a determining factor of the enhancement of nighttime uptake. When *Gyrodinium aureolum* was N-starved for 24 h, it exhibited an increase in nighttime NO_3^- uptake (Paasche *et al.* 1984) even though it did not show nighttime NO_3^- uptake before N starvation. N-starved dinoflagellates, *Pyrocystis noctiluca* and *Dissodinium lunula* were independent of the L:D cycle in their NO_3^- uptake capacity (Bhovichitra & Swift

1977). N limitation may enhance the potential for dark N uptake more than light uptake. Consequently, diel periodicity of N uptake becomes less evident.

The enhancement of light independence of N uptake might be an adaptive response to N limitation since N-starved phytoplankton could optimize their uptake capability under even low light. Cochlan *et al.* (1991) found that with increased N limitation, the relative dark uptake capacity increased four-fold for total (light + dark) NO_3^- uptake, and two-fold for total NH_4^+ uptake.

A consequence of enhanced dark N uptake by N starvation is the dampening of the diel N uptake periodicity. Laboratory studies by Harrison (1976) showed dark uptake by *Gonyaulax polydra* increased to ca. 40% of daytime uptake rate in N-starved cultures. On the other hand, in N-sufficient cultures, N uptake during nighttime was only ca. 20% of that during daytime. The absence of diel periodicity in NO_3^- uptake occurred in axenic cyclostat cultures (Picard 1976). Dark NO_3^- uptake capacity of cyclostat cultures of the prymnesiophyte, *Pavlova lutheri* and the chlorophyte, *Dunaliella tertiolecta* exceeded the supply rate of NO_3^- at high dilution rates, which suggested that the environment had less available N for cells (Laws & Caperon 1976; Laws & Wong 1978). The coccolithophore, *Emiliania huxleyi*, which was grown in both NO_3^- - and NH_4^+ -limited cyclostat cultures did not exhibit diel periodicity (Eppley *et al.* 1971).

There are two contrasting examples in field studies. In NO_3^- -depleted water off Peru with a dinoflagellate bloom dominated by *Gymnodinium sanguineum*, NO_3^- uptake during nighttime was ca. 50% of that during the

daytime (Dortch & Maske 1982). On the other hand, in the bloom off Baja California, which was dominated by *Gonyaulax polyedra*, night time NO_3^- uptake was 10 - 20% of daytime NO_3^- uptake (MacIsaac 1978). The later case had a higher NO_3^- concentration than the former case in the surface waters where phytoplankton resided. In addition, the nitracline off Baja California was shallower than off Peru and thus a shorter downward vertical migration in order to obtain NO_3^- . This result agreed with the field study by Harrison (1976), which revealed the dampening effect on N uptake by red tide populations dominated by *Gonyaulax polyedra*.

3) *Heterosigma carterae* and dark NO_3^- uptake

In the present study, high NO_3^- uptake occurred during the light and not during the dark before NO_3^- deprivation. Low NO_3^- uptake (81 - 90 h, 105 - 114 h) and even efflux of NO_3^- (32.5 - 42 h, 57 - 66 h) occurred at the end of dark periods. However, NO_3^- uptake rate in the dark by N-starved cells was positive and higher than by N-replete cells.

During diel migration of *Heterosigma carterae*, the cells stay close to the surface in the day time to carry out photosynthesis and migrate downwards to deeper water at night to take up nutrients (Watanabe *et al.* 1983; Yamochi & Abe 1984; Nagasaki *et al.* 1996). Considering that maximal nitrate reductase activity (Eppley & Harrison 1975) occurs during the day time, NO_3^- uptake during night time via vertical migration is not efficient (Raven 1986). In addition, diel migration costs are metabolically high. Therefore, night-time NO_3^- uptake does

not contribute to the entire supply of nutrients for *Heterosigma carterae*.

However, considering that N limitation increased the SAV ratio (Cochlan *et al.* 1991) and increased nitrate reductase activity during the dark period (Eppley & Harrison 1975), vertical migration at night might be more beneficial for N-starved *Heterosigma carterae* than N-replete cells.

CONCLUSIONS

This dissertation examined N uptake by the dinoflagellates, *Prorocentrum micans* and *Amphidinium carterae*, and the raphidophyte, *Heterosigma carterae* as a function of the photoperiod and N physiological states. The specific findings of the research are summarized below.

1. A change in the relative preference of the three N sources occurred during N deprivation. N-deplete *Prorocentrum micans* increased its preference for urea relative to both NH_4^+ and NO_3^- . N-deplete *Amphidinium carterae* enhanced its preference for NH_4^+ relative to both NO_3^- and urea, and its preference for urea relative to NO_3^- under the interaction of three N sources. The preference for NO_3^- was enhanced by N-deprived *Heterosigma carterae*.
2. Strong NH_4^+ influence on NO_3^- and urea uptake were observed in N-replete *Amphidinium carterae* and *Heterosigma carterae*. N-replete *Prorocentrum micans* only showed strong NH_4^+ influence on NO_3^- uptake, but not on urea uptake. N deprivation weakened the influence of NH_4^+ on urea uptake in *Heterosigma carterae*. The N uptake preference depended on the interactions of each N source.
3. NO_3^- uptake needed a longer acclimation period after the NO_3^- pulse in N-starved *Heterosigma carterae* grown under a light:dark cycle than under continuous lights. A short acclimation period for NO_3^- uptake occurred in

Prorocentrum micans, but not in *Amphidinium carterae* and *Heterosigma carterae* grown on three N sources. The duration of the acclimation periods appeared to be influenced by the light cycle and species specificity.

4. The uptake of NO_3^- by *Heterosigma carterae* was phased by a light:dark cycle. NO_3^- disappearance in the culture medium accompanied by a high uptake rate occurred mostly during the light periods and only a small disappearance accompanied by a low uptake rate and an efflux occurred during the dark periods. This uptake cycle may be due to nitrate reductase activity, which usually decreases at night. Diel vertical migration to take up NO_3^- in deeper water at night seems less likely than previously thought for *Heterosigma carterae*.

FUTURE RESEARCH SUGGESTIONS

The outstanding question is why N-deprivation changed the magnitude of N preference by marine phytoplankton. The impact of N deprivation on the mechanisms involved in the uptake of each N source needs further investigation. The change in the interaction among N sources during the N deprivation also needs to be examined under various conditions such as the availability of light, lower concentrations of N, and widely ranging periods of N starvation.

An increase in the preference for urea as a N source during N starvation seems a general phenomenon in marine phytoplankton, which was observed in this study on dinoflagellates and other previous studies on a diatom and coccolithophores. However, the evidence for a decrease in the preference for urea by *Heterosigma carterae* (raphidophyte) suggests species or even group specificity.

It was a surprise that N-replete *Heterosigma carterae* showed negative or very small NO_3^- uptake rates during dark periods because it is known to vertically migrate downwards at night, presumably to take up nutrients. N-deplete *Heterosigma carterae* showed dark uptake of NO_3^- . However, unfortunately the dark period occurred when the cells had taken up most of the re-added NO_3^- , and therefore it was not possible to determine the effect of N starvation on dark uptake. Therefore, it is more interesting to re-add a higher concentration of NO_3^- at the beginning of the dark period, which provides a longer period of observation to determine the influence of N deprivation on NO_3^- uptake in the dark.

Part II

RESULTS

Isotope fractionation

1) *Prorocentrum micans* grown on NH_4^+ , NO_3^- , and urea

In the N-sufficient phase (0 - 106 h), NO_3^- and urea were used along with NH_4^+ (Fig. 29). However, NO_3^- was completely consumed before urea. During growth mainly on NH_4^+ , the apparent isotope discrimination was relatively large and decreased upon exhaustion of NH_4^+ (Fig. 30). At this time (31 h), NH_4^+ had been completely incorporated into PN and $\delta^{15}\text{N}_{\text{PN}}$ was in good agreement with the expected value of -1.14‰ of $\delta^{15}\text{N}_{\text{AS}}$ (Table 3). NO_3^- uptake was accompanied by a small change due to both a smaller $\epsilon(\text{NO}_3^-)$ and a significant amount of preexisting PN produced during growth on NH_4^+ . In the 65 - 106 h time period, $\delta^{15}\text{N}_{\text{PN}}$ showed a slight increase due to the uptake of urea. At stationary phase, the $\delta^{15}\text{N}_{\text{PN}}$ was 0.24‰ . This value was in good agreement with the $\delta^{15}\text{N}_{\text{mx}}$ of 0.26‰ , which was expected when all three N sources were completely taken up. The model gave a good fit for the $\epsilon(\text{NH}_4)$ value of 12‰ . However, during the drawdown of NO_3^- and urea when the model used an $\epsilon(\text{urea})$ of 0‰ , it systematically overestimated $\delta^{15}\text{N}_{\text{PN}}$.

During the N re-supply phase, again, NH_4^+ and urea were immediately utilized, and NO_3^- uptake coincided with the complete consumption of NH_4^+ . Using the same variables as in the N-sufficient phase, the model gave a good fit for $\epsilon(\text{NH}_4^+)$. Again, the model systematically overestimated $\delta^{15}\text{N}_{\text{PN}}$ during the

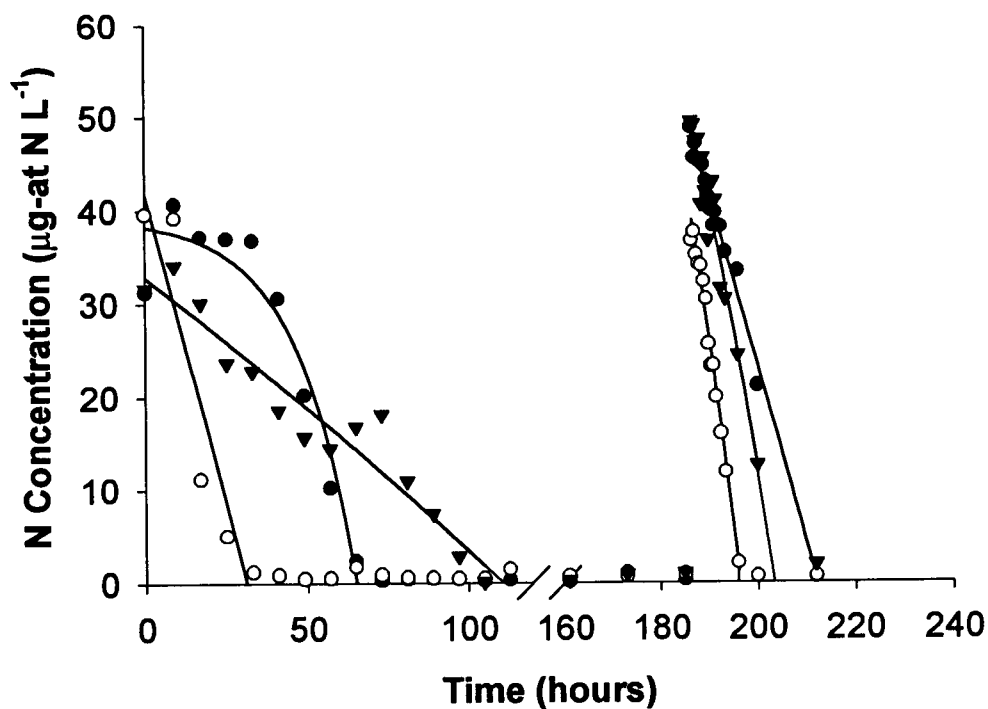


Figure 29 Time series of $[\text{NO}_3^-]$ (●), $[\text{NH}_4^+]$ (○) and [urea] (▼) during the growth of *Prorocentrum micans* grown on NO_3^- , NH_4^+ , and urea under continuous light. Culture was N-starved between 105 and 186.5 h and then $36.6 \mu\text{g-at N L}^{-1} \text{NH}_4^+$, $48.7 \mu\text{g-at N L}^{-1} \text{NO}_3^-$, and $49.4 \mu\text{g-at N L}^{-1}$ urea were added at 186.5 h. The best fits for the concentrations were determined by the dissolved N data using the equation: $y = a \cdot (1 - \text{EXP}(b \cdot (x - c)))$ where a is an initial N concentration, b is a co-efficient number, and c is the time when N reached 0, and are indicated by the solid lines.

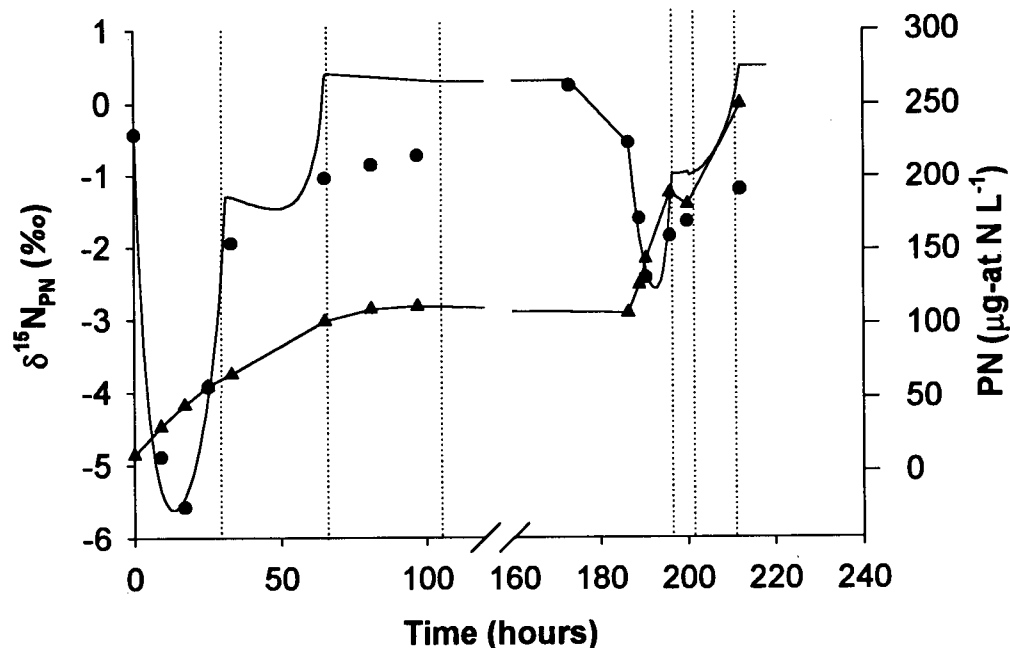


Figure 30 Time series of PN(▲) and $\delta^{15}\text{N}_{\text{PN}}$ (●) during the growth of *Prorocentrum micans* grown on NO_3^- , NH_4^+ , and urea under continuous light. Culture was N-starved between 105 and 186.5 h and then $36.6 \mu\text{g-at N L}^{-1} \text{NH}_4^+$, $48.7 \mu\text{g-at N L}^{-1} \text{NO}_3^-$, and $49.4 \mu\text{g-at N L}^{-1}$ urea were added at 186.5 h. The $\delta^{15}\text{N}_{\text{PN}}$ as predicted by the multiple N source uptake model is shown by the solid line. The 3 dotted lines indicate times when $[\text{NH}_4^+]$, $[\text{NO}_3^-]$ and $[\text{urea}]$ fits, determined by the dissolved N data to the concentration data in Fig. 29, reached 0, respectively.

Table 3. Listing of variables and definitions used in the multiple N source uptake model.

Variable	Definition	Value*
PN_m	Measured PN concentration	
ΣPN_x	Calculated PN concentration from dissolved N drawdown	
PN_i	Initial PN concentration	
$\delta^{15}N_{NS}$	$\delta^{15}N$ of the initial NO_3^- source	3.04‰
$\delta^{15}N_{AS}$	$\delta^{15}N$ of the initial NH_4^+ source	1.14‰
$\delta^{15}N_{US}$	$\delta^{15}N$ of the initial urea source	0.74‰
$\delta^{15}N_{MX}$	$\delta^{15}N$ of the initial mixed N sources (calculated from mass balance)	0.26-0.46‰
$\delta^{15}N_{PNI}$	$\delta^{15}N$ of PN_i	
$\varepsilon(NO_3)$	Isotope fractionation for the overall reaction: $NO_3^- \rightarrow PN$	
$\varepsilon(NH_4)$	Isotope fractionation for the overall reaction: $NH_4^+ \rightarrow PN$	
$\varepsilon(urea)$	Isotope fractionation for the overall reaction: Urea $\rightarrow PN$	0‰
Δ	Apparent isotope fractionation or discrimination, i.e. $\delta^{15}N_{PN} - \delta^{15}N_{st}$	

*: constant values are given.

consumption of NO_3^- and urea. All the base variables are summarized in Table

4. A sensitivity analysis is presented later.

2) *Amphidinium carterae* grown on NH_4^+ , NO_3^- , and urea

In the N-sufficient phase (0 - 101 h), NH_4^+ was utilized first followed by the simultaneous uptake of NO_3^- and urea (Fig. 31). Growth on NH_4^+ produced a large initial decrease in $\delta^{15}\text{N}_{\text{PN}}$ to values of -8.94 to -12.1‰ (Fig. 32). $\delta^{15}\text{N}_{\text{PN}}$ then increased to about -0.6 ‰ during the simultaneous growth on urea and NO_3^- (60 - 94 h) and finally reached 0.73‰ at the stationary phase. The model gave a relatively good fit for the NH_4^+ uptake phase with $\varepsilon(\text{NH}_4^+)$ values of 20‰. However, the model systematically underestimated $\delta^{15}\text{N}_{\text{PN}}$ during the simultaneous growth on urea and NO_3^- . $\delta^{15}\text{N}_{\text{ST}}$ of 0.76‰ showed a relatively good agreement with the initial $\delta^{15}\text{N}_{\text{MX}}$ (0.27‰).

In the N re-supply phase, NH_4^+ was taken up immediately, followed by simultaneous uptake of urea and NO_3^- . $\delta^{15}\text{N}$ was -0.24‰ (193 h) and, then, increased to 0.33 and 0.04‰ at 30 min and 1 h respectively after the re-addition of the three N sources. Positive $\delta^{15}\text{N}_{\text{PN}}$ values indicate more incorporation of ^{15}N into the cells than ^{14}N . Using the same variables as in the N-sufficient phase, the model systematically underestimated the $\delta^{15}\text{N}_{\text{PN}}$ during the growth on any N. A sensitivity study for *Amphidinium carterae* is also provided later.

Table 4 Variables and their values used in the multiple N source uptake model. *Prorocentrum micans*, *Amphidinium carterae*, and *Heterosigma carterae* were grown on multiple N sources (NO_3^- , NH_4^+ , and urea) under N-sufficient conditions. After 0 - 82 h of starvation, all three N sources were added simultaneously to the culture (i.e. N re-supply phase). *Heterosigma carterae* was grown on NO_3^- under NO_3^- -sufficient condition. After 52 h of N starvation, NO_3^- was added to the culture (i.e. N re-supply phase). Symbols are defined in Table 3.

Species	$\epsilon(\text{NH}_4^+)$ (‰)	$\epsilon(\text{NO}_3^-)$ (‰)	PN_i (μM)	$\delta^{15}\text{N}_i^*$ (‰)
N-sufficient phase				
<i>Prorocentrum micans</i>	12	9	12	- 0.42
<i>Amphidinium carterae</i>	20	0	3.04	0.27
<i>Heterosigma carterae</i>	24	9	3.87	- 1.36
<i>Heterosigma carterae</i>	----	5	5.1	1.08
N re-supply phase				
<i>Prorocentrum micans</i>	18	9	107.4	- 0.54
<i>Amphidinium carterae</i>	4	0	77.1	- 0.24
<i>Heterosigma carterae</i>	20	5	100	- 0.01
<i>Heterosigma carterae</i>	----	9	92.9	0.78

*: $\delta^{15}\text{N}_i$ in the initial N source

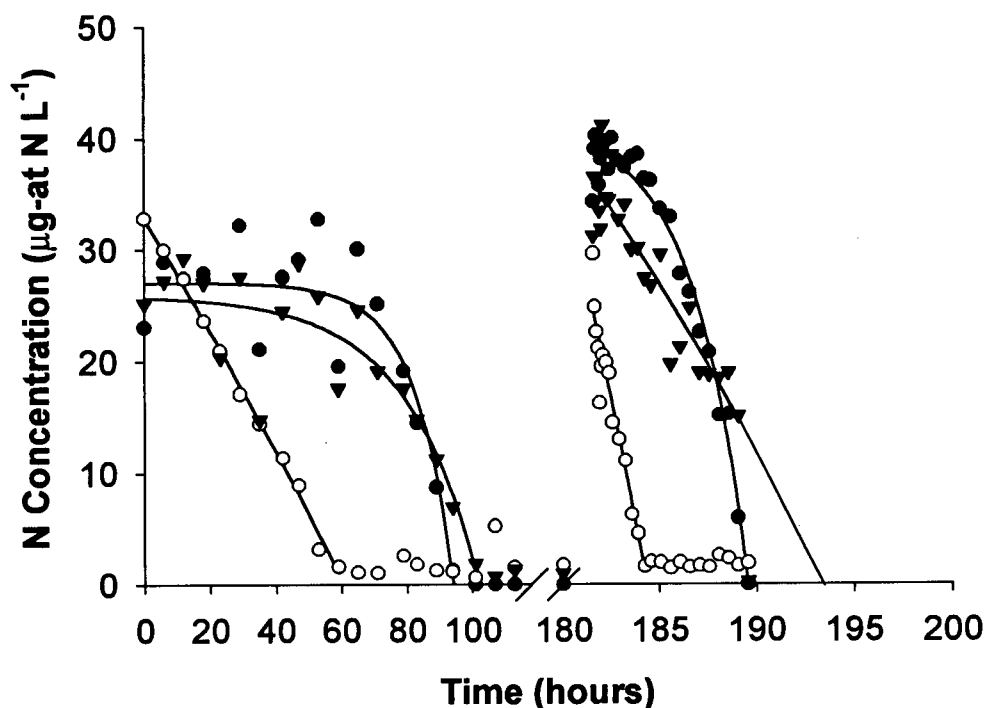


Figure 31 Time series of $[\text{NO}_3^-]$ (\bullet), $[\text{NH}_4^+]$ (\circ) and $[\text{urea}]$ (\blacktriangledown) during the growth of *Amphidinium carterae* grown on NO_3^- , NH_4^+ , and urea under continuous light. Culture was N-starved between 119 and 193.5 h and then $29.6 \mu\text{g-at N L}^{-1} \text{NH}_4^+$, $34.3 \mu\text{g-at N L}^{-1} \text{NO}_3^-$, and $31.2 \mu\text{g-at N L}^{-1} \text{urea}$ were added at 193.5 h. The best fits for the concentrations were determined by the dissolved N data using the equation: $y = a*(1-\text{EXP}(b*(x-c)))$ where a is an initial N concentration, b is a co-efficient number, and c is the time when N reached 0, and are indicated by the solid lines.

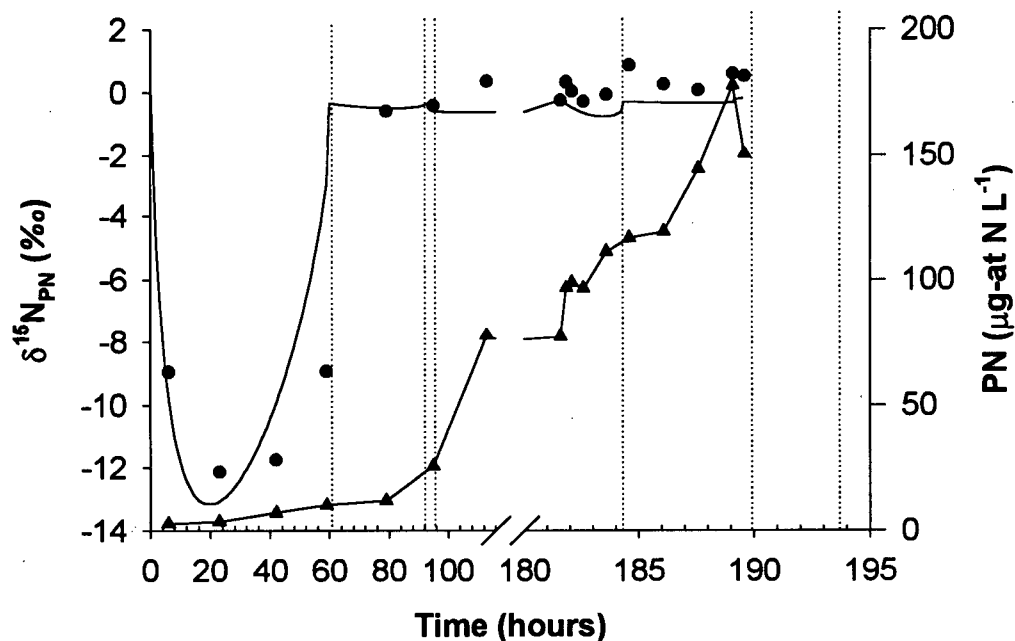


Figure 32 Time series of PN (▲) and $\delta^{15}\text{N}_{\text{PN}}$ (●) during the growth of *Amphidinium carterae* grown on NO_3^- , NH_4^+ , and urea under continuous light. Culture was N-starved between 119 and 193.5 h and then $29.6 \mu\text{g-at N L}^{-1} \text{NH}_4^+$, $34.3 \mu\text{g-at N L}^{-1} \text{NO}_3^-$, and $31.2 \mu\text{g-at N L}^{-1} \text{urea}$ were added at 193.5 h. The $\delta^{15}\text{N}_{\text{PN}}$ as predicted by the multiple N source uptake model is shown by the solid line. The 3 dotted lines indicate times when $[\text{NH}_4^+]$, $[\text{NO}_3^-]$ and $[\text{urea}]$ fits, determined by the dissolved N data to the concentration data in Fig. 31, reached 0, respectively.

3) *Heterosigma carterae* grown on NH_4^+ , NO_3^- , and urea

In the N-sufficient phase (0 - 175 h), the three N sources were utilized in sequence (Fig. 33). NO_3^- was taken up only when NH_4^+ decreased to $< 1 \mu\text{M}$. Large $\delta^{15}\text{N}_{\text{PN}}$ values such as -8.16, -13.3, and -10.6‰ were observed during the growth on NH_4^+ at 11, 36, and 49 h respectively (Fig. 34). The isotope discrimination decreased to a small value upon exhaustion of NH_4^+ . At stationary phase, the $\delta^{15}\text{N}_{\text{PN}}$ was -0.41‰. This is a little lower than the value of 0.46‰ for $\delta^{15}\text{N}_{\text{MX}}$. The model gave a relatively good fit. When the exhaustion of NH_4^+ occurred (68 h), $\delta^{15}\text{N}_{\text{PN}}$ (-2.32‰) was in good agreement with the expected values of -1.14‰ for $\delta^{15}\text{N}_{\text{AS}}$.

Since urea was hardly consumed in the N-replete phase, cells were not N-starved completely. NH_4^+ was used first and followed by NO_3^- and urea in the N re-supply phase. The $\delta^{15}\text{N}_{\text{PN}}$ showed a relatively large decrease which was well predicted by the model using the same variables as in the N-sufficient phase. An $\varepsilon(\text{NH}_4^+)$ value of 20‰ was used for the fit in N-deplete phase.

4) *Heterosigma carterae* grown on NO_3^-

Figure 35 shows the time series data for the nutrient fit. NO_3^- was taken up without showing a distinct lag phase. In the N-sufficient phase (0 - 63 h), the model gave a relatively good fit with $\varepsilon(\text{NO}_3^-)$ values of 5‰ (Fig. 36). However, $\delta^{15}\text{N}_{\text{PN}}$ at the beginning of the experiment was lower (1.08‰) than the expected value (3.04‰). During the log phase, the $\delta^{15}\text{N}_{\text{PN}}$ decreased to -1.04‰ at 48 h

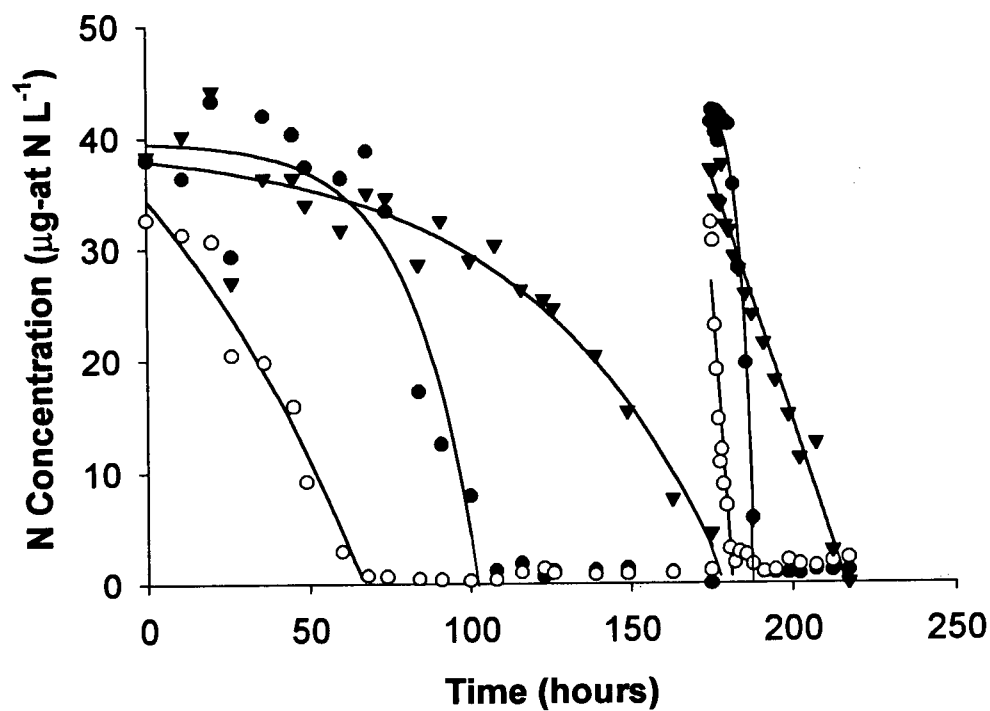


Figure 33 Time series of $[\text{NO}_3^-]$ (●), $[\text{NH}_4^+]$ (○) and [urea] (▼) during the growth of *Heterosigma carterae* grown on NO_3^- , NH_4^+ , and urea under continuous light. Culture was added $32.2 \mu\text{g-at N L}^{-1} \text{NH}_4^+$, $41.2 \mu\text{g-at N L}^{-1} \text{NO}_3^-$, and $37 \mu\text{g-at N L}^{-1}$ urea at 175 h. The best fits for the concentrations were determined by the dissolved N data using the equation: $y = a*(1-\text{EXP}(b*(x-c)))$ where a is an initial N concentration, b is a co-efficient number, and c is the time when N reached 0, and are indicated by the solid lines.

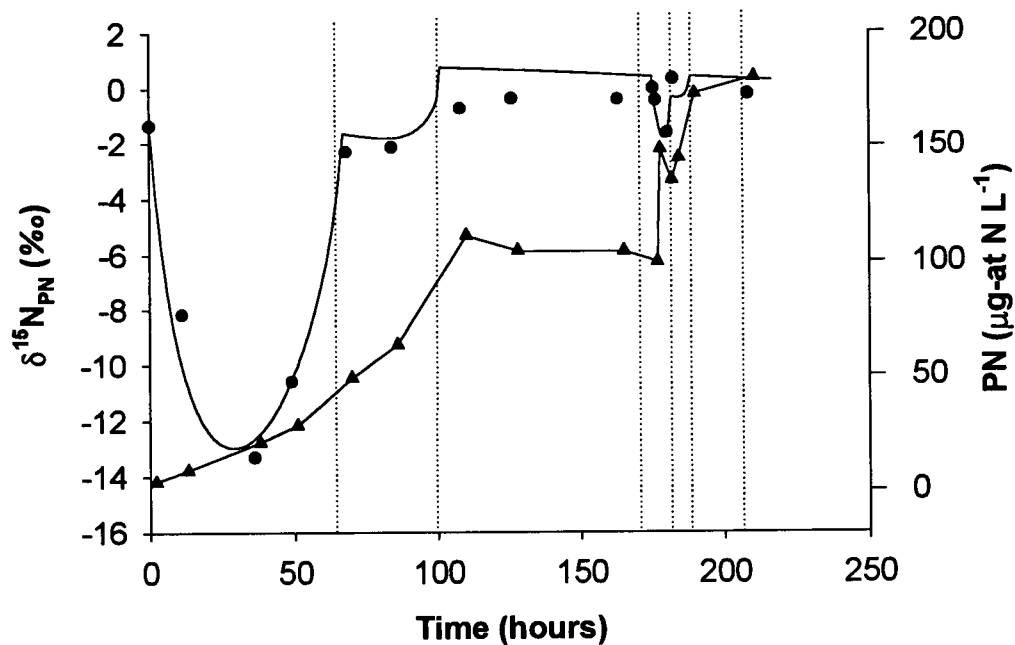


Figure 34 Time series of PN (▲) and $\delta^{15}\text{N}_{\text{PN}}$ (●) during the growth of *Heterosigma carterae* grown on NO_3^- , NH_4^+ , and urea under continuous light. Nitrogen additions at 175 h to the culture were $32.2 \mu\text{g-at N L}^{-1} \text{NH}_4^+$, $41.2 \mu\text{g-at N L}^{-1} \text{NO}_3^-$, and $37 \mu\text{g-at N L}^{-1}$ urea. The $\delta^{15}\text{N}_{\text{PN}}$ as predicted by the multiple N source uptake model is shown by the solid line. The 3 dotted lines indicate times when $[\text{NH}_4^+]$, $[\text{NO}_3^-]$ and [urea] fits, determined by the dissolved N data to the concentration data in Fig. 33, reached 0, respectively.

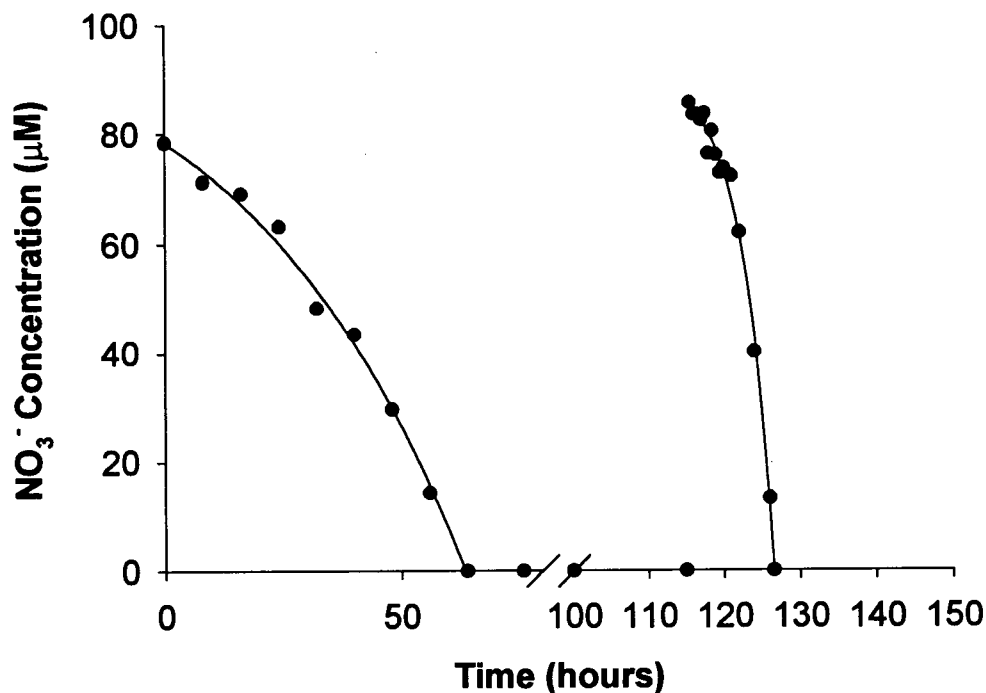


Figure 35 Time series of $[\text{NO}_3^-]$ during the growth of *Heterosigma carterae* grown on NO_3^- under continuous light. Culture was N-starved between 64 and 115.5 h and then $85.6 \mu\text{g-at N L}^{-1} \text{NO}_3^-$ was added at 115.5 h. The best fits for the concentrations were determined by the dissolved N data using the equation: $y = a \cdot (1 - \text{EXP}(b \cdot (x - c)))$ where a is an initial N concentration, b is a co-efficient number, and c is the time when N reached 0, and are indicated by the solid lines.

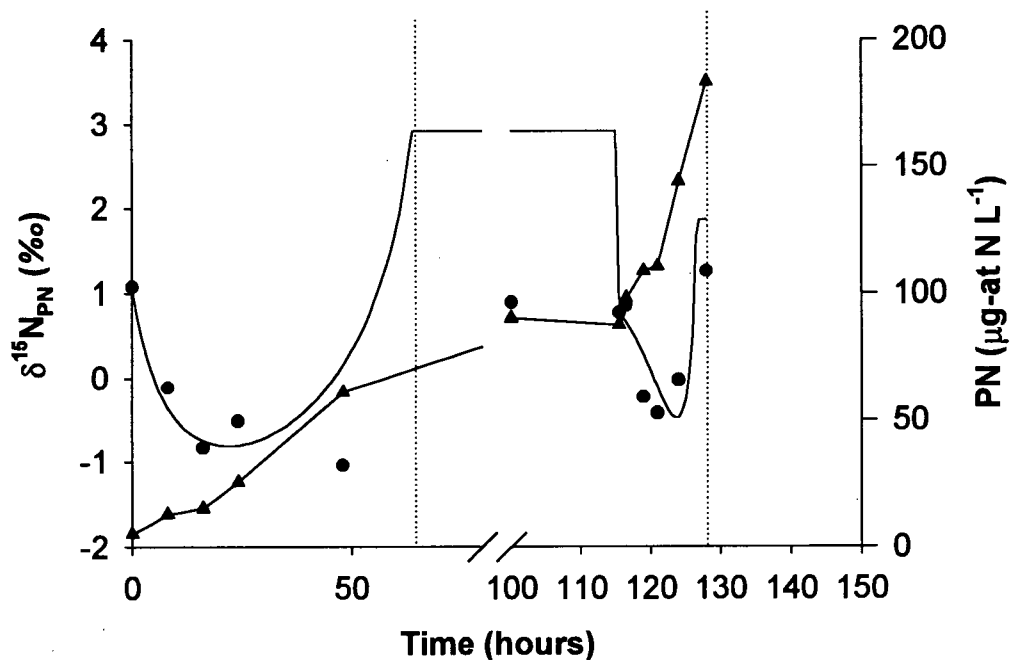


Figure 36 Time series of PN (▲) and $\delta^{15}\text{N}_{\text{PN}}$ (●) during the growth of *Heterosigma carterae* grown on NO_3^- under continuous light. Culture was N-starved between 64 and 115.5 h and then $85.6 \mu\text{g-at N L}^{-1} \text{NO}_3^-$ was added at 115.5 h. The $\delta^{15}\text{N}_{\text{PN}}$ as predicted by the N source uptake model is shown by the solid line. The dotted line indicates times when $[\text{NO}_3^-]$ fits, determined by the dissolved N data to the concentration data in Fig. 35, reached 0.

from the expected value for 3.04‰ for the NO_3^- source. During N starvation (100 h), the $\delta^{15}\text{N}_{\text{PN}}$ was 0.90‰, which was lower than the expected value of $\delta^{15}\text{N}_{\text{NS}}$ (3.04‰).

In the N re-supply phase, NO_3^- was not taken up immediately. Positive $\delta^{15}\text{N}_{\text{PN}}$ values (0.78 and 0.86‰) similar to the one in the stationary phase occurred when re-added NO_3^- was not utilized (115.5 - 118 h). At the end of this period of NO_3^- re-supply (119 h), $\delta^{15}\text{N}$ decreased again to -0.23‰. Then, negative values (-0.42 and -0.02‰) followed at 121 and 124 h respectively. During the exhaustion of NO_3^- (128 h), $\delta^{15}\text{N}_{\text{PN}}$ became positive (1.26‰) again. An $\varepsilon(\text{NH}_4^+)$ of 9‰ was used for the model fit.

SENSITIVITY ANALYSIS

Changes in various variables were made to study their effect on the $\delta^{15}\text{N}_{\text{PN}}$ in N-replete and N re-addition conditions. The value of $\epsilon(\text{urea})$ was taken as a constant of 0‰. Changes in the values of $\epsilon(\text{NH}_4^+)$, $\epsilon(\text{NO}_3^-)$, and PN_i are presented in Table 3.

1) *Prorocentrum micans* grown on NH_4^+ , NO_3^- , and urea

In N-replete phase, variations in the values of $\epsilon(\text{NH}_4^+)$ produced large changes in the $\delta^{15}\text{N}_{\text{PN}}$ (Fig. 37a). The $\epsilon(\text{NH}_4^+)$ that gave the best fit was 12‰. During this N-replete period, urea which has a lower ϵ value than NH_4^+ , was also taken up with NH_4^+ . The values of $\epsilon(\text{NO}_3^-)$ from various fits ranged from 5 to 9‰ (Fig. 37b). Since $\delta^{15}\text{N}_{\text{PN}}$ data during the drawdown of NO_3^- were lacking, it was impossible to obtain the best $\epsilon(\text{NO}_3^-)$. Changes in PN_i were made since PN_i concentration seemed large in this culture ($11.1 \mu\text{g-at N L}^{-1}$). PN_i values used for the fit ranged from 11 to $13 \mu\text{g-at N L}^{-1}$ (Fig. 37c). A higher PN_i value tended to improve the fit.

Again, variations in the values of $\epsilon(\text{NH}_4^+)$ produced a large change during the N-deplete phase (Fig. 38). Interestingly in the N-replete phase, the $\epsilon(\text{NH}_4^+)$ that gave the best fit, increased to 18‰ from 12‰.

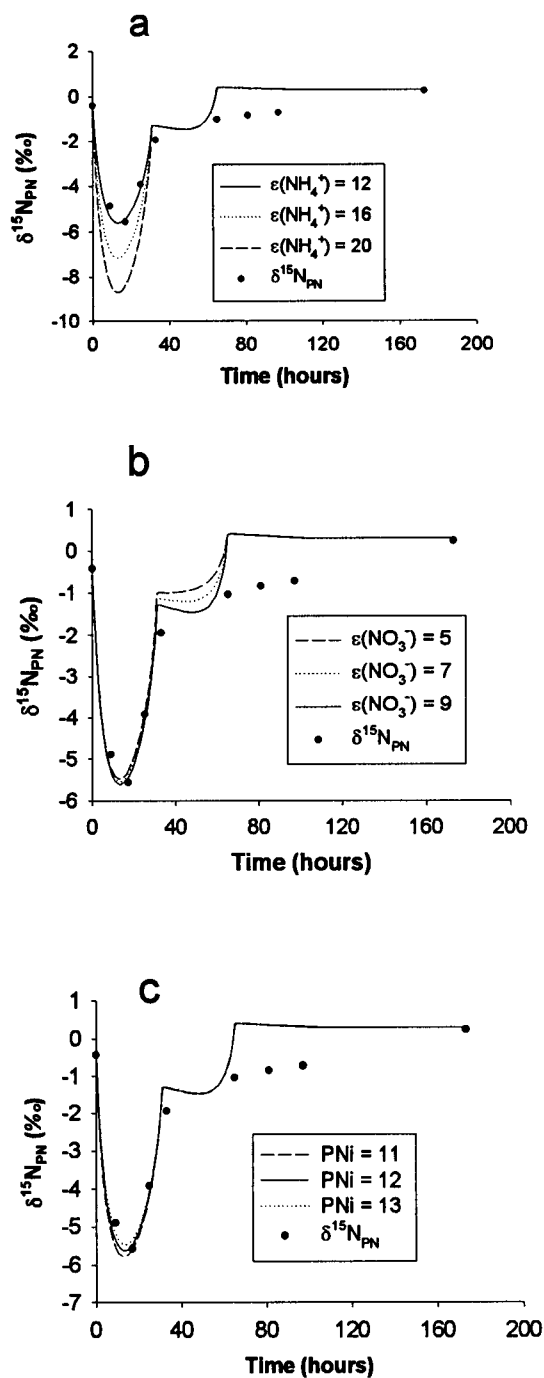


Figure 37 Response of the model to changes in a) $\epsilon(\text{NH}_4^+)$, b) $\epsilon(\text{NO}_3^-)$, and c) PN_i in the N-sufficient condition for *Prorocentrum micans* grown on three N sources. The solid line represents the response of the model using the base values indicated in Table 4.

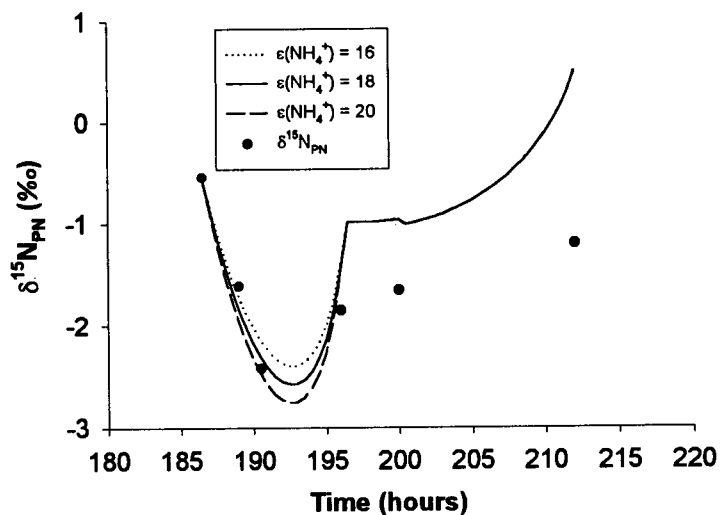


Figure 38 Response of the model to changes in $\varepsilon(\text{NH}_4^+)$ in the N re-supply phase for *Prorocentrum micans* grown on three N sources. The solid line represents the response of the model using the base variables indicated in Table 4.

2) *Amphidinium carterae* grown on NH_4^+ , NO_3^- , and urea

Changing $\epsilon(\text{NH}_4^+)$ values made a large difference in predicting $\delta^{15}\text{N}_{\text{PN}}$, however, it was not significant in the beginning (0 - 6 h) and the end (59 - 61 h) of NH_4^+ uptake (Fig. 39a). The model predicted the data well for growth on NH_4^+ for $\epsilon(\text{NH}_4^+)$ values of 18 - 22‰. $\epsilon(\text{NO}_3^-)$ decreased to a minimum value of 0‰ (Fig. 39b). Lower $\epsilon(\text{NO}_3^-)$ values tended to improve the fit.

For the N-deplete phase, $\epsilon(\text{NH}_4^+)$ ranged from 4 to 20‰ (Fig. 40). None of the $\epsilon(\text{NH}_4^+)$ values could fit the data during NH_4^+ drawdown. The model underestimated $\delta^{15}\text{N}_{\text{PN}}$ in the entire N-deplete phase.

3) *Heterosigma carterae* grown on NH_4^+ , NO_3^- , and urea

During the N-replete phase, the model predicted the data well for growth on NH_4^+ for $\epsilon(\text{NH}_4^+)$ values of 22 - 26‰ (Fig. 41a). The $\epsilon(\text{NH}_4^+)$ value that gave the best fit was about 24‰. PN_i had a large effect on the response of the model during the initial growth on NH_4^+ (Fig. 41b). Variations in the values of $\epsilon(\text{NH}_4^+)$ and PN_i produced large changes in the $\delta^{15}\text{N}_{\text{PN}}$ at low PN concentrations. The values of $\epsilon(\text{NO}_3^-)$ ranged from 5 to 9‰ (Fig. 41c). The $\epsilon(\text{NO}_3^-)$ value that gave the best fit was about 9‰.

After the re-addition of three N sources, the model predicted well the data for values of $\epsilon(\text{NH}_4^+)$ of 20‰ (Fig. 42). This value was smaller in magnitude than the one derived in the N-sufficient phase.

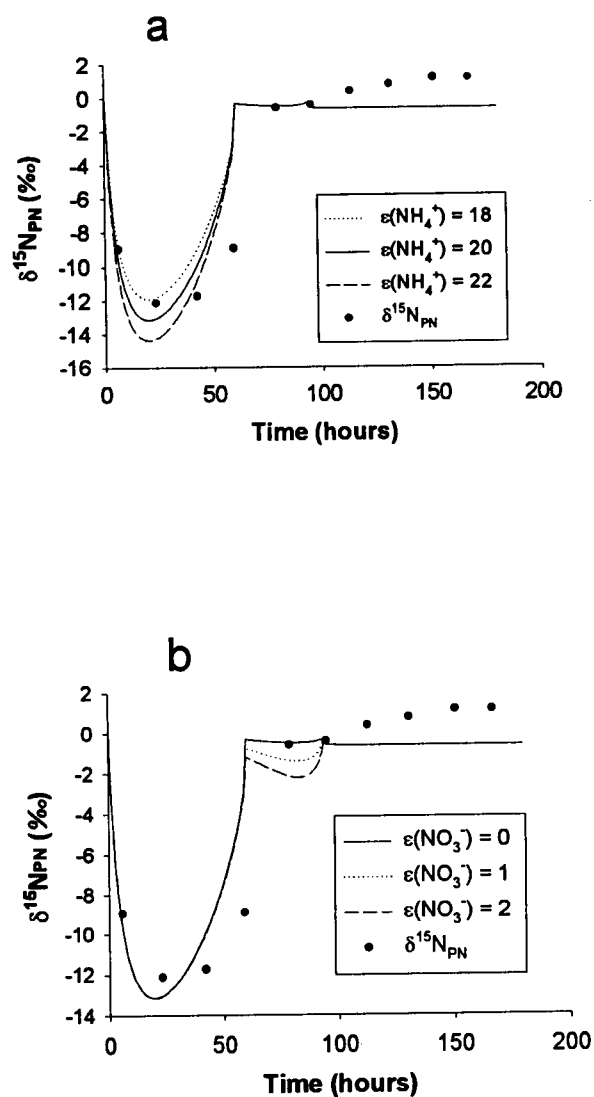


Figure 39 Response of the model to changes in a) $\epsilon(\text{NH}_4^+)$ and b) $\epsilon(\text{NO}_3^-)$ in the N-sufficient condition for *Amphidinium carterae* grown on three N sources. The solid line represents the response of the model using the base values indicated in Table 4.

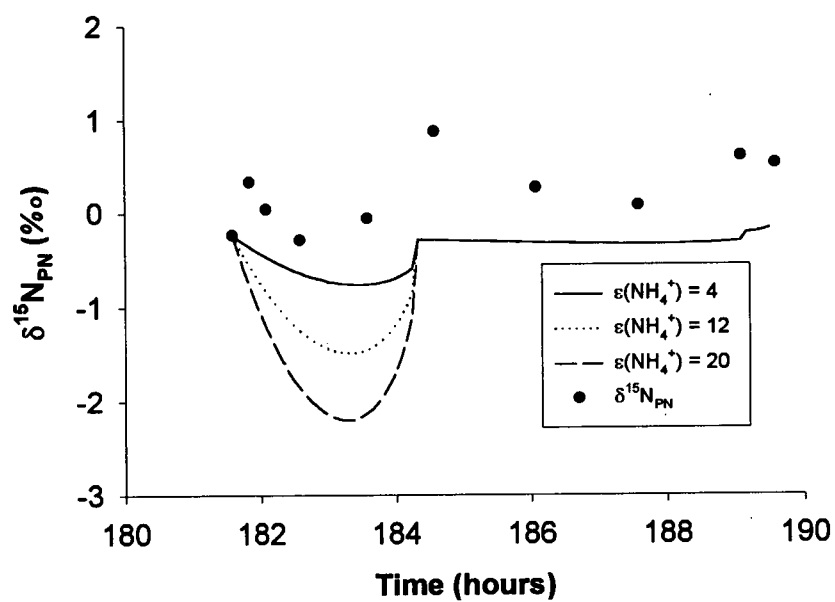


Figure 40 Response of the model to changes in $\epsilon(\text{NH}_4^+)$ in the N-sufficient condition for *Amphidinium carterae* grown on three N sources. The solid line represents the response of the model using the base values indicated in Table 4.

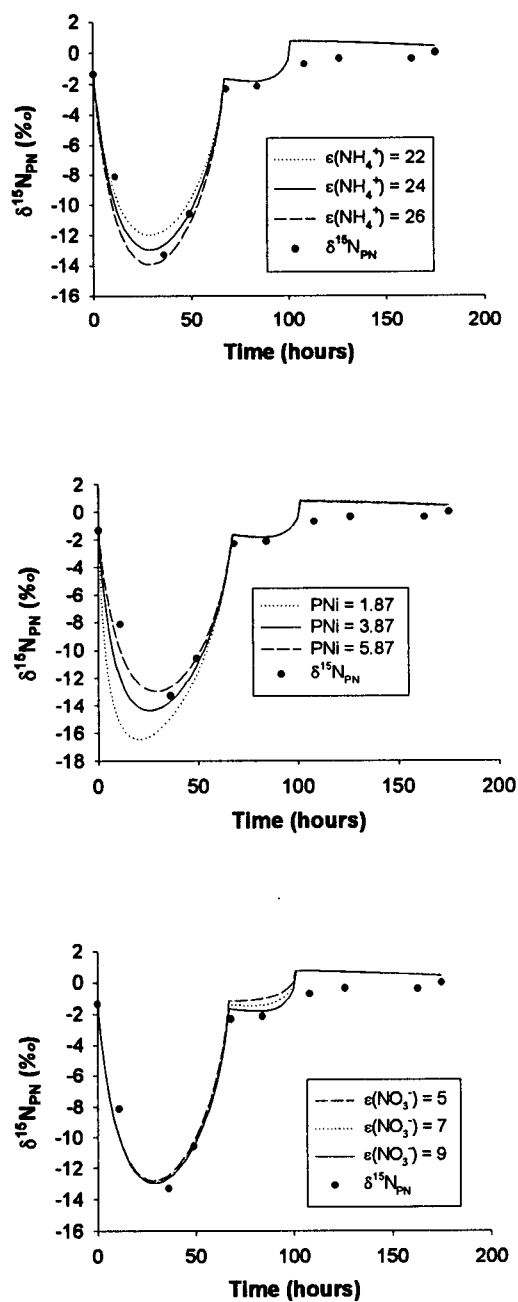


Figure 41 Response of the model to changes in a) $\epsilon(\text{NH}_4^+)$ and b) $\epsilon(\text{NO}_3^-)$ in the N re-supply phase for *Heterosigma carterae* grown on three N sources. The solid lines represent the response of the model using the base variables indicated in Table 4.

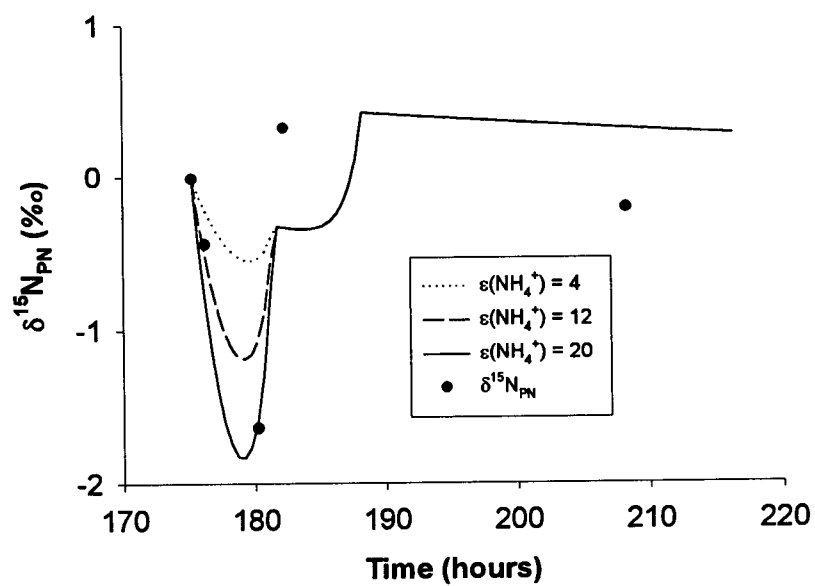


Figure 42 Response of the model to changes in $\epsilon(\text{NH}_4^+)$ in the N re-supply phase for *Heterosigma carterae* grown on three N sources. The solid line represents the response of the model using the base values indicated in Table 4.

4) *Heterosigma carterae* grown on NO_3^-

Variations in the values of $\epsilon(\text{NO}_3^-)$ produced large changes in the $\delta^{15}\text{N}_{\text{PN}}$ at low PN concentrations in N-replete phase (Fig. 43). The values of $\epsilon(\text{NO}_3^-)$ that fitted the data best was in the range of 5 - 7‰. The best fit value of $\epsilon(\text{NO}_3^-)$ in the N-deplete phase clearly increased (Fig. 44). An $\epsilon(\text{NO}_3^-)$ of 9 ‰ was used for the best fit model, although $\delta^{15}\text{N}_{\text{PN}}$ values at 119 and 121 h were lower than the predicted $\delta^{15}\text{N}_{\text{PN}}$ of $\epsilon(\text{NO}_3^-)$ of 11‰. The changes of $\epsilon(\text{NO}_3^-)$ had a large effect on the fit for the 121 -125 h time period, but a small effect on the fit immediately after the re-addition of NO_3^- (115.5 - 116 h) and near the completion of NO_3^- utilization (126 - 127 h).

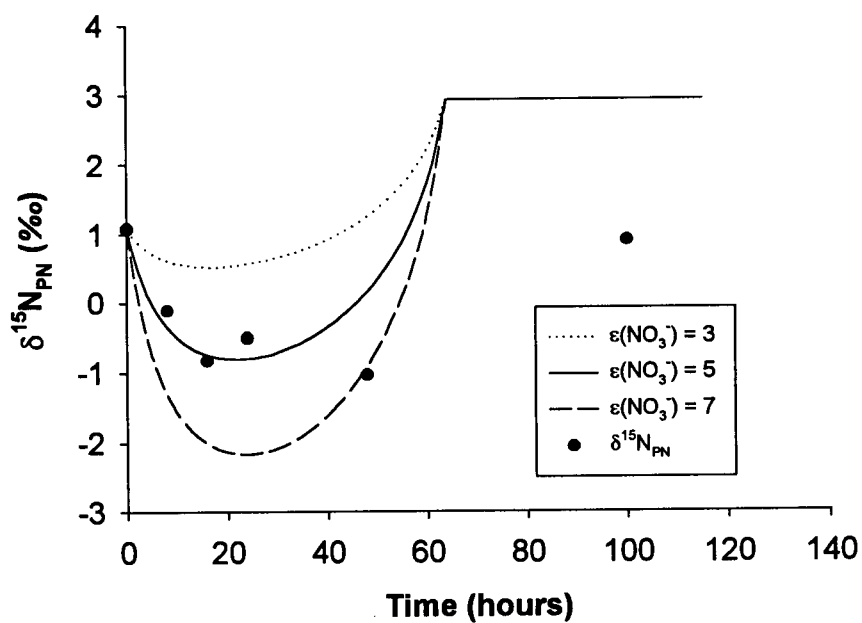


Figure 43 Response of the model to changes in $\epsilon(\text{NO}_3^-)$ in the N-sufficient condition for *Heterosigma carterae* grown on three N sources. The solid line represents the response of the model using the base values indicated in Table 4.

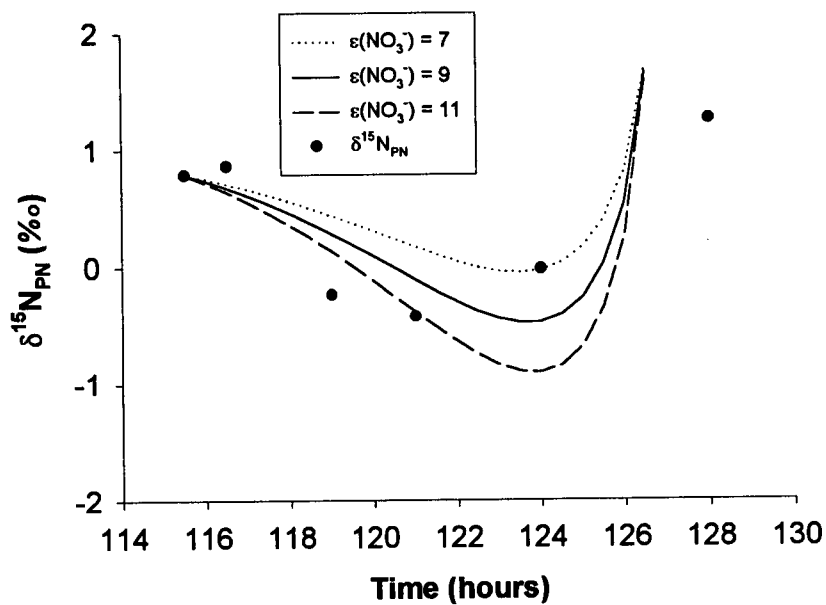


Figure 44 Response of the model to changes in $\epsilon(\text{NO}_3^-)$ in the N re-supply phase for *Heterosigma carterae* grown on three N sources. The solid lines represent the response of the model using the base variables indicated in Table 4.

DISCUSSION

The present study attempted to show that the $\delta^{15}\text{N}_{\text{PN}}$ resulting from the growth of two dinoflagellates and a raphidophyte in a medium containing NO_3^- or three N sources was predicted by the model. The model assumed $\delta^{15}\text{N}_{\text{PN}}$ was described as the weighted sum of the changes in $\delta^{15}\text{N}_{\text{PN}}$ resulted from the incorporation of each individual N source. Each N incorporation was treated as a unidirectional reaction and the total N incorporation was described as the sum of these reactions. The models fitted the data relatively well. However, during the simultaneous growth on two N sources, especially on NH_4^+ and urea, the prediction was difficult. For example, *Prorocentrum micans* had a much lower $\epsilon(\text{NH}_4^+)$ than the expected value of 20‰. The data for *Amphidinium carterae* and *Heterosigma carterae* were relatively well predicted by using the expected ϵ value of each N.

$\epsilon(\text{NO}_3^-)$

The $\epsilon(\text{NO}_3^-)$ value for *Amphidinium carterae* in N-replete condition that gave the best fit was 0‰. This value was lower than $\epsilon(\text{NO}_3^-)$ of 1.9 ± 0.3 ‰ obtained by Needoba (1997) for *Amphidinium carterae* grown on NO_3^- . $\epsilon(\text{NO}_3^-)$ of 0‰ is also lower than previous estimates for diatoms, a coccolithophore and even dinoflagellates. $\epsilon(\text{NO}_3^-)$ for the diatoms, *Chaetoceros debilis*, *Chaetoceros simplex*, *Skeletonema costatum*, *Thalassiosira weissflogii*, and *Ditylum brightwellii* were 4 - 5, 3.0 ± 0.5 , 2.2 ± 0.4 , 6.2 ± 0.3 , and 2.8 ± 0.3 ‰ respectively

(Needoba 1997; Waser *et al.* 1998a). The coccolithophore, *Emiliania huxleyi* had a N fractionation of $3.9 \pm 0.3\text{‰}$ (Needoba 1997). Dinoflagellates such as *Prorocentrum minimum* had $\epsilon(\text{NO}_3^-)$ of $2.4 \pm 0.3\text{‰}$ (Needoba 1997). Only *Heterosigma carterae* grown on NO_3^- whose best fit $\epsilon(\text{NO}_3^-)$ was 5‰ , showed a good agreement with these values. On the other hand, $\epsilon(\text{NO}_3^-)$ for *Heterosigma carterae* grown on three N sources appeared to be higher than 9‰ . A high $\epsilon(\text{NO}_3^-)$ was reported by Montoya and McCarthy (1995). These authors reported that diatoms such as *Thalassiosira weissflogii* and *Skeletonema costatum* had an ϵ of $9.7 - 15.4$ and $6.4 - 11.9\text{‰}$ respectively for a continuous culture experiment. Interestingly, 9.0‰ for *Skeletonema costatum* reported by Pennock (1996) was very close to the $\epsilon(\text{NO}_3^-)$ for *Heterosigma carterae* grown on three N sources in the present study. The discrepancy may be due to some process such as recycling of DON or NH_4^+ (Rees & Syrett 1979; Price & Harrison 1988; Pujo-Pay *et al.* 1997). This process was not accounted for the model and may produce discrepancies. At the moment, it is impossible to explain the reason of the discrepancy. The difference in isotope fractionation between dinoflagellates and flagellates on the one hand (i.e. low fractionation) (Montoya & McCarthy 1995) and coccolithophores and diatoms on the other hand (e.g. high fractionation) (Montoya & McCarthy 1995; Pennock *et al.* 1996) was not seen in this study. It has been hypothesized that the ability of dinoflagellates and flagellates to swim, decreases the zone of diffusion around the cell and results in the reduction of the potential of the fractionating step during the uptake of NO_3^- across the outer cell membrane (Montoya & McCarthy 1995). This process could explain the low

ϵ value observed. The silica shell of diatoms is considered to provide a barrier to NO_3^- uptake and results in higher discrimination of isotopes (Montoya & McCarthy 1995). These morphological effects on isotope fractionation remain unclear.

$\epsilon(\text{NH}_4^+)$

Growth on NH_4^+ in N-replete conditions was accompanied by very large values of $\epsilon(\text{NH}_4^+)$ ranging from 12 to 24‰. $\epsilon(\text{NH}_4^+)$ for *Heterosigma carterae* (18 - 22‰) and *Amphidinium carterae* (20‰) were in good agreement with previously reported values such as 25 - 26‰ for *Skeletonema costatum* (Pennock *et al.* 1996) and 18 - 20‰ for *Thalassiosira pseudonana* (Waser *et al.* 1998b). However, *Prorocentrum micans* had a very low $\epsilon(\text{NH}_4^+)$ of 12‰. This value is close to the estimates (6.5 - 9‰) of phytoplankton grown on NH_4^+ in coastal environments (Cifuentes *et al.* 1989; Montoya *et al.* 1991). Because of a very low $\epsilon(\text{NH}_4^+)$ and a linear uptake of NH_4^+ and urea in N-replete conditions, it is suspected that the cell might have experienced N starvation at the beginning of the experiment. An $\epsilon(\text{NH}_4^+)$ of 12‰ is very close to the values of N-starved *Emiliana huxleyi* and a diatom assemblage (Waser *et al.* unpublished results). However, NO_3^- concentration of the stock culture was 5.25 μM , thus *Prorocentrum micans* was not N-starved. One clue of this low $\epsilon(\text{NH}_4^+)$ was that cells had a high PN. The calculated PN was 11.1 $\mu\text{g-at N L}^{-1}$. This was the highest among other species in the present study. PN_i of *Amphidinium carterae* (grown on three N sources), *Heterosigma carterae* (grown on three N sources),

and *Heterosigma carterae* (grown on NO_3^-) were 4.7, 3.9, and 5.1 $\mu\text{g-at N L}^{-1}$ respectively. If the true PN_i is higher than the calculated PN_i , some of the discrepancy is explained. The PN of the first few points of *Prorocentrum micans* was 29.6 at 9 h and 45.2 $\mu\text{g-at N L}^{-1}$ at 17 h. The calculated PN_i s from these two measured PNs were 14.7 and 16.4 $\mu\text{g-at N L}^{-1}$ respectively. These numbers are higher than 11.1 $\mu\text{g-at N L}^{-1}$ of PN_i that was used for the model and the true PN_i is suspected higher than the calculated value. Another possibility for low $\epsilon(\text{NH}_4^+)$, again, may be the excretion of NH_4^+ (Rees & Syret 1979; Price & Harrison 1988). The hypothesis that mobile cells may have a lower ϵ value compared to non-mobile cells (Montoya & McCarthy 1995) could be another possibility for the low $\epsilon(\text{NH}_4^+)$. This species has the ability to swim as fast as 0.85 m h^{-1} (Edler & Olson 1985). In contrast, it is known that high $\epsilon(\text{NH}_4^+)$ values are found in chain-forming diatoms (Pennock *et al.* 1996; Waser *et al.* 1998a). *Chaetoceros debilis* and *Skeletonema costatum* had an $\epsilon(\text{NH}_4^+)$ of 25 and 26‰ respectively. These chain-forming diatoms discriminated against ^{15}N during NH_4^+ incorporation than mobile cells.

The mechanism of isotope fractionation for NH_4^+ and NO_3^- incorporation is still unclear, and so is the different ϵ values obtained (Waser *et al.* 1998a). Culture conditions such as NH_4^+ concentration, pH, and bubbling may affect ϵ values of NH_4^+ relative to NO_3^- because of efflux and influx of NH_3 (Hoch *et al.* 1992) and the loss of gaseous NH_3 from the culture medium at high pH (Waser *et al.* 1998b).

Effect of N deprivation

Physiological state of dinoflagellates and raphidophytes affected the $\delta^{15}\text{N}_{\text{PN}}$. After the re-addition of N sources, the positive values of $\delta^{15}\text{N}_{\text{PN}}$ were observed in the cultures of *Amphidinium carterae* grown on three N sources and *Heterosigma carterae* grown on NO_3^- . This phenomenon was observed in the study of coastal diatoms and the coccolithophore (Waser *et al.* 1998a). A positive number indicates that ^{15}N was incorporated more quickly than ^{14}N by the N-starved cells. One of the reasons for this inverse discrimination is the excretion of a ^{15}N -depleted compound by the N-starved cells. An example of such an excreted compound is NH_3 which is excreted by cells when it is incorporated into urea (Price & Harrison 1988). Amino acids can become enriched in ^{15}N for a while when cells accumulate ^{15}N -replete amino acids before the cells excrete some of these amino acids into the medium. Accumulating compounds indicate that the enzyme to aid the transformation to another compound may be rate limiting. Usually, intrinsic isotope fractionation (β) for the enzyme activity results in ^{15}N -replete substrate and ^{15}N -deplete products. However, the ϵ value for membrane diffusion of NH_3 is quite large (39‰) (Hermes *et al.* 1985), and results in excretion of ^{15}N -deplete NH_3 . In fact, the NH_4^+ concentration did not increase initially in *Amphidinium carterae* culture. Therefore, it is difficult to explain the inverse isotope discrimination by efflux of NH_3 for this species. Another possibility is the excretion of isotopically light amino acids as explained above. It is not possible to determine what ^{15}N -deplete compound was excreted in this study.

The $\epsilon(\text{NH}_4^+)$ of *Prorocentrum micans* grown on three N sources and the $\epsilon(\text{NO}_3^-)$ of *Heterosigma carterae* grown on NO_3^- increased after the cells became N-starved. *Prorocentrum micans* and *Heterosigma carterae* changed their best fit ϵ values from 12 to 20‰ and from 5 to 9‰ respectively. One possible explanation for an increased $\epsilon(\text{NH}_4^+)$ has to do with a change in the transport system (active transport versus passive diffusion) during N starvation. The increase in $\epsilon(\text{NO}_3^-)$ may be for a different reason than for $\epsilon(\text{NH}_4^+)$. Perhaps, the efflux of NO_3^- increased after N starvation due to a slowed assimilation, which allowed for more ^{15}N -replete NO_3^- to efflux and resulted in high ϵ values. Since *Heterosigma carterae* grown on NO_3^- in the N-replete phase had much lower $\delta^{15}\text{N}$ of PN_i (1.08‰) than the expected values of 3.04‰, the increased $\epsilon(\text{NO}_3^-)$ value in the N-deplete phase was of a concern. It is not clear at present why there is such a discrepancy between the measured $\delta^{15}\text{N}$ and the fit by the model. It is possible that DON may have been released into the medium (Rees & Syrett 1979; Price & Harrison 1988; Pujo-pay 1997). The PN concentration (90.6 $\mu\text{g-at N L}^{-1}$) at steady-state was in good agreement with the initial NO_3^- concentration (78.5 $\mu\text{g-at N L}^{-1}$) suggesting that the release of DON, if it occurred, was relatively small. Nonetheless, it is interesting that N-deprivation enhanced isotope fractionation and incorporated more ^{14}N than ^{15}N , which was the opposite of what was expected. Again, the hypothesis that mobile cells have lower ϵ values (Montoya & McCarthy 1995) could be one possibility of higher $\epsilon(\text{NH}_4^+)$ of N-starved *Prorocentrum micans* and $\epsilon(\text{NO}_3^-)$ of *Heterosigma carterae*.

During N starvation, cells tended to sink and stay at the bottom of the flask even though the flask was swirled by hand and after the re-addition of N sources, cells gradually dispersed in the medium again. The temporary loss of ability to move might result in the higher ϵ values for these species. On the other hand, *Amphidinium carterae* decreased its $\epsilon(\text{NH}_4^+)$ from 18 - 20‰ to < 4‰.

Previously, no change or decreased ϵ values were reported to be due to N deprivation in the study of the open ocean clone of *Emiliana huxleyi* and the coastal clone of the same species grown on three N sources respectively (Waser *et al.* 1998a). Diatoms grown on three N sources also showed decreased ϵ values after N deprivation (Waser *et al.* 1998a).

All species changed the mechanism of isotope fractionation during N deprivation. This may be due to the rate limiting transport across the membrane and diffusion to the cell that occurred during N deprivation (Wada & Hattori 1978; Mariotti *et al.* 1982; Handily & Raven 1992; Evens *et al.* 1996). Otherwise, the rate-limiting step was the reduction of NO_3^- to NO_2^- by nitrate reductase which was affected by N deprivation. At this time, it is impossible to tell which step, either at the cell membrane or at the nitrate reductase level, is responsible for the isotope fractionation. If the cell did not change the mechanism of isotope fractionation, it indicates that the cell has recovered quickly from the impact of N deprivation. Such a species is able to live in the oligotrophic ocean because it takes up episodically supplied NH_4^+ (Dugdale 1967) with the same mechanism that occurs under N-replete conditions.

Difficulties in predicting $\delta^{15}\text{N}_{\text{PN}}$ occurred during simultaneous uptake of two or three N sources. Since the purpose of this type of laboratory experiment involves the application for understanding N isotope fractionation in the ocean, interaction of each N is important for interpreting the $\delta^{15}\text{N}_{\text{PN}}$ in the ocean. For example, if NH_3 is released and recycled during the simultaneous uptake of NH_4^+ and urea, $\delta^{15}\text{N}_{\text{PN}}$ was much lower than $\delta^{15}\text{N}_{\text{PN}}$ grown on only NH_4^+ . Therefore, not only ϵ for each N source, but also the interaction of N sources needs to be considered in the model fit.

N availability affected N isotope fractionation. It is interesting to compare the results of acclimation to the N-deplete condition obtained in Part. I of this study. *Prorocentrum micans* and *Amphidinium carterae* showed a response to N depletion by enhancing their ability to take up the reduced N form and episodically supplied urea (Dugdale 1967) rather than NO_3^- , although they decreased their ability to take up NH_4^+ . However, none of species were able to keep the same isotope fractionation mechanism during the N deprivation. These observations indicate that marine phytoplankton have different methods and magnitudes of adaptation to N-deplete conditions.

CONCLUSIONS

N availability had a great impact on $\delta^{15}\text{N}$ incorporation by marine phytoplankton. ϵ (isotope fractionation) changed before and after N deprivation and following N re-supply. $\epsilon(\text{NO}_3^-)$ of *Heterosigma carterae* grown on NO_3^- increased during N starvation probably due to the increased efflux of ^{15}N -deplete DON. For cultures grown on three N sources, $\epsilon(\text{NH}_4^+)$ decreased in *Amphidinium carterae* and *Heterosigma carterae* and increased in *Prorocentrum micans*. The magnitudes of isotope fractionation were species specific. The multiple N source uptake model predicted $\delta^{15}\text{N}_{\text{PN}}$ well.

FUTURE STUDY

Species specificity on N isotope fractionation to the N availability needs further investigation since each species showed a different response to N deprivation. Differences in morphology of marine phytoplankton may influence the isotope fractionation. Therefore, the correlation of morphological features such as chain-formation, and motility of flagellates and low fractionation, and the existence of silica frustules of diatoms and high fractionation, needs further analysis as well as the physiological state. Simultaneous uptake of two N sources have a different impact on the $\delta^{15}\text{N}$ of the PN depending on the N forms and the species, which is critical for interpreting the $\delta^{15}\text{N}$ of the PN in the field. Thus, understanding of interactions between different N sources is required.

REFERENCES

- Altabet, M. A. and Francois, R. 1994. Sedimentary nitrogen isotopic ratio as a recorder for surface ocean NO_3^- utilization. *Global Biogeochem. Cycles* 8: 103-116.
- Amy, N. K. and Garrett, R. H. 1974. Purification and characterization of the nitrate reductase from the diatom *Thalassiosira pseudonana*. *Plant Physiol.* 54: 629-637
- Antia, N. J., Harrison, P. J., and Oliveira, L. 1991. The role of dissolved organic nitrogen in phytoplankton nutrition, cell biology and ecology. *Phycologia* 29: 1-89
- Avaria, P. S. 1982. Fenomenos de marea roja en el mar de Ch. *Cienc. Tecnol. Mar. (Valparaiso)* 6: 117-127.
- Bekheet, I. A. and Syrett, P. J. 1979. The uptake of urea by *Chlorella*. *New Phytol.* 82: 179-186.
- Berman, T. 1974. Urea in the waters of Lake Kinneret (Sea of Galilee). *Limnol. Oceanogr.* 19: 977-980.
- Bhovichitra, M. and Swift, E. 1977. Light and dark uptake of nitrate and ammonium by large oceanic dinoflagellates: *Pyrocystis noctiluca*, *Pyrocystis fusiformis*, and *Dissodinium lunula*. *Limnol. Oceanogr.* 22: 73-83.
- Buijsman, E., Jonker, P. J., Asman, W. A. H., and Ridder, T. B. 1991. Chemical composition of precipitation collected on a weather ship on the North Atlantic. *Atmos. Environ.* 25: 873-883.
- Calvert, S. E., Nielsen, B., and Fontugne, M. R. 1992. Evidence from nitrogen isotope ratios for enhanced productivity during formation of eastern Mediterranean sapropels. *Nature* 359: 223-225.
- Caperon, J. and Ziemann, D. A. 1976. Synergistic effects of nitrate and ammonium ion on the growth and uptake kinetics of *Monochrysis lutheri* in continuous culture. *Mar. Biol.* 36: 73-84.
- Cassie, V. 1981. Non-toxic blooms of *Prorocentrum micans* (Dinophyceae) in the Karamea Bight. *N. Z. J. Mar. Fresh Res.* 15: 181-184.

- Chang, F. H., Pridmore, R., and Boustead, N. 1993. Occurrence and distribution of *Heterosigma* cf. *Akashiwo* (Raphidophyceae) in a 1989 bloom in Big Blory Bay, New Zealand. In: Toxic phytoplankton blooms in the sea (eds.) T. Smayda, and Y. Shimizu. Proceedings of the Fifth International Conference on Toxic Marine Phytoplankton, Newport, Rhode Island, October, 1991, Elsevier, p. 675-680.
- Cifuentes, L. A., Fogel, M. L., Pennock, J. R., and Sharp, J. H. 1989. Biogeochemical factors that influence the stable nitrogen isotope ratio of dissolved ammonium in the Delaware Estuary. *Geochim Cosmochim Acta*. 53: 2713-2721.
- Cleveland, J. S., Perry, M. J., Kiefer, D. A., and Talbot, M. C. 1989. Maximal quantum yield of photosynthesis in the northwestern Sargasso sea. *J. Mar. Res.* 47: 869-86.
- Cochlan, W. P. and Harrison, P. J. 1991. Uptake of nitrate, ammonium, and urea by nitrogen-starved cultures of *Micromonas pusilla* (Prasinophyceae): transient responses. *J. Phycol.* 27: 673-679
- Cochlan, W. P., Harrison, P. J., and Denman, K. L. 1991. Diel periodicity of nitrogen uptake by marine phytoplankton in nitrate-rich environments. *Limnol. Oceanogr.* 36: 1689-1700
- Collos, Y. 1980. Transient situations in nitrate assimilation by marine diatoms. 1. Changes in uptake parameters during nitrogen starvation. *Limnol. Oceanogr.* 25: 1075-1081.
- Collos, Y. 1983. Transient situations in nitrate assimilation by marine diatoms. 4. Non-linear phenomena and the estimation of the maximum uptake rate. *J. Plankton Res.* 5: 677-691.
- Collos, Y., Maestrini, S. Y., and Robert, J.-M. 1989. High long-term nitrate uptake by oyster-pond microalgae in the presence of high ammonium concentrations. *Limnol. Oceanogr.* 34: 957-964.
- Conover, S. A. M. 1975. Nitrogen utilization during spring blooms of marine phytoplankton in Bedford Basin, Nova Scotia, Canada. *Mar. Biol.* 32: 247-261.
- Conway, H. L. 1977. Interactions of inorganic nitrogen in the uptake and assimilation by marine phytoplankton. *Mar. Biol.* 39: 221-232.

- Conway, H. L., Harrison, P. J., and Davis, C. O. 1976. Marine diatoms grown in chemostats under silicate or ammonium limitation. II. Transient response of *Skeletonema costatum* to a single addition of a limiting nutrient. Mar. Biol. 35: 187-199.
- Conway, H. L. and Harrison, P. J. 1977. Marine diatoms grown in chemostats under silicate or ammonium limitation. IV. Transient response of *Chaetoceros debilis*, *Skeletonema costatum*, and *Thalassiosira gravida* to a single addition of the limiting nutrient. Mar. Biol. 43: 33-43.
- Conway, H. L. and Whitledge, T. E. R. 1979. Distribution of fluxes and biological utilization of inorganic nitrogen during a spring bloom in the New York Bight. J. Mar. Res. 37: 657-668.
- Costas, E. 1990. Genetic variability in growth rates of marine dinoflagellates. Genetica 82: 99-102.
- Cresswell, R. C. and Syrett, P. J. 1979. Ammonium inhibition of nitrate uptake by the diatom, *Phaeodactylum tricornutum*. Plant Sci. Lett. 14: 321-325.
- Cullen, J. J., Stewart, E., Renger, E., Eppley, R. W., and Winant, C. D. 1983. Vertical motion of the thermocline, nitracline and chlorophyll maximum layers in relation to currents on the Southern California Shelf. J. Mar. Res. 41: 239-262.
- D'elia, C. F. and DeBoer, J. A. 1978. Nutritional studies of two red algae II. Kinetics of ammonium and NO_3^- uptake. J. Phycol. 14: 266-272.
- Demanche, J. M. and Curl, H. C. 1979. The rapid response of the marine diatom *Skeletonema costatum* to changes in external and internal nutrient concentration. Mar. Biol. 53: 323-333.
- Dortch, Q. and Maske, H. 1982. Dark uptake of nitrate and nitrate reductase activity of a red tide population off Peru. Mar. Ecol. Prog. Ser. 9: 299-303.
- Dortch, Q., Clayton, J. R. Jr., Thoresen, S. S., Bressler, S. L., and Ahmed, S. I. 1982. Response of marine phytoplankton to nitrogen deficiency: decreased nitrate uptake vs enhanced ammonium uptake. Mar. Biol. 70: 13-19.

- Dortch, Q., Clayton J. R. Jr., Thoresen, S. S., and Ahmed, S. I. 1984. Species differences in accumulation of nitrogen pools in phytoplankton. *Mar. Biol.* 81: 237-250.
- Dugdale, R. C. 1967. Nutrient limitation in the sea: dynamics, identification, and significance. *Limnol. Oceanogr.* 12: 685-695.
- Dugdale, R. C. and Goering, J. J. 1967. Uptake of new and regenerated forms of nitrogen in primary productivity. *Limnol. Oceanogr.* 12: 196-206.
- Edler, L. and Olsson, P. 1985. Observations on diel migration of *Ceratium furca* and *Prorocentrum micans* in a stratified bay in the Swedish west coast. In: *Toxic Dinoflagellates* (eds.) D. M. Anderson, A. W. White, and D. G. Baden, Elsevier, New York. p. 195-200.
- Eppley, R. W. and Coatsworth, J. L. 1968. Uptake of nitrate and nitrite by *Ditylum brightwellii* - kinetics and mechanisms. *J. Phycol.* 4: 151-156.
- Eppley, R. W., Coatsworth, J. L., and Solorzano, L. 1969. Studies of nitrate reductase in marine phytoplankton. *Limnol. Oceanogr.* 14: 194-205.
- Eppley, R. W. and Rogers, J. N. 1970. Inorganic nitrogen assimilation of *Ditylum brightwellii*, a marine plankton diatom. *J. Phycol.* 6: 344-351.
- Eppley, R. W., Rogers, J. N., McCarthy, J. J., and Sournia, A. 1971. Light/dark periodicity in nitrogen assimilation of the marine phytoplankters *Skeletonema costatum* and *Coccolithus huxleyi* in N-limited chemostat cultures. *J. Phycol.* 7: 150-154.
- Eppley, R. W., Renger, E. H., Venrick, E. L., and Mullin, M. M. 1973. A study of plankton dynamics and nutrient cycling in the central gyre of the North Pacific Ocean. *Limnol. Oceanogr.* 18: 534-551.
- Eppley, R. W. and Harrison, W. G. 1975. Physiological ecology *Gonyaulax polyedra*, a red water dinoflagellate of Southern California. In: *Proceedings of the First International Conference on Toxic Dinoflagellate Blooms.* (ed.) V. R. LoCicero. Massachusetts Science & Technology Foundation, Wakefield, Massachusetts, p. 11-22.
- Eppley, R. W., Rogers, E. H., and Harrison, W. G. 1979. Nitrate and phytoplankton production in southern California coastal waters. *Limnol. Oceanogr.* 24: 483-494.

- Evans, R. D., Bloom, A. J., Sukrapanna, S. S., Ehleinger, J. R. 1996. Nitrogen isotope composition of tomato (*Lycopersion esculentum* Mill. Cv. T-5) grown under ammonium or nitrate nutrition. *Plant Cell Environ.* 19: 1317-1323.
- Falkowski, P. G. 1975. Nitrate uptake in marine phytoplankton: (nitrate, chloride) - activated adenosine triphosphatase from *Skeletonema costatum* (Bacillariophyceae). *J. Phycol.* 11: 323-326.
- Falkowski, P. G. and Rivkin, R. B. 1976. The role of glutamine synthetase in the incorporation of ammonium in *Skeletonema costatum* (Bacillariophyceae). *J. Phycol.* 12: 448-450.
- Farrell, J. W., Pedersen, T. F., Calvert, S. E., and Nielsen, B. 1995. Sedimentary $^{15}\text{N}/^{14}\text{N}$ ratios reveal nutrient utilization history in the equatorial Pacific. *Nature* 377: 514-517.
- Fedorov, V. D., and Il'yash, V. 1992. Adaptive mechanisms in life-history strategies of microalgae. *Hydrobiol. J.* 28: 38-45.
- Fisher, T. R., Carlson, P. R., and Barber, R. T. 1982. Carbon and nitrogen primary productivity in three North Carolina estuaries. *Est. Coastal Shelf Sci.* 15: 621-644.
- Fitzgerald, G. P. 1968. Detection of limiting or surplus nitrogen in algae and aquatic weeds. *J. Phycol.* 4: 121-126.
- Florencio, F. J. and Vega, J. M. 1983. Utilization of nitrate, nitrite and ammonium by *Chlamydomonas reinhardtii*. *Planta* 158: 288-293.
- Francois, R., Altabet, A., and Burckle, L. H. 1992. Glacial to interglacial changes in surface nitrate utilization in the Indian sector of the Southern Ocean as recorded by sediment $\delta^{15}\text{N}$. *Paleoceanography* 7: 589-606.
- French, D. P., Smayda, T. J., Lassus, P., Arzul, G., Erard-Le Denn, E., Gentien, P., and Marceillou-Le Baut, C. 1995. Temperature regulated responses of nitrogen limited *Heterosigma akashiwo*, with relevance to its blooms. Harmful marine algal blooms. In: Proliferation d'algues marines nuisibles. p. 585-590.
- Glivert, P. M. and Goldman, J. C. 1981. Rapid ammonium uptake by marine phytoplankton. *Mar. Biol. Lett.* 2: 25-31.

- Goericke, R., Montoya, J. P., and Fry, B. 1994. Physiology of isotope fractionation in algae and cyanobacteria. In: Stable isotope in ecology and environmental science. (eds.) K. Lajtha and R. H. Michener. Blackwell Scientific Publications. p. 187-221.
- Goldman, J. C., McCarthy, J. J., and Peavey, D. G. 1979. Growth rate influence on the chemical composition of phytoplankton in oceanic waters. *Nature (Lond.)* 279: 210-215.
- Goldman, J. C., Taylor, C. D., and Glibert, P. M. 1981. Non-linear time-course uptake of carbon and ammonium by marine phytoplankton. *Mar. Ecol. Prog. Ser.* 6: 137-148.
- Goldman, J. C. and Glibert, P. M. 1982. Comparative rapid ammonium uptake by four species of marine phytoplankton. *Limnol. Oceanogr.* 27: 814-827.
- Grant, B. R., Madgwick, J., and Dalpont, G. 1967. Growth of *Cylindrotheca closterium* var. *californica* (Mereschk) Rieman & Lewin on nitrate, ammonia, and urea. *Aust. J. Mar. Freshwater Res.* 18: 129-135.
- Guerrero, M. G., Vega, J. M., and Losada, M. 1981. The assimilatory nitrate-reducing system and its regulation. *Ann. Rev. Plant Physiol.* 32: 169-204.
- Hallegraeff, G. M. 1991. Aquaculturists' guide to harmful Australian microalgae. CSIRO, Hobart.
- Halstead, B. W. 1965. Poisonous and Venomous Marine Animals of the World, vol. 1 U. S. Govt. Printing Office, Washington, D. C., p. 159.
- Handily, L. L. and Raven, J. A. 1992. The use of natural abundance of nitrogen isotopes in plant physiology and ecology. *Plant Cell Environ.* 15: 965-985.
- Hara, T. 1990. *Heterosigma akashiwo* (HADA) HADA. In: *Nihon no akashiwo seibutsu*. (eds.) Y. Fukuyo, H. Takano, M. Chihara, and K. Matsuoka. Uchida Rokkakueho, Tokyo. p. 346-347.
- Harrison, P. J., Waters, R. E., and Taylor, F. J. R. 1980. A broad spectrum artificial seawater medium for coastal and open ocean phytoplankton. *J. Phycol.* 16: 28-35.
- Harrison, P. J. and Turpin D. H. 1982. The manipulation of physical, chemical and biological factors to select species from natural phytoplankton

- communities. In: Marine Mesocosms: Biological and chemical research in experimental ecosystems. (eds.) G. D. Grice and M. R. Reeve. Springer-Verlag, New York. p. 275-289.
- Harrison, P. J., Druehl, L. D., Lloyd, K. E., and Thompson, P. A. 1986. Nitrogen uptake kinetics in three-year classes of *Laminaria groenlandica* (Laminariales: Phaeophyta). Mar. Biol. 93: 29-35.
- Harrison, P. J., Parslow, J. S., and Conway, H. L. 1989. Determination of nutrient uptake kinetic parameters: a comparison of methods. Mar. Ecol. Prog. Ser. 52: 301-312.
- Harrison, W. G. 1976. Nitrate metabolism of the red tide dinoflagellate *Gonyaulax polyedra* Stein. J. Exp. Mar. Biol. Ecol. 21: 199-209.
- Harrison, W. G. 1983. The time-course of uptake of inorganic and organic nitrogen compounds by phytoplankton from the eastern Canadian Arctic: A comparison with temperate and tropical populations. Limnol. Oceanogr. 28: 1231-1236.
- Harrison, W. G., Platt, T., and Lewis, M. R. 1987. F-Ratio and its relationship to ambient nitrate concentration in coastal waters. J. Plankton Res. 9: 235-248.
- Harrison, W. G. 1992. Regeneration of nutrients. In: Primary productivity and biogeochemical cycles in the sea. (eds.) P. G. Falkowski, and A. D. Woodhead. Plenum Press, New York. p. 385-407.
- Harvey, H. W. 1953. Synthesis of organic nitrogen and chlorophyll by *Nitzschia closterium*. J. Mar. Biol. Ass. U. K. 31: 477-487.
- Harvey, G. W. 1966. Microlayer collection from the sea surface by new method and initial results. Limnol. Oceanogr. 11: 608-612.
- Hata, M., Abe, S., and Hata, M. 1982. Occurrence of peridinin-chlorophyll a-protein complex in red tide dinoflagellate *Prorocentrum micans* Bull. Jap. Soc. Scient. Fish. 48: 459-461.
- Hattori, A. 1958. Studies on the metabolism of urea and other nitrogenous compounds in *Chlorella ellipsoidea*. II. Changes in levels of amino acids and amides during the assimilation of ammonia and urea by nitrogen-starved cells. J. Biochem. (Tokyo) 45: 57-64.

- Hattori, H., Yuki, K., Zaitsev, Y. P., and Motoda, S. 1983. A preliminary observation on the neuston in Suruga Bay. *La Mer* (B Soc. Franco-jap. Oceanogr., Tokyo) 21: 11-20.
- Hersey, R. L. and Swift, E. 1976. Nitrate reductase activity of *Amphidinium carteri* and *Cachnina riei* (Dinophyceae) in batch culture: Diel periodicity and effects of light intensity and ammonia. *J. Phycol.* 12: 36-44.
- Hedrich, R. and Schroeder, J. I. 1989. The physiology of ion channels and electrogenic pumps in higher plants. *Annu. Rev. Plant Physiol.* 40: 539- 569.
- Herdman, E. C. 1924a. Notes on dinoflagellates and other organisms causing discoloration of the sand at Port Erin. III. *Liverpool Biol. Soc. Proc. Trans.* 38: 58-63.
- Herdman, E. C. 1924b. Notes on dinoflagellates and other organisms causing discoloration of the sand at Port Erin. IV. *Liverpool Biol. Soc. Proc. Trans.* 38: 75-84.
- Hermes, J. D., Weiss, P. M., and Cleland, W. W. 1985. Use of nitrogen-15 and deuterium isotope effects to determine the chemical mechanism of phenylalanine ammonia-lyase. *Biochemistry* 24: 2959-2967.
- Hipkin, C. R., Al-Bassam, B. A., and Syrett, P. J. 1980. The roles of nitrate and ammonium in the regulation of the development of nitrate reductase in *Chlamydomonas reinhardtii*. *Planta* 150: 13-18.
- Hoch, M. P., Foge, M. L., and Kirchman, D. L. 1994. Isotope fractionation associated with ammonium uptake by a marine bacterium. *Limnol. Oceanogr.* 37: 1447-1459.
- Hoe Chang, F. 1993. Occurrence and distribution of *Heterosigma akashiwo* (Raphidophyceae) in a 1989 bloom in Big Glory Bay, New Zealand. In: *Toxic Phytoplankton Blooms in the Sea*. (eds.) T. J. Smayda and Y. Shimizu. Elsevier, Amsterdam. p. 675-679.
- Hoe Chang, F and Page, M. 1997. Influence of light and three nitrogen sources on growth of *Heterosigma carterae* (Raphidophyceae). *N. Z. J. Mar. Freshwat. Res.* 29: 299-304.
- Honjo, T. 1992. Harmful red tides of *Heterosigma akashiwo*. NOAA Tech. Rep. NMFS 111: 27-32

- Honjo, T. 1993. Overview on bloom dynamics and physiological ecology of *Heterosigma akashiwo*. In: Toxic Phytoplankton Blooms in the sea. (eds.) T. J. Smayda and Y. Shimizu. Elsevier, New York. p. 33-41.
- Honjo, T. and Tabata, K. 1985. Growth dynamics of *Olisthodiscus luteus* in outdoor tanks with flowing coastal water and in small vessels. Limnol. Oceanogr. 30: 653-664.
- Horiguchi, T. 1990. *Prorocentrum micans* Ehrenberg. In: Nihon no akashiwo seibutsu. (eds.) Y. Fukuyo, H. Takano, M. Chihara, and K. Matsuoka. Uchida Rokkakueho, Tokyo. p. 28-29.
- Horrigan, S. G. and McCarthy, J. J. 1981. Urea uptake by phytoplankton at various stages of nutrient depletion. J. Plankton Res. 3: 403-414.
- Horrigan, S. G. and McCarthy, J. J. 1982. Phytoplankton uptake of ammonium and urea during growth on oxidized forms of nitrogen. J. Plankton Res. 4: 379-389.
- Hulbert, E. M. 1957. The taxonomy of unarmored Dinophyceae of shallow embayments on Cape Cod, Massachusetts. Biol. Bull. 112: 196-219.
- Ignatiades L. 1986. Annual variability of [^{14}C] urea utilization by natural marine phytoplankton. British Phycol. J. 21: 209-215.
- Ikawa, M. and Sasner, J. J. Jr. 1975. Chemical and physiological studies on the marine dinoflagellate *Amphidinium carterae*. In: Proceedings of the first international conference on toxic dinoflagellate blooms (ed.) V. R. LoCicero. The Massachusetts Science and Technology Foundation, Wakefield, Massachusetts. p. 323-332.
- Jones, M. N. 1984. Nitrate reduction by shaking with cadmium, alternative to cadmium columns. Water Res. 18: 643-646.
- Khan, S., Arakawa, O. and Onoue, Y. 1997. Neurotoxins in a toxic red tide of *Heterosigma akashiwo* (Raphidophyceae) in Kagoshima Bay, Japan. Aqua. Res. 28: 9-14.
- Lanskaya, L. A. 1971. Cultivation of algae. In: Ecological physiology of marine planktonic algae. Naukova Dumka Press, Kiev. p. 5-21.
- Larsen, J. and Moestrup, O. 1989. Guide to Toxic and Potentially Toxic Marine Algae. Fish Inspection Service, Ministry of Fisheries, Copenhagen.

- Larsen, J. and Moestrup, O. 1992. Potentially toxic phytoplankton. 1. Haptophyceae (Prymnesiophyceae). Ices Identif. Leaflet. Plankton. 179: 11.
- Laws, E. and Caperon, J. 1976. Carbon and nitrogen metabolism by *Monochrysis lutheri*: measurement of growth-rate-dependent respiration rates. Mar. Biol. 36: 85-97.
- Laws, E. A. and Wong, D. C. L. 1978. Studies of carbon and nitrogen metabolism by three marine phytoplankton species in nitrate-limited continuous culture. J. Phycol. 14: 406-416.
- Lee, R. B. 1980. Sources of reductant for nitrate assimilation in non-photosynthetic tissue: a review. Plant Cell Environ. 3: 65-90.
- Lehman, J. T. and Scavia, D. 1982. Microscale patchiness of nutrients in plankton communities. Science 216: 729-730.
- Lesser, M. P. 1996. Acclimation of phytoplankton to UV-B radiation: oxidative stress and photoinhibition of photosynthesis are not prevented by UV-absorbing compounds in the dinoflagellate *Prorocentrum micans*. Mar. Ecol. Prog. Ser. 132: 287-297.
- Levasseur, M. E., Harrison, P. J., Heimdahl, B. R., and Therriault, J-C. 1990. Simultaneous nitrogen and silicate deficiency of a phytoplankton community in a coastal jet-front. Mar. Biol. (Berl.) 104: 329-338.
- L'Helguen, S., Made, C., and Le Corre, P. 1996. Nitrogen uptake in permanently well-mixed temperate coastal waters. Estuar. Coast. Shelf Sci. 42: 803-818.
- Liebig, J. 1846. Chemistry in its application to agriculture and physiology. 4th ed. Taylor and Walter, London.
- Liu, M. S. and Hellebust, J. A. 1976. Effects of salinity and osmolarity of the medium on amino acid metabolism in *Cyclotella cryptica*. Can. J. Bot. 54: 938-948.
- Lobban, C. S., Harrison, P. J., and Duncan, M. J. 1985. The physiological ecology of seaweeds. Cambridge University Press, Cambridge, England. p. 242.
- Lobban, C. S. and Harrison, P. J. 1994. Seaweed ecology and physiology. Cambridge University Press. New York, New York.

- Lui, N. S. T. and Roels, O. A. 1970. Nitrogen metabolism of aquatic organisms. I. The assimilation and formation of urea in *Ochromonas malhamensis*. Arch. Biochem. Biophys. 139: 269-277.
- Lund, B. A. 1987. Mutual interference of ammonium, nitrate, and urea on uptake of ^{15}N sources by the marine diatom *Skeletonema costatum* (Grev.) Cleve. J. Exp. Mar. Biol. Ecol. 113: 167-180.
- MacIsaac, J. J. 1978. Diel cycles of inorganic nitrogen uptake in a natural phytoplankton population dominated by *Gonyaulax polyedra*. Limnol. Oceanogr. 23: 1-9.
- MacIsaac, J. J. and Dugdale, R. C. 1972. Interactions of light and inorganic nitrogen in controlling nitrogen uptake in the sea. Deep-Sea Res. 19: 209-232.
- Maguer, J. F., Le Corre, P., and L'Helguen, S. 1995. Nitrogen sources for phytoplankton in shallow well-mixed waters of the western English Channel: Importance of the regenerated production. J. Rech. Oceanogr. 21: 103-108.
- Malone, T. C., Garside, C., Haines, K. C., and Roels, O. A. 1975. Nitrate uptake and growth of *Chaetoceros* sp. in large outdoor cultures. Limnol. Oceanogr. 20: 9-19.
- Mariotti, A., Germon, J. C., Hubert, P., Kaiser, P., Letolle, R., Tardieux, A., and Tarcieux, P. 1981. Experimental determination of nitrogen kinetic isotope fractionation: some principles; illustration for the denitrification and nitrification processes. Plant Soil 62: 413-430.
- Marriott, A., Marriott, F., Champigny, M., Amarger, N., and Moyse, A. 1982. Nitrogen isotope fractionation associated with nitrate reductase activity and uptake of NO_3 by Pearl Millet. Plant Physiol. 69: 880-884.
- Martin, G. W. 1929. Dinoflagellates from marine and brackish waters of New Jersey. Univ. Iowa Stud. Nat. Hist. 12: 3-32.
- McCarthy, J. J. 1980. Nitrogen. In: The physiological ecology of phytoplankton. (ed.) I. Morris. Blackwell Sci. Publ., Oxford, England. p.191-233
- McCarthy, J. J. 1981. The kinetics of nutrient utilization, p. 211-233. In: Physiological bases of phytoplankton ecology. (ed.) T. Platt. Can. Bull. Fish. Aquat. Sci. 210. p. 211-233.

- McCarthy, J. J. and Eppley, R. W. 1972. A comparison of chemical, isotopic, and enzymatic methods for measuring nitrogen assimilation of marine phytoplankton. *Limnol. Oceanogr.* 17: 371-382.
- McCarthy, J. J. and Goldman, J. C. 1979. Nitrogenous nutrition of marine phytoplankton in nutrient depleted waters. *Science* 203: 670-672.
- McCarthy, J. J., Taylor, W. R., and Taft, J. L. 1977. Nitrogenous nutrition of the plankton in the Chesapeake Bay. 1. Nutrient availability and phytoplankton preferences. *Limnol. Oceanogr.* 22: 996-1011.
- Mitamura, O., Saijo, Y., Hino, K., and Barbosa, F. A. R. 1995. The significance of regenerated nitrogen for phytoplankton productivity in the Rio Doce Valley lakes Brazil. *Arch. Hydrobiol.* 134: 179-194.
- Molloy, C. J. and Syrett, P. J. 1988a. Interrelationships between uptake of urea and uptake of ammonium by microalgae. *J. Exp. Mar. Biol. Ecol.* 118: 85-95.
- Molloy, C. J. and Syrett, P. J. 1988b. Effect of light and N deprivation on inhibition of nitrate uptake by urea in microalgae. *J. Exp. Mar. Biol. Ecol.* 118: 97-101.
- Montaya, J. P. and McCarthy, J. J. 1995. Isotopic fractionation during nitrate uptake by phytoplankton grown in continuous culture. *J. Plankton Res.* 17: 439-464.
- Montaya, J. P., Horrigan, S. G., and MacCarthy, J. J. 1991. Rapid, storm-induced changes in the natural abundance of ^{15}N in a planktonic ecosystem. *Geochim. Cosmochim. Acta.* 55: 3267-3638.
- Morris, I. and Syrett, P. J. 1963. The development of nitrate reductase in *Chlorella* and its repression by ammonium. *Arch. Mikrobiol.* 47: 32-41.
- Nagasaki, K., Itakura, I., Imai, I., Nakagiri, S., and Yamaguchi, M. 1996. The disintegration process of a *Heterosigma akashiwo* (Raphidophyceae) red tide in northern Hiroshima Bay, during the summer of 1994. In *Proceedings of the 7th International Conference on Toxic Phytoplankton*.
- Nagasaki, K and Yamaguchi, M. 1997. Isolation of a virus infectious to the harmful bloom causing microalga *Heterosigma akashiwo* (Raphidophyceae). *Aquat. Microb. Ecol.* 13: 135-140.

- Needoba, J. 1997. Nitrogen isotope fractionation by four groups of phytoplankton grown on nitrate. BSc dissertation, University of British Columbia, Vancouver.
- Ohmori, M., Ohmori, K., and Strotmann, H. 1977. Inhibition of nitrate uptake in a blue-green alga, *Anabaena cylindrica*. Arch. Microbiol. 114: 225-229.
- Paasche, E. 1971. Effect of ammonia and nitrate on growth, photosynthesis, and ribulosediphosphate carboxylase content of *Dunaliella tertiolecta*. Physiol. Plant. 24: 294-299.
- Paasche, E. and Kristiansen, S. 1982. Nitrogen nutrition of the phytoplankton of the Oslofjord. Estuarine Coastal Shelf Sci. 14: 237-249.
- Paasche, E., Bryceson, I., and Tange, K. 1984. Interspecific variation in dark nitrogen uptake by dinoflagellates. J. Phycol. 20: 394-401.
- Pachard, T. T. and Blasco, D. 1974. Nitrate reductase activity in upwelling regions. 2. Ammonia and light dependence. Tethys 6: 269-280.
- Park, J. S. 1989. Studies on red tide phenomena in Korean coastal waters. In: Red Tides (eds.) T. Okaichi, D. M. Anderson, and T. Nemoto. Elsevier, New York. p. 37-40.
- Parslow, J. S., Harrison, P. J., and Thompson, P. A. 1984a. Development of rapid ammonium uptake during starvation of batch and chemostat cultures of the marine diatom *Thalassiosira pseudonana*. Mar. Biol. 83: 43-50.
- Parslow, J. S., Harrison, P. J., and Thompson, P. A. 1984b. Saturated uptake kinetics: transient response of the marine diatom *Thalassiosira pseudonana* to ammonium, nitrate, silicate or phosphate starvation. Mar. Biol. 83: 51-59.
- Parsons, T. R., Stronach, J., Borstad, G. A., Louttit, G., and Perry, R. I. 1981. Biological fronts in the Strait of Georgia, British Columbia and their relation to recent measurements of primary productivity. Mar. Ecol. Prog. Ser. 6: 237-242.
- Parsons, T. R., and Harrison, P. J. 1983. Nutrient cycling in marine ecosystems. In: physiological plant ecology IV. Ecosystem Processes : Mineral Cycling, Productivity and Pollution. (eds.) B. Richards and J. L. Charley. Springer-Verlag, Heidelberg. p. 85-115.

- Pennock, J. R., Velinsky, D. J., Ludlam, J. M., and Sharp, J. H. 1996. Isotopic fractionation of ammonium and nitrate during uptake by *Skeletonema costatum*: implications for $\delta^{15}\text{N}$ dynamics under bloom conditions. *Limnol. Oceanogr.* 41: 451-459.
- Picard, G. A. 1976. Effects of light and dark cycles on the relationship between nitrate uptake and cell growth rates of *Chaetoceros* sp. (STX-105) in continuous culture. Ph.D. Thesis, Dept. Biology, City Univ. of New York, N. Y. p. 220
- Pingree, R. A., Holligan, P. M., and Mardell, G. T. 1978. The effects of vertical stability on phytoplankton distributions in the summer on the northwest European Shelf. *Deep-Sea Res.* 25: 1011-1028.
- Price, N. M., Cochlan, W. P., and Harrison, P. J. 1985. Time course of uptake of inorganic and organic nitrogen by phytoplankton in the Strait of Georgia: comparison of frontal and stratified communities. *Mar. Ecol. Prog. Ser.* 27: 39-53.
- Price, N. M. and Harrison P. J. 1987. Comparison of methods for the analysis of dissolved urea in seawater. *Mar. Biol.* 94: 307-317.
- Price, N. M. and Harrison, P. J. 1988. Uptake of urea C and urea N by the coastal marine diatom *Thalassiosira pseudonana*. *Limnol. Oceanogr.* 33 : 528-537.
- Probyn, T. A. and Chapman, A. R. O. 1982. Nitrogen uptake characteristics of *Chordaria flagelliformis* (Phaeophyta) in batch mode and continuous mode experiments. *Mar. Biol.* 71: 129- 133.
- Pujo-Pay, M., Conan, P., and Raimbault, P. 1997. Excretion of dissolved organic nitrogen by phytoplankton assessed by wet oxidation and super(15)N tracer procedures. *Mar. Ecol. Prog. Ser.* 155: 99-111.
- Pybus, C. 1984. Unusual concentrations of the dinoflagellate *Ceratium tripos* in Galway Bay. *Ir. Nat. J.* 21: 317-320.
- Raven, J. A. 1986. Physiological consequences of extremely small size for autotrophic organisms in the sea. In: *Photosynthetic picoplankton.* (eds.) T. Platt, and W. K. W. Li. *Can. Bull. Fish. Aquat. Sci.* 214. p. 1-70.

- Ree, T. A. V. and Syrett, P. J. 1979. Mechanisms for urea uptake by the diatom *Phaeodactylum tricornutum*: the uptake of thiourea. *New Phytol.* 83: 37-48.
- Reed, R. H. 1990. Solute accumulation and osmotic adjustment. In: *Biology of Red Algae*. (eds.) K. M. Cole and R. G. Sheath. Cambridge University Press. p. 147-170.
- Rees, T. A. V. and Syrett, P. J. 1979. The uptake of urea by the diatom *Phaeodactylum*. *New Phytol.* 82: 169-178.
- Reid, F. M., Lange, C. B., and White, M. M. 1985. Microplankton species assemblages at the Scripps Pier from March to November 1983 during the 1982 - 1984 El Niño event. *Botanica Mar.* 28: 443-452.
- Reisner, G. S., Gering, R. K., and Thompson, J. F. 1960. The metabolism of nitrate and ammonia by *Chlorella*. *Plant Physiol.* 35: 48-52.
- Remsen C. C. 1971. The distribution of urea in coastal and oceanic waters. *Limnol. Oceanogr.* 16: 732-740.
- Remsen, C. C., Carpenter, E. J., and Schroeder, B. W. 1972. Competition for urea among estuarine microorganisms. *Ecology* 53: 921-926.
- Rhee G-Y. and Lederman, T. C. 1983. Effects of nitrogen sources on P-limited growth of *Anabaena flos-aquae*. *J. Phycol.* 19: 179-185.
- Ricketts, T. R. 1988. Homeostasis in nitrogenous uptake/assimilation by the green alga *Platymonas (Tetraselmis) striata* (Prasinophyceae). *Annals. Bot.* 61: 451-458.
- Robert, J-M. and Maestrini, S. Y. 1986. Absorptions simultanees des ions NO_3 et NH_4 par trois diatomées de claires à huitres, en culture axénique. *Phycologica* 25: 152-159.
- Rosenberg, G., Probyn, T. A., and Mann, K. H. 1984. Nutrient uptake and growth kinetics in brown seaweeds: response to continuous and single additions of ammonium. *J. Exp. Mar. Biol. Ecol.* 80: 125-146.
- Ryther, J. H. and Dunstan, W. M. 1971. Nitrogen, phosphorus and eutrophication in the coastal marine environment. *Science* 171: 1008-1013.
- Sampayo, M. A. de M. 1985. Encystment and excystment of a Portuguese isolate of *Amphidinium carterae* in cultures. In: *Toxic Dinoflagellates*.

- (eds.) D. M. Anderson, A. White, and D. G. Baden. Elsevier, New York. p. 125-130.
- Satoh, Y. and Hanya, T. 1981. The distribution of urea in Lake Yunoko. Jap. J. Limnol. 42: 254-258.
- Serra, J. L., Llama, M. J., and Codenas, E. 1978. Nitrate utilization by the diatom *Skeletonema costatum*. 2. Regulation of nitrate uptake. Pl. Physiol. 62: 991-994.
- Sharp, J. H. 1983. The distributions of inorganic nitrogen and dissolved and particulate organic nitrogen in the sea. In: Nitrogen in the marine environment. (eds.) E. J. Carpenter and D. G. Capone. Academic Press, New York, N.Y. p. 1-35.
- Smith, F. W. and Thompson, J. F. 1968. Regulation of nitrate reductase in *Chlorella*. Plant Physiology 43: 58.
- Slawyk, G. and MacIsaac, J. J. 1972. Comparison of two automated methods in a region of coastal upwelling. Deep-Sea Res. 19: 521-524.
- Solomonson, L. P. and Barver, M. J. 1990. Assimilatory nitrate reductase: functional properties and regulation. Annu. Rev. Plant Physiol. Plant Molec. Biol. 4: 225-253.
- Steinmann, J. 1976. Untersuchungen über den bakteriellen Abbau von Harnstoff und Harnsäure in der Westlichen Ostsee. Botanica Mar. 19: 47-58.
- Suttle, C. A. and Harrison, P. J. 1988. Rapid ammonium uptake by freshwater phytoplankton. J. Phycol. 24: 13-16.
- Suttle, C. A., Chan, A. M., and Cottrell, M. T. 1990. Infection of phytoplankton by viruses and reduction of primary productivity. Nature 347: 467-469.
- Sweeney, B. M. 1975. Red tides I have known. In: Proceedings of the first International Conference on Toxic Dinoflagellate Blooms. (ed.) LoCicero, V. R. Massachusetts Science & Technology Foundation. Wakefield, Massachusetts. p. 225-234.
- Sweeney, B. M. 1983. Circadian time-keeping in eukaryotic cells, models and hypotheses. Prog. Phycol. Res. 2: 189-225.

- Syrett, P. J. 1953. The assimilation of ammonia by nitrogen-starved cells of *Chlorella vulgaris*. I. The correlation of assimilation with respiration. *Ann. Bot.* 17: 1-19.
- Syrett, P. J. 1981. Nitrogen metabolism of microalgae. In: *Physiological bases of phytoplankton ecology*. (ed.) T. Platt. *Can. Bull. Fish. Aquat. Sci.* 210. p. 182-210.
- Syrett, P. J. 1988. Uptake and utilization of nitrogenous compounds. In: *Biochemistry of the Algae and Cyanobacteria*. (eds.) L. J. Rogers and J. R. Gallon. Oxford: Clarendon Press. p. 23-39.
- Syrett, P. J. and Morris, I. 1963. The inhibition of nitrate assimilation by ammonium in *Chlorella*. *Biochem. Biophys. Acta.* 67: 566-575.
- Syrett, P. J. and Peplinska, A. M. 1988. Effects of nitrogen-deprivation, and recovery from it, on the metabolism of microalgae. *New Phytol.* 109: 289-296.
- Taylor, F. J. R. 1992. The taxonomy of harmful marine phytoplankton, *G. Bot. Ital.* 126: 209-219.
- Taylor, F. J. R. and Haigh, R. 1993. The ecology of fish-kills blooms of the chloromonad flagellate *Heterosigma* in the Strait of Georgia and adjacent waters. In: *Toxic phytoplankton Blooms in the Sea* (ed.) T. J. Smayda and T. Shimizu. Elsevier, Amsterdam. p. 705-710.
- Thacker, A. and Syrett, P. J. 1972a. Disappearance of nitrate reductase activity from *Chlamydomonas reinhardtii*. *New Phytol.* 71: 435-441.
- Thacker, A. and Syrett, P. J. 1972b. Assimilation of nitrate and ammonium by *Chlamydomonas reinhardtii*. *New Phytol.* 71: 423-434.
- Thurberg, E. P. and Sasner, J. J. Jr. 1973. Biological activity of a cell extract from the dinoflagellate *Amphidinium carteri*, *Chesapeake Sci.* 14: 48-51.
- Timperley, M. H., Vigor-Brown, R. J., Kawashima, M., and Ishigami, M. 1985. Organic nitrogen compounds in atmospheric precipitation: their chemistry and availability to phytoplankton. *Can. J. Fish. Aquat. Sci.* 42: 1171-1177.
- Tischner, R. and Lorenzen, H. 1979. Nitrate uptake and nitrate reduction in synchronous *Chlorella*. *Plant* 146: 287-292.

- Turley, C. M. 1986. Urea uptake by phytoplankton at different fronts and associated stratified and mixed waters on the European Shelf. *British Phycol. J.* 21: 225-238.
- Turpin, D. H. and Harrison, P. J. 1978. Fluctuations in free amino acid pools of *Gymnodinium simplex* (Dinophyceae) in response to ammonia perturbation. Evidence for glutamine synthetase pathway. *J. Phycol.* 14: 461-464.
- Turpin, D. H. and Bruce, D. 1990. Regulation of photosynthetic light harvesting by nitrogen assimilation in the green alga *Selenastrum minutum*. *FEBS* 263: 99-103.
- Thomas, T. E. and Harrison, P. J. 1987. Rapid ammonium uptake and nitrogen interactions in five intertidal seaweeds grown under field conditions. *J. Exp. Mar. Biol. Ecol.* 107: 1-8.
- Thompson, P. A., Levasseur, M. E., and Harrison, P. J. 1989. Light-limited growth on ammonium vs nitrate: What is the advantage for marine phytoplankton? *Limnol Oceanogr.* 34: 1014-1024.
- Tischner, R., Ward, M. R., and Huffaker, R. C. 1989. Evidence for a plasma-membrane-bound nitrate reductase involved in nitrate uptake of *Chlorella sorokiniana*. *Planta* 178: 19-24.
- Tomas, C. R. 1978. *Olisthodiscus luteus* (Crysoophyceae) I. Effect of salinity and temperature on growth, motility and survival. *J. Phycol.* 14: 309-313.
- Tomas, C. R. 1982. *Olisthodiscus luteus* (Chrysophyceae). V. Its occurrence, abundance and dynamics in Narragansett Bay, Rhode Island. *J. Phycol.* 16: 157-166.
- Uchida, T. 1976. Excretion of ammonia by *Prorocentrum micans* Ehrenberg in urea-grown culture. *Jap. J. Ecol.* 26: 42-44.
- Ullrich, W. R. 1987. Nitrate and ammonium uptake in green algae and higher plants: mechanism and relationship with nitrate metabolism. In: *Inorganic nitrogen metabolism*. (eds.) W. R. Ullrich, P. J. Aparicio, P. J. Syrett, and F. Castillo. Springer-Verlag, Berlin, Heidelberg, New York. p. 32-38.
- Ullrich, W. R., Larsson, M., Larsson, C-M., Lesch, S., and Novacky, A. 1984. Ammonium uptake in *Lemna gibba* G1, related membrane potential changes, and inhibition of anion uptake. *Physiol. Plant.* 61: 369-376.

- Vernet, M, Neori, A., and Haxo, F. T. 1989. Spectral properties and photosynthetic action in red-tide populations of *Prorocentrum micans* and *Gonyaulax polyedra*. Mar. Biol. 103: 365-371
- Wada, E. and Hattori, A. 1978. Nitrogen isotope effects in the assimilation of inorganic nitrogenous compounds. Geomicrobiol. J. 1: 85-101.
- Wada, E. 1980. Nitrogen isotope fractionation and its significance in biogeochemical processes occurring in marine environments. In: Isotope Marine Chemistry. (eds.) E. Goldberg, Y. Horibe, and K. Saruhashi. Uchida Rokakukuhō, Tokyo. p. 375-398.
- Walsh, J. J., Whitley, T. E., Barvenik, F. W., Wirick, C. D., and Howe, S.O. 1978. Wind events and food chain dynamics within the New York Bight. Limnol. Oceanogr. 23: 659-683.
- Wang, Z., Zhang, Q., Lu, Y., and Lu, H. 1996. The effects of nutrients, vitamins and trace metals on the growth of the red tide organism *Prorocentrum micans*. Donghai Mar. Sci. 14: 33-38.
- Wangersky, P. J. and Guillard, R. L. 1960. Low molecular weight organic base from the dinoflagellate *Amphidinium carteri*. Nature (London) 185: 689-690.
- Ward, A. K. and Wetzel, R. G. 1980. Interactions of light and nitrogen source among planktonic blue-green algae. Arch. Hydrobiol. 90: 1-25.
- Waser, N. A. D., Yin, K., Yu, Z., Tada, K., Harrison, P. J., Turpin, D. H., and Calvert, S. E. 1998a. Nitrogen isotope fractionation associated with growth of marine diatoms and coccolithophores on the combined nitrate, ammonium and urea sources. Mar. Ecol. Prog. Ser. 169: 29-41.
- Waser, N. A. D., Harrison, P. J., Nielsen, B., and Calvert, S. E. 1998b. Nitrogen isotope fractionation during the uptake and assimilation of nitrate, nitrite, ammonium, and urea by a marine diatom. Limnol. Oceanogr. 43: 215-224.
- Watanabe, M., Nakamura, M., and Kohata, K. 1983. Diurnal vertical migration and dark uptake of nitrate and phosphate of the red tide flagellates, *Heterosigma akashiwo* HADA and *Chattonella antiqua* (HADA) ONO (Raphidophyceae). Jpn. J. Phycol. 31: 161-166.

- Wheeler, P. A., Glibert, P. M., and McCarthy, J. J. 1982. Ammonium uptake and incorporation by Chesapeake Bay phytoplankton: Short-term uptake kinetics. *Limnol. Oceanogr.* 27: 1113-1128.
- Wheeler, P. A., Olson, R. J., and Chisholm, S. W. 1983. Effects of photocycles and periodic ammonium supply on three marine phytoplankton species. II. Ammonium uptake and assimilation. *J. Phycol.* 19: 528-533.
- Wood, G. J. and Flynn, K. J. 1995. Growth of *Heterosigma carterae* (Raphidophyceae) on nitrate and ammonium at three photon flux densities: Evidence for N stress in nitrate-growing cells. *J. Phycol.* 31: 859-867.
- Yamochi, S. 1983. Mechanisms for outbreak of *Heterosigma akashiwo* red tide in Osaka Bay, Japan. Part 1. Nutrient factors involved in controlling the growth of *Heterosigma akashiwo* Hada. *J. Oceanogr. Soc. Jap.* 39: 310-316.
- Yamochi, S. and Abe, T. 1984. Mechanisms to initiate a *Heterosigma akashiwo* red tide in Osaka Bay. Part 2. Diel vertical migration. *Mar. Biol.* 83: 255-261.
- Yamochi, S. 1989. Mechanisms for outbreak of *Heterosigma akashiwo* red tide in Osaka Bay, Japan, In: *Red Tides* (eds.) T. Okaichi, D. M. Anderson, and T. Nemoto. Elsevier, New York. p 253-256.
- Yin, K. 1988. Short-term interaction between nitrate and ammonium uptake for cells of a marine diatom grown under different degrees of light limitation. M.Sc. Thesis, University of British Columbia, Vancouver.
- Yokote, M., Honjo, T., and Asakawa, M. 1985. Histochemical demonstration of a glycocalyx on the cell surface of *Heterosigma akashiwo*. *Mar. Biol. (Berl.)* 88: 295-299.

APPENDIX 1

Equations used to calculate growth rates

Growth rates (d^{-1}) were calculated from fluorescence values between the beginning and the end of log phase according to the following equation:

$$\mu = \ln (F2/F1) / (t2-t1)$$

where F2 and F1 are the fluorescence values at time 2 (t2) and time 1 (t1), respectively and are reported as the mean ($n = 3$) ± 1 S. D. for triplicate cultures.

In vivo fluorescence was measured with a Turner Designs model 10 fluorometer.